ABSTRACT

GOETZ, AMBER KRISTINA. Gene expression profiling in testis and liver of mice to identify modes of action of conazole toxicities. (Under the direction of David Dix.)

Conazoles are a class of azole fungicides used in both pharmaceutical and agricultural applications. This study focused on 4 conazoles that exhibit a range of carcinogenic and reproductive effects, in order to identify common and unique modes of action. Conazoles target cytochrome P450s (CYPs), and the inhibition and induction of various CYP activities may be part of the toxic modes of action in liver and testis. We used gene expression profiling to characterize a broader range of conazole effects and to identify additional modes of action. Adult male CD-1 mice were dosed daily by gavage for 14 days with fluconazole, propiconazole, myclobutanil or triadimefon (three doses each). Relative liver weight increased following fluconazole and propiconazole exposure, and histological analysis revealed centrilobular hepatocyte hypertrophy in response to all 4 conazoles. No weight or histological changes were observed in testis, and serum testosterone and luteinizing hormone were also unchanged. Microarrays queried expression of 16,475 genes, and identified 2,081 and 1,424 differentially expressed genes in liver and testis, respectively, following conazole exposure. Of these genes, 118 in the liver and 94 in the testis were common to two or more conazoles. The majority of differentially expressed genes related to stress response, oxidative stress, xenobiotic metabolizing enzymes, steroidogenesis or carcinogenesis. Expression profiles between conazoles and between liver and testis affected similar biological pathways, suggesting the potential for common modes of action.

GENE EXPRESSION PROFILING IN TESTIS AND LIVER OF MICE TO IDENTIFY MODES OF ACTION OF CONAZOLE TOXICITIES

by
AMBER KRISTINA GOETZ

A thesis submitted to the Graduate Faculty of
North Carolina State University
in partial fulfillment of the
requirements for the Degree of
Master of Science

TOXICOLOGY

Raleigh

2003

APPROVED BY:

_____
Dr. Charlotte Farin

_____
Co-chair of Advisory Committee
Dr. David Dix

_____
Co-chair of Advisory Committee
Dr. Robert Smart

DEDICATION

This thesis and all the work that has been put in to it are dedicated to my parents, who have provided me with support both emotionally and financially. They would not let me stop when I finished undergraduate school, they wouldn't let me settle when those paychecks bounced during my stint as a zookeeper, and they always gave motivational support through both the good times and the bad.

PERSONAL BIOGRAPHY

I was born into an Air Force family in Ohio, moving rapidly to Florida and Maine where I attended a rural school emphasizing strong family values and involvement in community life. Throughout my early years I assisted my family in caring for a variety of farm animals and at the age of 10 decided to breed rabbits. This interest expanded to extensive volunteer work at the Caribou veterinary clinic. As a Girl Scout, I was selected to represent the State of Maine at a National training program in Animal Care and Management at the Bronx Zoological Park.

Each of these experiences and opportunities led me to the Zoology program at the University of Maine Orono. At UMaine Orono I was introduced to the study of the taxonomy of cumaceans as well as work in the field of DNA analysis. Due to my interest and skill in the laboratory, I was selected as an undergraduate to participate in a graduate research program off the coast of Mexico.

Following graduation, I continued to work in a veterinary clinic and then as a zoo attendant specializing in the care of domestic and exotic animals. In the fall of 2001 I entered the graduate program in Zoology at North Carolina State University (NCSU) with the support of the U.S. Environmental Protection Agency (EPA). My interest in research was refocused to toxicology, such that shortly after my admittance in the Zoology program I transferred into NCSU's Toxicology program.

In fact, I have recently entered into NCSU's Doctoral program in Toxicology, and upon completion of my Master's work will continue my research in reproductive toxicology at the U.S. EPA.

AKNOWLEDGMENTS

First and foremost, thanks to Dr. David Dix for giving me the opportunity to volunteer in his lab at the EPA during the summer of 2001, and continuing to support my efforts and interest in the field of reproductive toxicology. His interest in this project drove my enthusiasm to dive into this research headfirst to do the best I could possibly do.

I'd also like to thank a number of people at North Carolina State University: Dr. Copeland for helping me gain acceptance into the Master's program in Zoology; Dr. Grossfeld for teaching me the true meaning of graduate studies; Dr. Robert Smart and Dr. Charlotte Farin for sitting on my committee with Dr. David Dix and providing advice and support throughout; and of course, to all my professors for opening my eyes, broadening my mind and testing my abilities.

TABLE OF CONTENTS

LIST OF FIGURES

LIST OF TABLES

LIST OF TABLES CONTINUED

Page

INTRODUCTION

Conazoles are a class of azole fungicides used in the prevention and treatment of fungal infections. Agriculturally, their potent fungicidal activity is useful for fungal growth control on fruit, vegetable, cereal crops and seed treatment. Clinical uses include treatment for local and systemic infections (Schlüter, 1988). Conazoles can be differentiated into two categories, based on their azole ring structure. Imidazoles such as ketoconazole and miconazole have a 1,3-N-substituted azole ring and triazoles such as propiconazole, triadimefon and fluconazole have a 1,2,4-N-substituted azole ring (Figure 1). Imidazoles bind via their N-3 and triazoles bind via their N-4 of the azole ring to the heme protein of cytochrome P450s (CYPs). Determination of CYP-binding affinity depends heavily on the non-ligand hydrophobic component of the chemical structure of the selected conazole (Vanden Bossche, 1990). Despite their chemical structure differences, they still have the same antifungal activity by the same molecular mechanism. The variability in affinities is one reason why several different conazoles are used to treat different fungal infections.

Conazoles specifically inhibit ergosterol biosynthesis, a main constituent required for the bioregulation of membrane fluidity and integrity of fungal cell walls (Ghannoum and Rice, 1999). A decrease in ergosterol levels inhibits cell growth and proliferation. The heme protein of 14α-demethylase (Cyp51) co-catalyzes the cyp-dependent 14α-demethylation of lanosterol to ergosterol. Studies indicate the azole moiety of conazoles bind to the heme protein of CYP51a1, inhibiting functionality of the enzyme thus inhibiting ergosterol biosynthesis (Ghannoum and Rice, 1999). Plasma-bound chitin synthesis enzymes of the fungal cell wall become uncoordinated with the accumulation of C-14-methylated sterols and fungal cells burst due to changes in membrane permeability (Huss et al., 2002, Vanden Bossche et al., 1990).

Conazoles not only inhibit prokaryotic CYP51 but also affect mammalian CYP enzymes. Conazoles can act as both inducers and inhibitors of CYP450s, depending on the tissue and specific conazole (Ronis et al., 1994). Ergosterol biosynthesis inhibiting fungicides have complex effects on the hepatic microsomal monooxygenase systems of vertebrate species. This creates the possibility for a common mode of action for conazole toxicities via modulation of CYP enzymes common to liver metabolism in vertebrates. Disruption of metabolic processes can have serious effects on the organism as a whole, from changes in hormone synthesis to decreased clearance of toxic xenobiotics from the animal. Numerous studies have tested the *in vivo* effects of various conazoles and demonstrated common rodent toxicities including liver tumors primarily in mice, thyroid tumors in rats, and in some cases developmental and reproductive lesions (Zarn et al., 2003).

As of June 2002 1,925 Cyp genes had been named across many species and classified into at least 60 distinct families (Nelson, 2003). Cyp genes were arranged into families based on their nucleotide sequence similarity to one another. Genes with 40% or greater similarity are grouped into families designated with an Arabic numeral (e.g. CYP1) and further subdivided into subfamilies if similarity is 55% or greater and designated with a letter (e.g. CYP1a). In humans, there are currently 57 distinct Cyp genes, sorted into 18 families and 42 subfamilies (Nebert, 2002).

The major site of Cyp gene expression is in the liver, however there are many other tissues that contain appreciable levels of CYPs (e.g. kidney, intestine and gonads). Major sites of metabolism by specific CYPs contain larger concentrations of those CYPs, however lower concentrations of many CYPs are found in tissues throughout the body, including the skin (Hodgson and Smart, 2001). This large range of CYP enzymes throughout the body

indicates the importance of CYPs and their enzymatic activities in many physiological processes.

Despite specificity of the different CYP families and subfamilies for endogenous substrates, exogenous compounds can also modulate the expression and activity of many CYPs. Numerous CYPs respond to xenobiotic challenge with induction, increased levels of activity, protein expression, and increased gene transcription, or post-translational protein stabilization. Some of the main drug-metabolizing hepatic CYPs are 1A2, 2C9, 2C19, 2D6, and 3A4, which are all encoded by separate genes, have different in their amino acid composition; and therefore differing substrate specificities (McGinnity, 2001). However, CYP substrate specificities tend to be broad, with overlap between numerous CYPs and substrates. Part of an organism's defense system involves CYPs that specifically bind exogenous compounds to metabolize and target the unwanted compounds for excretion. However, some exogenous compounds bind CYPs and other enzymes not designed to handle the metabolism of foreign compounds. Non-specific binding of exogenous compounds to arbitrary enzymes inhibits enzymatic reactions of those enzymes with their preferred substrates.

Cytochrome P450 genes encode for membrane-bound, heme-containing terminal oxidase enzymes that catalyze NADPH-dependent oxidation of drugs, chemicals and carcinogens. CYP enzymes form multienzyme complexes with cofactors flavin adenine dinucelotide/ flavin mononucleotide-dependent (FAD/FMN-dependent) NADPH-cytochrome P450 reductases and cytochrome b_5. Since CYPb_5 oxidase is a major source for superoxide ions, metabolism of several substrates by CYPs will generate O_2^- radicals in the liver. This increase in free radicals sets the stage for oxidative stress in the liver such as lipid

peroxidation and cell death (Hodgson and Smart, 2001). CYPs are responsible for the formation and degradation of endogenous sterol and steroid compounds, vitamin D_3, cholesterol, bile acid synthesis, and prostaglandin synthesis as well as metabolism of exogenous compounds (xenobiotics) foreign to the body (Honkakoski and Neghishi, 2000, Peterson and Graham, 1998). CYPs act on many endogenous substrates introducing oxidative, peroxidative and reductive changes into small molecules of widely different chemical structures. Clearance of xenobiotics and endogenous compounds from the body requires two or more phases of metabolism to reduce a compound to a more water-soluble intermediate for excretion. Mammalian phase I CYP-enzyme isoforms are microsomal monooxygenases that oxidize oxygen-containing compounds to more soluble intermediates by reducing the oxygen to a water molecule and preparing the remaining intermediate for further conjugation reactions by phase II enzymes (Hodgson and Smart, 2001).

Digestion and detoxification are the two most important functions of the liver, and liver cells always maintain high metabolic rates and active vesicular transport. Hepatocarcinogenesis in the rodent model is a result of increased CYP levels leading to oxidative stress, mitogenesis and altered foci development ultimately leading to neoplasia (Harada et al., 2003). Studies have shown fungicides, including conazoles, can act as both inducers and inhibitors of CYPs affecting the activity and expression of a number of CYP enzymes (Tiboni et al., 1999, Mitra et al., 1996). As stated earlier, conazoles have complex effects on hepatic microsomal monooxygenase systems in vertebrates. Fluconazole has been shown to inhibit CYPs involved in the liver-mediated metabolism of toxic intermediates. Inhibition of one of the more important drug metabolizing hepatic enzymes, Cyp2c9, is significantly increased with co-administration of fluconazole *in vitro* and *in vivo* (Miners and

Birkett, 1998). *In vivo* studies have demonstrated that fluconazole administered in feed at dose levels of 10 and 20 mg/kg cause increases in liver weight and hepatic CYPs along with hepatocellular hypertrophy (Paulus et al., 1994). Male rats treated at doses up to 10 mg/kg/day fluconazole had increased occurrence of hepatocellular adenomas (Pfizer, 1998).

Fluconazole is used as a common pharmaceutical in human medicine, used for the treatment of several yeast infections including oropharyngeal and esophageal candidiasis, and cryptococcal meningitis infections. Primary route of clearance in humans is renal excretion, and for the most part it's excreted unchanged in the urine of rats (Paulus et al., 1994). The clearance and half-life of fluconazole is prolonged in children compared to adults, yet the plasma concentrations measured were lower in children. The volume of distribution, amount of drug in the body to the concentration of drug in the plasma, is high for fluconazole (Pfizer, 1998, Shrikhand et al., 2000). A high volume of distribution demonstrates fluconazole has a large range of distribution, including intracellular spaces. However, a two-year carcinogenicity studies in rats and mice at doses up to 10 mg/kg/day revealed no evidence of carcinogenic potential. Adverse effects of fluconazole include gastrointestinal upset and hepatic injury. As the dose of fluconazole is elevated above therapeutic and threshold levels, it loses specificity for its target enzyme (14α-demthylase), producing inhibitory effects on other CYP-mediated steps in the steroid cascade.

Myclobutanil has also been shown to cause treatment-related hepatic hypertrophy and increased liver weights in both rats and mice. 13 week subchronic feeding studies in rats revealed a lowest observed adverse effect level (LOAEL) of 3000 parts per million (ppm) based on increased liver weight, hepatocellular hypertrophy and necrosis of the liver (EPA, 2000). Similarly in the subchronic feeding study with mice, a LOAEL of 1000 ppm produced

hepatocytic hypertrophy and swollen vacuolated centrilobular hepatocytes as well as hepatocyte necrosis and other hepatic affects (EPA, 2000). 2-year chronic feeding/ carcinogenicity studies in mice defined a LOAEL of 500 ppm for males with observable effects of increased liver weight and incidence and severity of centrilobular hepatocyte hypertrophy along with focal hepatocellular alterations and necrosis (EPA, 2000).

The pesticide propiconazole induces activities of Cyp1a1, 1a2, 2b1/2, 2b6 and 3a4. These CYPs mainly degrade xenobiotics in the liver. Propiconazole also inhibits liver Cyp2c11 and steroidogenic Cyp19 (aromatase) in reproductive and other tissues *in vitro* (Vinggaard et al., 2000). In a rat 2-year carcinogenicity study a LOAEL was defined with 500 ppm based on hepatocyte changes (EPA, 1999). 2-year feeding studies in mice defined a LOAEL of 500 ppm as well, based on decreased body weight, increased liver lesions and weights along with significant increases in adenomas and carcinomas of the liver in males (EPA, 1999). Additional feeding studies with doses of 20mg/kg body weight or greater produced slight effects on liver parameters were (Zarn et al., 2003). Propiconazole has been shown to significantly induce Cyp1a1 activity in quail kidney microsomes (Ronis et al., 1998) as well as brown trout hepatic microsomes (Egaas et al., 1999). Such reports indicate fungicides can affect multiple species with similar targets of toxicity.

Triadimefon is an agricultural triazole fungicide that inhibits CYP2a6 in both rats (at 30 mg/kg/day for 7 days in males) and mice (at 50 mg/kg/day for 7 days in males) (Schmidt, 1983). In 2-year chronic feeding studies in mice, 2,000 ppm increases the incidence of enlarged livers, hyperplastic nodules and increased liver weights (EPA, 1994).

In addition to adverse effects on the liver, triadimefon also causes thyroid carcinomas in the rat (EPA, 1996, Office of Prevention: Bayleton, 1996). The hypothalamic pituitary

thyroid axis has a negative feedback mechanism to control the concentration of thyroid hormone in the blood. Thyroid-releasing hormone (TRH) from the hypothalamus stimulates release of thyroid-stimulating hormone (TSH) from the pituitary, which acts on the follicular cells of the thyroid to produce and secrete thyroid hormones triiodothyronine and thyroxin (T_3 and T_4 respectively). Circulating levels of thyroid hormone act on the hypothalamus and pituitary in a negative feedback manner to inhibit release of TRH and TSH when concentrations are high and vice versa at low concentrations of blood thyroid hormone levels.

Several pesticides have been shown to have antithyroid effects (disruption of thyroid-pituitary homeostasis), causing a reduction in thyroid hormone levels, increase in TSH and eventually increased thyroid cancer potential in rodents (Hurley et al., 1998). There are several mechanisms of action by antithyroid chemicals, one of which is the enhancement of normal levels of metabolism and excretion of thyroid hormone by the liver. Increased clearance of thyroid hormone (T_3 and T_4) is facilitated through the action of uridine diphosphate (UDP) glucoronosyltransferase. This accelerated depletion of thyroid hormone stimulates the hypothalamus and pituitary to release TRH and TSH in order to stimulate the thyroid's release of T_3 and T_4. When the stores of T_3 and T_4 are depleted, follicular cells undergo hyperplasia to compensate for the increased demand of T_3 and T_4 (Hurley et al., 1998). This induction of cell growth could be the mechanism leading to thyroid carcinomas. Triadimefon is one such fungicide that induces thyroid adenomas in the male rat (Office of Prevention: Bayleton, 1996). Induction in hepatic CYP enzymes has been correlated with induction of glucuronosyl transferase activity; thus, the increased clearance of thyroid hormone may be a secondary effect of conazole toxicity in the liver leading to thyroid toxicity.

Regulation of steroidogenesis is primarily at the level of transcriptional regulation for genes encoding various steroidogenic CYP450 enzymes. The CYP genes are regulated in tissue-specific, developmentally programmed, and hormonally regulated fashion. There are substantial differences in the expression of these genes among various mammals (for example, rodents do not express the gene for CYP17 in their adrenals, while humans do). Several conazoles are known to inhibit specific steroidogenic CYP enzymes. CYP19 (aromatase) activity is inhibited through the binding of the conazole to the CYP450 heme iron, the same mechanism used on CYP51. Inhibition of CYP19 blocks the conversion of androstenedione to estrone and testosterone to estradiol (Figure 2). Fluconazole, propiconazole and triadimefon are examples of conazoles that inhibit aromatase activity (Paulus et al., 1994, Vinggaard et al., 2000). CYP17 (17α-hydroxylase and 17,20-lyase) enzymes also have an impact on the steroidogenic biosynthetic pathway (Figure 3). Imbalances in steroidogenic enzymes will cause fluctuations in hormone levels, which could disrupt the hypothalamic pituitary gonad axis (HPG). In the testis, luteinizing hormone (LH) modulates the production of testosterone in leydig cells. Follicle-stimulating hormone (FSH) modulates estradiol synthesis (testosterone conversion by CYP19) in sertoli cells (Figure 4). LH and FSH are both secreted by the anterior pituitary in response to gonadotropin-releasing hormone (GnRH) from the hypothalamus. Thus, monitoring LH and FSH levels could be useful in understanding conazole effects on steroidogenesis. However, in this study we plan to use gene expression profiles to delineate the mode of action for conazoles on reproductive toxicities and confirm the variations in hormone levels.

The sterol biosynthesis pathway in vertebrates and fungal cells stems from the same starting material, lanosterol is the precursor to cholesterol in vertebrates and ergosterol in

fungal cells. The difference lies in the enzymes involved in the pathways to the different steroids produced. CYP51, however, is involved in both pathways (Vanden Bossche et al., 1990). The effects of conazoles on CYP51 interrupt normal steroid biosynthesis leading to abnormal levels of cholesterol precursors (zymosterol) and levels of cholesterol itself (Zarn et al., 2003). This imbalance leads to abnormal steroid and hormone levels in the system and thus disruptions occur at the whole organism level (Zarn et al., 2003).

Azole-induced disruption of CYP51 metabolism of lanosterol to cholesterol in sterol biosynthesis occurs at several steps in the metabolism of lanosterol. CYP 51 is involved in the metabolism of lanosterol to follicular fluid meiosis-activating sterol (FF-MAS); which is further metabolized to testis meiosis-activating sterol (T-MAS), two precursors to zymosterol and thus cholesterol (Zarn et al., 2003). FF-MAS and T-MAS have been shown to induce resumption of meiosis in cultured mouse oocytes, and significantly increase expression levels of sterol 14α-demethylase (CYP51) in post meiotic spermatids compared to pre-meiotic spermatids (Zarn et al., 2003). These studies are indicative of an important role for the different MAS sterols on development of the testis, spermatids and oocyte development (Zarn et al., 2003).

Besides the previously discussed agriculturally and common clinical uses of azole compounds, they are also used for the treatment of estrogen-responsive tumors in humans. Ketoconazole is an example of one such compound used in the treatment of prostate carcinomas (Harris et al., 2002) while anastrazole and letrozole are examples of azoles used in the treatment of breast cancer (Buzdar, 2002). These compounds target specific enzymes in the steroidal biosynthesis pathway (CYP17, 20-lyase by ketoconazole and CYP19 by anastrazole and letrozole), inhibiting the synthesis of steroids in a beneficial way for these

patients. However, excess exposure to these azole compounds by a general healthy population will overload the xenobiotic metabolizing capacity in these individuals, not only inhibiting CYP51A1 involved in fungal cholesterol biosynthesis but endogenous metabolizing levels of the individual such as CYP51 and CYP19 (aromatase). Such disruption can cause an imbalance in the normal functioning levels of androgens and estrogens as well other regulating factors (Zarn et al., 2003).

Other conazole treatment- related reproductive effects include changes in reproductive tissue weights and lesions (Zarn et al., 2003, EPA, 2000, Office of Prevention: Bayleton, 1996). The numerous interrelationships between the various cells constituting the testis and the existence of a complex hormonal regulatory system with both positive and negative feedback controls makes the testis a target organ for a variety of chemicals. Any impact on regulation mechanisms of the testis can affect the proper function of the testis.

In vitro studies confirm fluconazole as a steroid transformation inhibitor of the synthesis of corticosterone, testosterone, 17β-estradiol and aromatase (CYP19). This frequency of endocrine imbalance occurs at significantly higher dose levels in rodent models relative to therapeutic dose levels (Paulus et al., 1994). This data supports our hypothesis that a possible common mode of action in the toxicity of conazoles involves the modulation of steroidogenic CYP enzymes in the testis and other target organs.

Propiconazole and triadimefon have been proven to inhibit aromatase activity in *in vitro* studies (Vinggard, 2000). Propiconazole has also been shown in reproductive studies (rat) to reduce testis and epididymus weights in the pups at levels as low as 21mg/kg body weight. Additionally, at doses of 256mg/kg body weight or greater, an increase in rat testis weights has been observed in short term studies (Zarn et al., 2003). In a 2-generation rat

reproduction study, triadimefon was found to increase testosterone levels but FSH levels remained unchanged (WHO 1985, Zarn et al., 2003). This study suggests the inhibition of aromatase produced the increased levels of testosterone. Triadimefon treatment has also been shown to induce relative weight increases in testis (EPA, 1996, Office of Prevention: Bayleton, 1996).

In a two-year carcinogenicity study with rats, treatment with doses of 200 ppm myclobutanil or greater resulted in several reproductive related effects in the male rat (EPA, 1995). Reduced testis weight, testis atrophy, epididymus necrosis, reduced or absent spermatid production and atrophy of the prostate were all observed in this study (Zarn et al., 2003, EPA, 1995).

For this study, we selected four conazoles (Figure 1) that would give us a range of apparent toxicities (Table 1). This allows comparisons to be made across species, tissues and toxicities for the four conazoles. These four conazoles produce a range of effects including liver tumors in mice, thyroid tumors in rats, disruption of steroidogenesis and adverse effects on development and reproduction. Additionally, comparisons can be made between each chemical's affect on gene expression in the relevant target tissues (liver and testis). The doses chosen for this study are based on two-year cancer bioassays and multigeneration reproductive tests, in order to allow comparison of our gene expression results with the cancer and reproductive outcomes.

In this study, we focused on three hypotheses and three specific aims. The first hypothesis we set out to study was the modulation of CYPs and related xenobiotic metabolizing enzymes (XMEs) in the liver and testis represents a common mode of action for multiple toxicities to conazoles in the different tissues. The second hypothesis in this study is

modulation of additional XMEs and regulatory genes such as those involved in cell cycle regulation also represent a possible common mode of action among conazoles. The third hypothesis, the modulation of CYPs and enzymes involved in steroidogenesis may be common among conazoles, was also looked at in this study. To study the thousands of genes of interest simultaneously, microarrays were used to examine the global gene expression changes. Our three specific aims for this study were to develop an ideal microarray analysis procedure for this type of data set, look for common modes of action among the four individual conazoles as well as look for common modes of action among the conazoles across the different tissues.

In order to test our hypotheses that (1) the common mode of action for conazole-toxicity in the liver and testis is modulation of Cyps and additional genes involved in the multiple cell cycle regulation processes and (2) male reproductive toxicity by multiple conazoles is facilitated through inhibition of steroidogenic CYP enzymes, RNA was extracted from both tissues and gene expression changes were analyzed through the use of microarrays. It is our understanding that the modulation of various Cyp genes in both the liver and testis will promote cellular dysfunction, a precursor to tumor formation in the liver and disruption of normal spermatogenesis in the testis. Profiling the gene expression changes of additional genes will promote identification of probable biological pathways affected by conazole exposure and broaden the mechanistic picture of conazole-induced toxicity of the liver and testis. Particular genes of interest included those involved in steroidogenesis and in particular, the biosynthesis of estrogens from androgens by the CYP19 enzyme, aromatase. It has been well documented the inhibition of aromatase leads to dysfunction at several steps in spermatogenesis in adult males (Hess et al., 2001, Nitta et al., 1993). In addition to

microarray analysis of the liver and testis, the histopathology of both tissues was used for detection of changes in tissue morphology. Additional measures including serum hormone levels for LH and testosterone were measured to look for disturbances in hormone production levels. Several hepatic cytochrome P450 isozyme activity measures were included to measure the amounts of activity change between the treatment dose groups and controls. These measures are good indicators of differences in xenobiotic metabolizing functioning among the different conazoles.

The use of microarrays is a relatively new technique that is becoming a common component in toxicological research. Microarrays are an ideal toxicological tool since they have the ability to show relative changes in expression for thousands of genes from the same tissue, dose and time point. The ability to define probable modes of action for a class of chemicals based on gene expression profiles of multiple genes and identifying the subsets that are affected relative to one another and other samples demonstrates the power of microarray technology. This method of analysis is part of an emerging field of toxicology referred to as toxicogenomics, the study of gene expression changes induced (or suppressed) by toxic compounds. The goals of toxicogenomics are to create gene expression profiles that identify mechanistic markers of various toxicities, to elucidate the molecular mechanisms involved in cellular responses to toxic insult and to extrapolate this information from one species to another. The use of microarrays to measure the effects of conazoles on gene expression provides insight into the mechanism of toxicity by this class of compounds. Identifying patterns of gene expression and relating them to other effects (e.g. histopathology) might allow us to better understand the common and unique aspects of these four conazoles' toxicity.

For this study, glass slide oligonucleotide microarrays were chosen to measure the expression of almost 16,000 genes. Traditional toxicological end points still need to be measured to assess the dose-response relationships of route, timing and duration of exposure through histological, hormone and weight measures. These measures will indicate if there are general or organ-specific effects and provide a foundation for interpreting gene expression results.

In this study, microarray analysis and gene expression profiling was used to determine if the expression of Cyp and other genes in liver and testis correlate with a conazoles' potential for cancer and reproductive effects.

MATERIALS AND METHODS

Animals

Adult CD-1 mice were received from Charles River Laboratories postnatal day (PND) 35-39. The U.S. EPA NHEERL Institutional Animal Care and Use Committee approved all procedures. Mice were acclimated for 10 days before dosing. Mice were assigned to treatment groups by randomization to ensure equivalent weight means across the dose groups prior to dosing. All mice were singly housed in the animal facility with a 12:12-h light:dark cycle under controlled temperature (72˚ F) and humidity (45%) with unlimited access to feed and water. Each experimental group consisted of six males treated with a given test compound and 18 males were treated with the respective vehicle solvent in each stage of the study (Figure5). The study was split into two stages due to the size of the study. Fluconazole and propiconazole were run in stage one; myclobutanil and triadimefon were run in stage two with appropriate controls.

Chemicals and Treatment

Propiconazole was the kind gift of Syngenta Crop Protection Inc., Greensboro NC; Fluconazole and Myclobutanil were purchased from LKT Laboratories Inc., St. Paul MN; and Triadimefon the kind gift of Bayer Crop Science, Kansas City KS. All four chemicals were technical grade, at purities above 95%. Each conazole was dissolved in a 7.5% Alkamuls EL-620/ distilled water solution. Alkamuls EL-620 was the kind gift of Rhodia Inc., West Point GA. All mice were dosed from PND51 to PND65. All treatments were administered by gavage, the morning of 14 consecutive days. Propiconazole treatment

groups received 10, 75 or 150 mg/kg/day. Fluconazole treatment groups received 2, 25 or 50 mg/kg/day. Triadimefon treatment groups received 5, 50 or 115 mg/kg/day. Myclobutanil treatment groups received 10, 75 or 150 mg/kg/day (Table 5). Following the final dosing, animals were transferred to a holding room in the surgery suite with similar environment conditions the night before terminal harvests to avoid stress of moving the day of harvest. At the end of stage one dosing (fluconazole and propiconazole treated groups), the mice were euthanized by IP injection of Nembutal (90 mg/kg body weight, 1.75:5 dilution in saline). Stage two mice (triadimefon and myclobutanil treatment groups) were euthanized using CO_2.

Adrenals, brain, left and right epididymus, liver, left and right testes, seminal vesicles, spleen and prostate were weighed. Right testis was placed in Bouin's fixative at 4ºC for 24 hours, transferred to 25% ethanol (EtOH) for 3 hours, to 50% EtOH for 3 hours, to 70% EtOH for 18 hours and repeated until yellow color disappears with wash, stored in 70% EtOH. The liver was fixed in 10% formalin at 4ºC, washed in EtOH and stored in 70% EtOH. Whole thyroid was fixed in 10% formalin at 4ºC, washed in EtOH and stored in 70% EtOH for histopathological evaluation. Several pieces of liver and left testis (~50 mg each) were snap-frozen in liquid nitrogen for RNA isolation. The remaining portions of liver were placed in cold KCl for microsomal preparation.

Analysis of covariance was used to detect effect of each treatment on organ weights after adjusting for body weight. Pairwise t-tests were performed to test for differences between each treatment and its control group on weights that had significant overall treatment effects ($p<0.05$).

Serum Hormone Levels

Testosterone serum levels were assayed using the Coat-a-count Total Testosterone Kit (Diagnostic Products Corp.). Radioimmunassay results were measured using the Wallac model 1272 automatic gamma counter and serum assays were run in duplicate. Luteinizing hormone (LH) levels were measured using a modified rat LH kit with Delfia supplies (PerkinElmer Life Sciences Inc.). Statistical analysis was performed using analysis of variance, measures with $p<0.05$ were considered significant from controls. For significant effects found, Student's t-test on least-squares means was used to identify differences between controls and individual treatment groups.

DNA Microarray Design

Microarrays were printed on UltraGAP Corning glass slides using the mouse genome oligonucleotide set v1.1 (Qiagen Inc.) by the DNA Microarray Facility at Duke University Medical Center (Durham, NC). This set includes 17,664 oligonucleotides and interrogates the expression of 16,473 genes. Probes were designed from UniGene Build Mm 83 and 89 maintained by the Mouse Reference Sequence Database, National Center of Biotechnology Information (NCBI).

RNA Isolation and Probe Labeling

Total RNA from testis and liver was isolated using TRI Reagent and the manufacturer's protocol (Molecular Research Center Inc., Cincinnati OH). Before the RNA was allowed for use in the microarray analysis, several quality criteria had to be met (Figure 6). Spectrophotometer readings comparing A260:A280 greater than 1.6 were subjected to

further rigorous testing using F191 and R644 HSP 70-1 primers for genomic DNA contamination inspection through polymerase chain reaction (PCR) checks. Once samples were clean of DNA, the samples were further analyzed using the Agilent BioAnalyzer to compare the 28S to 18S ribosomal RNA ratio for the integrity of the RNA samples. If the samples met these criteria, they were aliquoted into 10 or 15ug aliquots and stored in –80˚C. 15µg of total RNA from each tissue sample were used in the microarray hybridizations. CyScribe™ cDNA Post Labeling Kit was used to make fluorescent cDNA targets for glass slide microarray hybridization (Amersham Biosciences Corp., Piscataway, NJ). Total RNA from individual samples was reverse transcribed in the presence of an optimized nucleotide mix containing anchored oligo (dT) (deoxythymidine) to incorporate aminoallyl-dUTP (AA-dUTP) during cDNA synthesis. Amino allyl-modified cDNA targets were chemically labeled using Amersham's CyDye cyanine3 (Cy3) for the reference cDNA channel and cyanine (Cy5) for the experimental cDNA channel. Labeled cDNA probes were purified using Qiagen's QIAquick PCR purification kit. Reference RNA was a compilation of 40µg total RNA from each treated and control sample used in each microarray experiment. A total of 24 liver and 24 testis samples were analyzed.

Hybridization, Scanning and Quantitation

To study the underlying mechanism of conazole-mediated toxicity, liver samples from the high-dose treatment groups from each of the four conazoles were analyzed on DNA microarrays. Hybridizations were set up in four blocks, one sample from each treatment and control group (6 arrays). This generated 4 replicates per treatment, 6 slides per batch and 24 slides per tissue (figure 7). Cy5 (treatment) and Cy3 (reference) labeled cDNA targets were

combined and hybridized to microarrays 14 to 18 hours (overnight) at 42ºc. After hybridization, microarrays were washed, dried and scanned using the ScanArray 4000 (Perkin-Elmer Life Sciences, Boston, MA). Fluorescence intensities of the Cy5 and Cy3 channels were quantitated using ScanArray express software (Perkin-Elmer Life Sciences).

Data from ScanArray Express was converted to excel file format and read into SAS software. Intensity values were transformed to the log (base 2) scale. For each slide and channel, histograms were generated to show the distribution of the measures: mean spot intensity, median spot intensity, mean background intensity and median background intensity. These mean and median values were calculated for all pixels from each probe on the array. Additional histograms were plotted for each slide showing the distribution of the Cy5/Cy3 ratio and the background-(bak) adjusted ratio: (Cy5-bak)/(Cy3-bak).

Saturation of spots on the arrays was looked at, however no significant problems were presented. Maximum percent saturation was defined as greater than 25% saturated pixels/ spot.

The data were normalized by slide using an intensity dependent local regression procedure (SAS Proc Loess) (SAS, 1999). The model used is $\log_2(Cy5/Cy3) = \log_2((Cy5 \times Cy3)^{1/2}) + \varepsilon$, where ε is the regression value defined as the error. A smoothing parameter of 0.2 was used (fraction of the data considered as a local neighborhood). Residuals from this model were further used in the analysis for each gene. The log ratio intensity values of each slide were centered on zero across all neighborhoods of intensity (Figures 18 & 19).

To differentiate between genes that are expressed in a sample from those that are not expressed, an intensity-above-background cutoff value or multiple of background is generally used to give reliable intensity signals. In this study, plots were generated for each

slide to compare the gene probe intensities for the oligonucleotides to negative control and empty locations. From examination of these plots, each slide/spot type had a chosen cutoff where the empty spots were less than 90% and negative controls were less than 80% of the spots remaining. With these cutoff criteria, the oligo proportion of spots must be at least 30% or greater; otherwise the slide was excluded from analysis. From this step, each spot was defined for each label (oligo, negative control, empty), to be either present or absent.

Genes with intensity to background ratios above the threshold values were further analyzed based on their data consistency within the treatment groups. If the genes passed the following cutoff conditions, they were included for further analysis: (1) the gene was 'present' in all four Cy5 (experimental) spots of at least one treatment group; (2) the gene was 'present' in at least 3 of 4 treated spots of at least two treatment groups; (3) the gene was 'present' in at least 20 of the 24 Cy3 (reference) spots in the experiment.

For each gene, a two-way analysis of variance (ANOVA) was performed to look for effects of block and treatment. Within the ANOVA, four pairwise t-tests were calculated, one to test differences between each treatment (fluconazole, propiconazole, triadimefon and myclobutanil) and the appropriate control. Genes with a significant p-value ($p \leq 0.05$) for one or more of the four tests was selected for further analysis. For the purposes of this exploratory analysis, no adjustments were made for multiple comparisons.

Quantitative real time RT-PCR

Quantification of select gene transcripts was carried out by quantitative real time polymerase chain reaction (qRT-PCR). 1 μg each of DNase-treated RNA sample was reverse transcribed with random hexamer primers using Taqman Reverse Transcription

Reagents (Applied Biosystem (ABI) N8080234) according to manufacturer's instructions. cDNA from each reaction was diluted to a concentration of 10 ng/ul. Five microlitres (50ng) of each cDNA was used in each PCR reaction. For real time PCR reactions that used ABI primers/probes (cyp2c40, cyp2c55, cyp2b10, cyp24m cyp8b1), the cDNA was mixed with TaqMan Universal PCR Master Mix (ABI 4304437) and amplified according to manufacturer's instructions. The quantitation of Hsp 70-3, cyp17 and cyp19 were done using custom made primers and dual-labeled fluorescent probes synthesized by Integrated DNA Technologies (Coralville, IA) (Table 3). The PCR master mix for the custom made primers and probes contained 0.4mM dNTP, 0.24mM each forward and reverse primer, 0.025uM probe, 0.25 unit Taq DNA polymerase (Promega M1668) mixed with 0.25 units of Platinum Taq antibody (Invitrogen 10965-028), 10X Promega Taq buffer and MgCl (10mM MgCl for Hsp 70-3, 9mM MgCl for Cyp17, and 8mM MgCl for Cyp19). PCR cycling conditions were initial 95° denaturation for 3 minutes followed by 40 cycles of 95° for 15 seconds, 56° for 20 seconds and 72° for 10 seconds. Quantitative real time PCR was performed in a BioRad iCycler using the appropriate filter set. All samples were run in duplicate sets within the same plate for each assay. For each assay, the same RNA samples (4 per treatment group) were used as those in the microarray analysis. The threshold cycle for the duplicate sets were averaged and compared using the student's unpaired t-test between appropriate treatment and control groups. Differences were considered significant when $p \leq 0.05$. To determine fold change between treatment and control, the data was transformed from exponential to linear terms by using the means of each treatment and control group in the following equation: $2^{(\text{treatment mean} - \text{control mean})}$. The inverse of this value represents the fold change of the gene in the treatment group relative to control (Livak and Schmittgen, 2001).

RESULTS

Organ Weights

Liver weights increased following exposure to three of the four conazoles tested in this study. Fluconazole treatment increased liver weights at mid dose (25 mg/kg) and high dose (50 mg/kg) groups relative to control (by 9.05% and 12.97% of body weight respectively) (Figure 8 & Table 2). Propiconazole treatment increased liver weights at both the mid dose (75 mg/kg) and high dose (150 mg/kg) relative to the control (by 18.63% and 36.59% of body weight respectively). Myclobutanil treatment groups' increased liver weights at the mid dose group (75 mg/kg) relative to its control (by 13.88% of body weight). High dose myclobutanil showed evidence of a positive trend in weight increase ($p = 0.052$).

Other tissue weight increases included the seminal vesicle weight increase at mid dose (25 mg/kg) fluconazole (Figure 10) along with increased testis and spleen weights at high dose (150 mg/kg) propiconazole exposure (Figures 9 and 11). Mid dose (75 mg/kg) myclobutanil presented a trend in decreasing testis weights ($p = 0.052$). Triadimefon treatment groups did not show any significant changes in weights among the organs weighed.

Histopathology

The histopathology of the liver, thyroid and testis of each treatment group were observed for abnormalities. Conazole treated livers demonstrated positive trends in dose response to hypertrophy. Fluconazole treated livers displayed diffuse mild centrilobular hepatocyte hypertrophy with cytoplasmic granularity at mid dose (25 mg/kg) and diffuse moderate centrilobular to midzonal hepatocyte hypertrophy at high dose (50 mg/kg).

Propiconazole treated livers presented diffuse moderate centrilobular to midzonal hepatocyte hypertrophy at both mid (75 mg/kg) and high dose (150 mg/kg) (Figure 12). Myclobutanil mid dose treatment effects on the liver were mild centrilobular to midzonal hepatocyte hypertrophy, similar to the high dose treatment for this fungicide. Triadimefon, similar to the other treatments, did not show any abnormalities in the low dose treatment group relative to the controls. Triadimefon did, however, present livers with mild centrilobular to midzonal hepatocyte hypertrophy in both the mid and high dose treatment groups, just as myclobutanil did.

Thyroid sections did not show any significant difference between the treated and controls. Nor did testis histopathology reveal any effects in the treatment groups relative to controls (Figure 13).

Serum Hormone Levels

Testosterone (T) and Luteinizing Hormone (LH) serum levels were measured in the low, mid and high dose conazole treatment groups. No significant changes were found among the conazoles relative to the controls (Figure 14).

Microarray Analysis Procedure

Histograms created to show the distribution of the intensity values in terms of using the median or mean values of the intensity and background values showed the mean histograms better approximated a normal distribution than the median histograms, therefore the mean was chosen for analysis (Figure 15). Additional histograms representing the distributions of the Cy5/Cy3 ratios and background adjusted Cy5/Cy3 ratios were plotted.

The distribution of the background-adjusted ratios did not follow a normal distribution, in addition, negative and zero values occurred with these adjusted ratios. Analysis on the log scale becomes problematic with negative and zero values. The Cy5/Cy3 ratio without adjustment for background was chosen for use in analysis (Figure 16).

Saturation of spots were analyzed, maximum percent saturation was defined as greater than 25% saturated pixels per spot. Across the 48 slides and 2 channels, saturation was only 3% of the spots. For most slides the saturated pixel value was close to 0.3%. No adjustment was made for saturation.

Mean intensity to background ratio graphs were generated for each channel (Cy3 and Cy5) on each slide to compare the gene probe intensities for the oligonucleotides to negative controls and empty locations (signal to background ratio values). Comparison of signal to background ratios (S/B) for each label (gene specific oligo spots, negative control and empty locations) was used to determine the threshold value for each microarray on an individual basis (Figure 17). Threshold value represents local background intensity of each spot and the nonspecific binding for each spot. Spots that met or exceeded the threshold value were defined as 'present'. Intensity threshold values identified gene specific oligo spots that were 'present' or 'absent'. Threshold values were set for each channel, Cy3 and Cy5, of each array. Gene-specific oligo spots had to remain 30% or greater than the threshold value whilst negative controls were less than 20% and empty locations less than 10% of the threshold values. Based on these criteria, threshold values ranged from 1.2 to 6.5 with the majority of threshold values settling around 2.0. From examination of these plots, only 2 slides were excluded from the analysis. This analysis left 10,266 genes in the liver and 11,317 in the testis for further analysis.

ANOVA and pairwise t-tests were carried out to define effects of block and treatment identifying a total of 3,187 genes from the liver data and 2,346 genes from the testis data as differentially expressed.

Gene Expression Profiles in Liver and Testis

In the adult mouse liver, fluconazole differentially expressed 515 genes, increased the expression of 111 genes and decreased the expression of 404 genes ($p \leq 0.05$). Propiconazole differentially expressed 420 genes, increasing 248 and decreasing expression of 172 genes. Myclobutanil differentially expressed 505 genes, increasing 136 and decreasing expression of 369 genes and triadimefon differentially expressed 983 genes, increasing 590 and decreasing expression of 393 genes, relative to comparative controls ($p \leq 0.05$) (Table 4).

Genes altered by conazole exposure in the liver included 15 CYP genes (Table 10). Four Cyp gene profiles were differentially expressed in the same manner by more than one conazole, CYP 2c40 (suppressed by fluconazole, propiconazole and myclobutanil), CYP 2c55 (induced by propiconazole, myclobutanil and triadimefon), CYP 2b10 (induced by fluconazole and propiconazole) and CYP 24 (induced by propiconazole and triadimefon). Other CYP genes: 2c29, 2j5 and 2j9 were differentially expressed by more than one conazole, however their expression profiles differed by direction of induction or suppression. Several additional genes associated with cancer, steroidogenesis and oxidative stress displayed significant deviations in gene expression profiles relative to controls as well (Tables 12,13 & 14).

Five genes or cDNAs were differentially expressed following exposure to all three of the agricultural conazoles in the liver. Phosphomannomutase 2 (increased by propiconazole; decreased by myclobutanil and triadimefon); carboxylesterase 2 (Ces2) (increased by all three conazoles); two RIKEN cDNAs with similarity to oxidoreductases (both increased by all three conazoles); and a RIKEN cDNA of unknown function (increased by propiconazole; decreased by myclobutanil and triadimefon).

In the conazole-treated testis, fluconazole differentially expressed 492 genes, increasing the expression of 223 and decreasing the expression of 269 genes. Propiconazole differentially expressed 229 genes, increasing 108 and decreasing the expression of 121 genes relative to control ($p \leq 0.05$). Myclobutanil differentially expressed 623 genes, increasing 184 and decreasing the expression of 439 genes and triadimefon differentially expressed 278 genes, increasing 122 and decreasing the expression of 156 genes, relative to controls ($p \leq 0.05$) (Table 4).

Following conazole exposure in the testis, expression of 3 CYP genes were altered relative to controls (Table 16). Expression of Cyps 2b9 and 24 was affected in the same manner by more than one conazole (propiconazole and myclobutanil induced CYP24, myclobutanil and triadimefon induced CYP2b9). Cyp 8b1 gene expression was suppressed by fluconazole.

Several cancer-related genes (met and fyn proto-oncogenes and RAB3B) were differentially expressed in the testis; however, no common genes were affected between any of the four conazoles (Table 19). Several other genes associated with xenobiotic metabolism, steroidogenesis, spermatogenesis and oxidative stress were also identified as genes whose expression was altered by conazole exposure in this study (Tables 17,18 & 20).

Comparison of gene expression profiles between the two tissues identified seven genes differentially expressed in both tissues (liver and testis) (Table 9). CYP 8b1 decreased in triadimefon treated liver and fluconazole treated testis. Cyp24 increased in propiconazole and triadimefon treated livers as well as the propiconazole and myclobutanil treated testes. A similar pattern of differential gene expression between tissues suggests these CYPs have an important function in both the liver and testis upon exposure to conazoles. Genes associated with xenobiotic metabolism, steroidogenesis and oxidative stress were similarly differentially expressed between the two tissues albeit the patterns in expression, whether increased or decreased were not identical between the tissues.

Quantitative real time RT-PCR

To validate microarray results in this study, genes showing altered gene expression profiles were selected for analysis. CYPs, testis, steroidogenesis and oxidative stress related genes were chosen (Tables 6 and 7). Four individual RNA samples from each high dose treatment group were reverse transcribed once and divided among the different PCR reactions to ensure equivalent cDNA populations were tested in each assay for each sample. Tables 5 & 6 show results using the qRT-PCR method and significant changes in gene transcript levels between controls and treatment groups. Both liver and testis results demonstrate some similar findings in the microarray analysis with exception of a few additional findings in the qRT-PCR method. Fold changes for liver Cyp2c55 expression by qRT-PCR are considerably higher than the microarray results. In addition to finding similar treatment effects by the same conazoles, qRT-PCR found fluconazole to increase expression of Cyp2c55. (Fluconazole induced Cyp2c55 gene expression by 1.5 fold in the microarray

analysis but the difference was not significant from the control.). Relative to the microarray results; qRT-PCR results demonstrated there were changes in several of the gene transcript levels measured, strengthening the microarray results.

DISCUSSION:

In this study using adult male mice, we monitored organ weight, histology, serum hormone levels, hepatic CYP450 activities, and gene expression by DNA microarray and qRT-PCR to assess the effects of conazole exposure in the liver and testis. The goal of this study was to generate data and hypotheses concerning the modes of action for the toxicities of the various conazoles.

Effects on organ weights, histology and hepatic P450 activities.

Organization of the liver is structured by hexagonal shaped lobules, centered on hepatic veins. At each corner of the lobule there is a portal vein importing blood from the gastrointestinal tract, hepatic artery supplying blood from central circulation, and a bile duct. Each lobule of the liver is sectioned into three zones, the first zone circumferences the portal ducts, where hepatocytes first receive incoming blood and its high concentrations of oxygen, nutrients, hormones and xenobiotic compounds. The third zone is referred to as the centrilobular portion of each lobule; these hepatocytes receive less oxygenated blood and greater concentrations of metabolites however they also contain the greatest concentration of cytochrome P450 enzymes. Hepatocytes between the portal ducts and central veins are referred to as midzonal hepatocytes (Hodgson and Smart, 2001). Greater concentrations of cytochrome P450 enzymes in the centrilobular region set the stage for greater xenobiotic metabolism and predispose the hepatocytes to greater susceptibility for toxic damage.

Increased liver weights in fluconazole and propiconazole treated mice correlated with histopathological lesions in livers from the same treatment groups. The diffuse centrilobular and midzonal hepatocyte hypertrophy suggests increased enzymatic activity in the liver. In

response to chemical injury, cells respond by increasing enzymes necessary to metabolize foreign compounds. The zonation of damage, common localization of CYP450s in the liver and hypertrophy of these cells suggests there is an increase in CYP450 enzyme production. Myclobutanil liver weights were slightly elevated at mid-dose (75mg/kg bw); which mid-dose histology results echoed with mild centrilobular to midzonal hepatocyte hypertrophy compared to controls. Triadimefon liver weights were not significantly altered however, the histology results indicated mild hepatocytic hypertrophy similar to the myclobutanil treated animals.

Increased hepatic CYP450 activity levels resulted in increased alkoxyresorufin O-dealkylation (AROD) metabolism (see appendix). Fluconazole and myclobutanil induced Benzyloxyresorufin (BROD), ethoxyresorufin (EROD), methoxyresorufin (MROD) and pentoxyresorufin (PROD) metabolism. Propiconazole induced BROD, MROD and PROD activities, and triadimefon induced BROD and PROD activities. Fluconazole was the most potent CYP450 inducer among the four conazoles.

The hepatocyte hypertrophy, increased liver weight and multiple induction of AROD activities suggests a possible common mode of conazole toxicity in the liver through increased CYP450 and subsequent metabolism of the different conazoles for clearance. The increased demand on the hepatocytes for metabolism of conazoles may not only induce increased production of CYP enzymes but also overload the cell's ability to protect and repair itself against conazole exposure. Suppressed regulation of normal cell function increases hepatocyte susceptibility to cell cycle and DNA replication dysfunction.

Results from this study correlate with previous work on these four conazoles, indicative of similar effects in the liver. However, longer-term studies have shown that

propiconazole and triadimefon also produce tumors in mice, while fluconazole and myclobutanil do not. In this short-term study, myclobutanil and fluconazole increased liver weights, caused mild to diffuse hepatocytic hypertrophy, increased expression of several CYP genes and increased various AROD activities in the liver – very similar to triadimefon and propiconazole. This discordance of effects and outcomes indicates mechanisms of which liver tumor formation occurs are not yet understood. Further analysis beyond weight changes, CYP activity and histology are needed to identify carcinogenic conazoles.

Organ weight changes in the testis among the different conazoles did not show a common pattern of effects. There was a significant increase in testis weight at high dose propiconazole, but no other conazoles caused a consistent, dose-responsive change in testis weight. Testis histology also did not yield any definitive findings among the different conazole treatment dose groups compared to controls. This could be due to the doses used, the duration of exposure, and the resistance of the adult mouse testis o conazole effects. The average length of time for the development of spermatogonia to spermatozoa takes 34.5 days in the mouse, the spermatogonial stages last 7 days, meiosis lasts 13 days and spermiogenesis up to 14 days (Russell et al., 1990). Dosing began at PND51, around the time the first spermatozoa have developed. It is possible, and likely, that a longer exposure period would have recreated effects similar to what has been reported in the two-year cancer bioassays and multigeneration reproductive tests, especially for myclobutanil. However, we chose the 14 day time-point to balance the opportunity for shorter-term effects (e.g. gene expression, CYP enzyme activity) with longer-term effects on organ weights and histology. It is known that fluconazole, propiconazole and triadimefon have the ability to inhibit steroidogenic CYPs such as CYP19 (aromatase) (Paulus et al., 1994, Sanderson et al., 2002, Vingaarrd, 2000,

Nitta et al., 1993). Aromatase is the rate-limiting enzyme responsible for the conversion of androgens to estrogens and it has been proven that estrogens are required for normal spermatid maturation (Nitta et al., 1993, Shetty et al., 1998). If dosing for this study had been extended longer, it may have been possible that some effects stemming from disrupted steroidogenesis would have been observed.

Differential Gene Expression in conazole-treated liver and testis in vivo.

In order to broaden our understanding of the molecular effects of conazoles in target organs, and correlate the effects with conazole toxicities, liver and testis RNAs from conazole-treated mice were analyzed on DNA microarrays. Using the parameters described for microarray analysis, hundreds of genes were differentially expressed in both tissues in response to conazole exposure. These differentially expressed genes were divided into various subsets based on similarities in gene expression between conazoles, tissues or biological functions.

Propiconazole are triadimefon have been classified as carcinogenic compounds, producing tumors in mice and rat models (EPA, 1999, EPA, 1996). Of the genes differentially expressed by propiconazole (420) or triadimefon (983), 45 of those genes were modified in their gene expression profiles solely by these two conazoles. Several of these genes have not yet been identified by their biological function, of the genes that have, their functions range from vitamin D_3 metabolism (Cyp24) to cell adhesion (protocadherins gamma 3).

Multigenerational reproductive studies have shown that myclobutanil causes effects in the male rat reproductive tract; injuries include testis atrophy, reduced testis weights and

epididymus necrosis (EPA, 2000). These relatively low-dose effects are unique to myclobutanil, as compared to the other conazoles in this study. Over 500 genes were differentially expressed by myclobutanil alone. Focusing on the 86 genes significantly different from controls with a p-value of 0.01 or less, biological processes range from spermatogenesis (Azi1) to zona pellucida binding (AS-A) and apoptosis (Fn14).

These unique subsets of genes modulated by either the two liver tumor-inducing conazoles (propiconazole and triadimefon) or the testicular toxicant myclobutanil may provide insight into the tissue-specific effects and diverse outcomes. The differential gene expression patterns for propiconazole and triadimefon in the liver, and myclobutanil in the testis suggests there is not just one biological pathway affected by these conazoles. These profiles suggest that a number of different cellular processes respond to the exposure and effects of these conazoles.

Cytochrome P450 gene expression

In the liver, twelve Cyp genes were differentially expressed relative to controls, and expression of four of these Cyp genes was affected by two or more conazoles. In the testis, three Cyp genes were differentially expressed relative to controls.

One of the conazole-affected Cyp genes was CYP2c40, for which expression was decreased in the liver by fluconazole, myclobutanil and propiconazole. CYP2c40 is a member of the CYP2C family, which is involved in inactivating exogenous substrates and in arachidonic acid metabolism. In some cases though, CYP2Cs can actually activate xenobiotics (Lewis 2001). CYP2c40 is primarily expressed in the liver, kidney, intestine and brain of mice (Roman 2002, Luo et al., 1998). CYP2C enzymes metabolize arachidonic acid

(AA) to epoxyeicosatrienoic acids (EETs) (potent vasodilators). Several other antimycotics such as ketoconazole and miconazole also selectively inhibit epoxygenase activity, blocking the metabolism of AA to EETs (Roman 2002). It appears these antimycotics bind to the heme of CYPs, blocking substrate binding to the CYP and subsequent substrate metabolism. Evidence suggests CYP2c40 plays an important role in hepatic as well as extrahepatic physiology, including modulation of fluid and electrolyte transport, vascular tone, release of neuropeptides and xenobiotic metabolism (Luo et al., 1998). In this study, Cyp2c40 expression was suppressed by three of the four conazoles, how this might relate to epoxygenase inhibition remains to be determined.

Another member of the CYP2C family, CYP2c55, had increased gene expression in the liver by all three agricultural conazoles (myclobutanil, propiconazole and triadimefon). The fold-increase in expression of CYP2c55 was greater in the liver by all three conazoles than for any other gene, suggesting that this monooxygenase enzyme is extremely important in metabolism of all three conazoles. Alternatively, it might be that increased Cyp2c55 expression was in response to enzymatic inhibition. In future studies, it will be critical to understand the relationship between Cyp gene expression and enzyme activity in response to conazoles. If CYP2c55 enzymatic activity also increased, it seems critical to understand what role it plays in conazole metabolism and toxicity.

Expressions of two other Cyps were altered by conazoles in both liver and testis. Cyp8b1 expression was suppressed by triadimefon in the liver and by fluconazole in the testis. CYP8b1 is a sterol 12 alpha-hydroxylase microsomal enzyme involved in the synthesis of bile acids. The synthesis and excretion of bile acids is a major pathway of cholesterol catabolism in mammals. Cholesterol conversion into hydrophilic and readily excreted bile

acid is an important pathway for the elimination of cholesterol. Bile acid synthesis is under tight regulation through classic feedback mechanisms, ensuring sufficient catabolization of cholesterol and adequate emulsification of dietary cholesterol in the intestine (Li-Hawkins et al., 2002). An increase in bile acids will decrease Cyp 8b1 and Cyp 7a1 (7α-hydroxylase) transcription to prevent further synthesis of bile acids (Yang et al., 2002). CYP8b1 catalyzes the conversion of CYP7a1 from 7α-hydroxy-4-cholesten-3-one to 7α, 12α-dihydroxy-4-cholesten-3-one; ratio of these acids determines the level of cholic acid to chenodeoxycholic acid. The ratio of these two acids determines the level of cholesterol saturation in bile (Hunt et al., 2000). Additionally, the expression of Cyp7a1 will increase when cholesterol accumulates in the liver. As part of this negative feedback mechanism, CYP8b1 will synthesize cholate, a primary bile acid that inhibits the activation of CYP7a1 (Li-Hawkins et al., 2002). Thus, decreased expression of Cyp8b1, as observed in liver with triadimefon, could decrease cholate synthesis, increasing cholesterol saturation of the bile acid pool. A decrease in the levels of CYP8b1 will disrupt the regulation of CYP7a1 conversion of cholesterol to bile acid, allowing increased bile acid production and decreased levels of cholesterol in the liver.

Expression of CYP8b1 in the testis has been detected from PND11 onward in mice (Choudhary et al., 2003), coincident with the appearance of meiotic spermatocytes. Cyp8b1 expression levels are low relative to other CYPs in the testis, and little is known about CYP8b1 function in the testis. CYP8b1 expression in the liver is regulated by thyroid hormone - thyroidectomy in rats produces a substantial increase in CYP8b1 activity, and CYP8b1 mRNA levels are promptly reduced with T_4 treatment (Andersson et al., 1999). There was a slight (1.2 fold) increase in thyroid hormone receptor expression in the testis.

This may have resulted in increased responsiveness to thyroid hormone, and produced the decrease in CYP8b1 expression in testis following fluconazole exposure.

Cyp24 was the second Cyp gene differentially expressed in both the liver and testis. Both propiconazole and triadimefon in the liver, and myclobutanil and propiconazole in the testis induced Cyp24 expression. This increased expression in the liver by propiconazole and triadimefon could be related to the ability of these conazoles to cause liver tumors. Normally, Cyp24 is expressed at low levels in the adult mouse liver relative to other tissues measured (e.g. kidney and brain) (Choudhary et al, 2003), and our qRT-PCR work was not able to detect liver Cyp24 levels. Increased expression of Cyp24 by propiconazole and myclobutanil in the testis also highlights this gene, though its biological function in the testis is unknown. Cyp24 (vitamin D-24-hydroxylase) is a mitochondrial hydroxylase that degrades and deactivates 25-hydroxyvitamin D_3 and 1α,25-dihydroxyvitamin D_3 to 24,25-dihydroxyvitamin D_3 and 1,24,25-trihydroxyvitamin D_3, respectively (Akeno et al., 1997). The active form of vitamin D_3 plays an important role in calcium homeostasis, and is an inducer of cell differentiation in a variety of normal and malignant cell types. The vitamin D receptor is not only found in classical vitamin D responsive organs like the kidney and bone, but also in several cancer cell lines (Halline et al., 1994). 1α,25-dihydroxyvitamin D_3's growth inhibiting and differentiation-inducing effects are beneficial to tumor suppression (Halline et al., 1994). In our study, increased expression of Cyp24 suggests there was a subsequent deactivation of 25-hydroxyvitamin D_3 and 1α,25-dihydroxyvitamin D_3, suppressing the effects of vitamin D_3 in normal calcium balance and cell differentiation. Increased expression levels of CYP24 have also been found in prostatic cancer cells (Farhan and Cross, 2002). The fact that Cyp24 expression was possibly increased in liver by the

carcinogenic conazoles and by myclobutanil in the testis suggests CYP24 might play a role in the formation of liver tumors or reproductive effects.

Conazole effects on oxidative stress related gene expression

Numerous proteins are involved in protecting cells from reactive oxygen species (ROS) formed during regular cellular and xenobiotic metabolism. Glutathione (GSH) protects cells from oxidative stress by binding electrophiles, neutralizing and inactivating electrophilic effects on cellular proteins and DNA. GSH also serves as a cofactor in reactions against chemical intermediates such as the GSH redox cycle, which requires NADPH as a cofactor (Hodgson and Smart, 2001). When concentrations of GSH decrease in the cell, decreases in NADPH levels and induction of apoptosis occur (Pierce et al., 2000, Hancock et al., 2001, Lavrentiadou et al, 2001). Binding of nucleophilic GSH to toxic intermediate electrophiles requires Glutathione S-transferase (GST). Glutathione S-transferases (Gst) are phase II conjugation enzymes, responsible for adding side groups to metabolized xenobiotics to aid in increased water solubility and clearance of the compounds. GST-alpha 2 (Yc2) is an isoenzyme that is not found in rats fed normal diets, and only in livers with preneoplastic nodules (Hayes et al, 1991). Decreased glutathione levels are also indicative of increased oxidative stress. Thus increased expression of GST Yc2 in the livers from propiconazole and triadimefon-treated mice suggests this particular GST may play a protective role in these livers perhaps in order to prevent tumor formation.

Oxidative stress increases levels of GST, glutathione peroxidase and heat shock proteins (HSP) (Raza et al., 2002). In addition, fluconazole selectively sensitizes mutated Gst genes, indicative of peroxide formation by fluconazole (Veal et al., 2002). GST, NADH

dehydrogenase, Glutathione peroxidase and HSPs were affected by several of the conazoles in this study. Several homodimers of GST were differentially expressed in the liver by the various conazoles, and increased expression of GST pi2 by propiconazole in the testis, suggesting GST plays a protective role against cell injury.

NADPH and NADH are necessary cofactors in the catalytic activity of CYP monooxygenation reactions. Increased levels of NADPH and NADH cofactors elevate levels of reactive oxygen species (ROS) formation and induction of lipid peroxidation in several cell types (Bondy and Naderi, 1994, Ohmori et al., 1993, Rashba-Step and Cederbaum, 1994). Several NADH dehydrogenases showed increased expression by conazoles in the liver and testis. Inhibition of NADH dehydrogenase occurs upon addition of antioxidants (Reyes et al., 1995). NADH dehydrogenase is an enzyme involved in the respiratory chain in mitochondria involved in ATP synthesis. Increased expression of NADH dehydrogenase by triadimefon in the liver implicates increased ATP synthesis, suggesting increased energy demands on the cells and consistent with the observed hypertrophy.

HSPs are involved in regulating protein folding and chaperone transport of proteins to the nucleus for target receptor binding. HSPs detect damaged proteins and protect cells from oxidative stress induced proteotoxicity (Liu et al., 1996, Su et al., 1999). Studies on the relationship between heat-shock gene expression and the severity of pathologic liver injury (and lipid peroxidation) have shown increased mRNA HSP70 levels in rats fed diets containing alcohol, although protein levels remained unchanged relative to controls (Nanji et al, 1995). The close relationship found in this study between increased oxidative stress and HSP70 mRNA, but not protein, suggested there may have been binding of HSP70 protein to damaged proteins, reducing the levels of HSP70 and inducing the expression of HSP70.

Alternatively, increased HSP70 expression may have been a cellular adaptive response to alcohol-induced oxidative stress (Nanji et al, 1995). HSP70-4 levels were decreased in fluconazole treated liver, and propiconazole treated testis. This pattern of differential gene expression suggests oxidative stress was not a main component of conazole toxicity in the liver and testis. Ferredoxin and ferritin, genes related to oxidative stress, were differentially expressed in the liver by triadimefon. Ferridoxin reductase transfers electrons from NADPH to CYPs via ferridoxin in mitochondria. DNA damage and ROS can induce ferridoxin reductase transcription and sensitize cells to ROS-mediated apoptosis (Liu et al., 1996). Triadimefon increased ferridoxin levels suggesting an increase in CYP activity and oxidative stress in the liver. Ferritin is the major form of iron storage in cells, release of stored ferritin is involved in lipid peroxidation, a major side effect of oxidative stress. Release of ferritin is mediated through superoxide-dependent reactions (Kukielka and Cederbaum, 1996). Triadimefon decreased expression of ferritin in the liver, suggesting a cellular protective mechanism preventing further release and availability of iron for lipid peroxidation reactions.

Conazole effects on cancer and cell cycle-related gene expression

Several cancer-related genes were differentially expressed among the four conazole-treated liver groups. T lymphoma oncogene gene expression was increased by fluconazole and propiconazole. The T lymphoma oncogene regulates T cell growth and differentiation, and increased expression indicates an immune response in the fluconazole and propiconazole-treated animals.

The majority of oncogenes differentially expressed were related to the Ras oncogene family, which function primarily in cell proliferation and regulating various steps of vesicular

traffic in eukaryotic cells. RAS-related genes are expressed during cell division and shut off when mitosis is complete. In general, RAB proteins are small GTPases involved in regulatory roles in intercompartmental vesicular transport and exocytosis, they have been found to be up regulated in many hepatocellular carcinoma cases (Lewin 2000, Barbosa et al., 1995, He et al., 2002). RAN proteins play several roles in DNA replication, RNA export and protein import as well as monitoring DNA synthesis before onset of mitosis. RAN protein activity appears to be regulated in the S phase of cell proliferation (Di Matteo et al., 1995). The Ras-related genes, Rab (1, 3c, 3d, 4a, 4b, 36), Rap (2b) and Ran were not expressed in any discernible pattern. Six Ras related genes were up regulated and three Ras related genes were down regulated in the liver following various conazole exposures. Given the number of Ras genes affected, it appears vesicular transport within hepatocytes are affected by conazole exposure.

Cell cycle-related genes affected include the protocadherins gamma subfamily c3 and beta 16, both members of the cadherin subfamily involved in calcium-dependent cell-cell adhesion. Research has shown levels of protocadherins significantly decreases in cancerous cells and that over-expression of protocadherins suppresses tumor formation in a nude mouse model (Okazaki et al., 2002). Increased expression of these same protocadherins in response to propiconazole and triadimefon suggests they may be a protective response in the liver.

Several additional genes were down regulated in livers from propiconazole and triadimefon-treated mice, one of which codes for the ATPase H+ transporting vacuolar proton pump. Without proper functioning of this proton pump, intracellular pH levels become acidic, which is a precursor for apoptosis (Gottlieb and Dosanjh, 1996). The other down-regulated gene was transthyretin (TTR), a plasma protein carrier known to bind with

both retinol (vitamin A) and thyroxine (T_4) for their transport into the liver. The liver is a major site of catabolism of TTR, which is taken up by hepatocytes through TTR-specific receptors. It's been shown that TTR is regulated by hepatocyte nuclear factor-3 (HNF-3 α, β and γ), HNF-6, AP-1 and C/EBPα, β and γ proteins (Vallet et al., 1995). Propiconazole increased AP-1 gene expression and triadimefon increased C/EBPβ gene expression. An increase in the expression of these transcription factors might potentiate an increase in the expression of TTR, but we observed the opposite in our study. It has also been shown, however, that when TTR is bound to T_4, there is a 20% increase in hepatocyte cell surface binding, suggesting TTR would be taken up by hepatocytes and degraded, thus promoting further transcription of the TTR protein. When TTR is complex bound to retinol and its retinol-binding protein, there is a 70% decrease in cell surface binding (Sousa and Saraiva, 2001). This decrease in hepatocyte uptake and increase in plasma concentrations of TTR may create a feedback loop to suppress further transcription of TTR. To test for this possible mechanism in future studies, T_4 levels would need to be measured.

Looking at the genes affected by the two liver-tumor inducing conazoles, three biological processes stand out: detoxification, tumor suppression, and tumor promotion. It appears there is a mix of responsive genes trying to protect the liver, and leading up to tumor formation. Characterizing these gene expression effects takes us one step closer to understanding the mechanisms of conazole toxicity in the liver.

Conazole effects on testicular function gene expression

Three Cyp genes and numerous other metabolic enzymes were differentially expressed in the testis in response to the four conazoles. These included GSTpi2, which was

increased by propiconazole treatment in the testis, similar to the various homodimers of GST in the liver.

Several genes known to be critical to testicular function were differentially expressed, including Feminization I homolog a (Fem1), which was decreased by myclobutanil. Fem1 is normally highly expressed in adult testis, involved in primarily in sex determination (Ventura-Holman et al, 1998). Tousled-like kinase 2 (Tlk) was decreased by propiconazole in the testis as well. Tlk is predominantly expressed in pachytene spermatocytes and round spermatids. Studies suggest Tlk plays a part in protein phosphorylations involved in regulation of spermatogenesis (Shalom and Don, 1999). Suppression of Tlk by propiconazole suggests conazoles may have an effect on normal spermatogenesis function.

Arylsulfatase A (AS-A) was differentially expressed in the testis by myclobutanil. AS-A is involved in the binding of sperm to the zona pellucida. This glycoprotein is a lysosomal enzyme, which plays a key role in the degradation of sulfated glycolipids, zona pellucida proteins 2 and 3, and the activation of the acrosome reaction during fertilization (Kreysing et al 1994, Tantibhedhyangkul et al 2002). Due to its promotion of sperm activation, the observed decrease in AS-A gene expression by myclobutanil may be indicative of a checkpoint for the spermatozoa. If the mature spermatozoa have not developed properly, this reduction in AS-A may prevent fertilization of abnormal spermatozoa and it's damaged DNA.

Another spermiogenesis related gene differentially expressed by myclobutanil was 5-azacytidine induced gene 1 (Azi1). Azi1 is an acrosomal protein with expression first detected in the pre-acrosomal region of pachytene spermatocytes. Azi1 has also been shown to regulate chromosomal segregation during meiosis (Aoto et al, 1995). Decreased levels of

Azi1 may play a protective role as a preventative to block damaged spermatogonia from developing into abnormal spermatozoa.

A number of cancer and cell cycle related genes were also affected by conazole treatment in the testis. RAD50 homolog gene expression was increased by myclobutanil, it functions in protein complexes central to metabolism of chromosome breaks and is essential to prevention of growth defects and cancer predisposition (Bender et al., 2002). Loss of RAD50 will produce stem cell failure in spermatogenic cells (Bender et al., 2002). Induction of RAD50 by myclobutanil in the testis suggests that myclobutanil may be disrupting normal DNA repair or recombination in the gametes.

Various genes were affected in the testis, ranging from CYPs to metabolic enzymes, cancer and cell cycle related genes. Despite the lack of common differential gene expression patterns among the four conazoles, several common mechanisms of cell protection (3β HSD induction) and survival against oxidative stress (GST, Cytochrome c oxidase) occur across the different conazole treatment groups.

Conazole effects on steroidogenesis related gene expression

Many enzymes are involved in the synthesis of steroids. The common precursor to all steroids is cholesterol, derived from lanosterol just as ergosterol is in the fungal cell membrane. CYP genes are the prominent source of enzymes involved in steroidogenesis, including CYP11a side chain cleavage and CYP19 aromatase. 17β-hydroxysteroid dehydrogenase (17β HSD) is another steroidogenic enzyme that catalyzes the reductive conversion of inactive androstenedione to biologically active testosterone. Multiple 17β HSD genes are differentially expressed in cancer cell lines, types 2 and 3 17β HSD are

expressed greater in malignant prostate tissue, yet types 1, 4 and 5 are not (Koh et al., 2002). 17β HSD levels are high in the liver, predominantly responsible for the inactivation of sex steroids from the blood circulation (Mustonen et al, 1997). 17β HSD types 1 and 3 predominantly catalyze the reductive reaction of androstenedione to testosterone and are preferentially located in the gonads. Types 2 and 4 preferentially catalyze the opposite reaction, thereby inactivating the sex steroids. 17β HSD type 5 has only recently been characterized and is found primarily in the liver, suggesting it plays a role in deactivating sex steroids as well (Mustonen et al, 1997). Triadimefon and myclobutanil differentially expressed several types of 17β HSD in the liver. Type 2 (decreased by triadimefon), 3 (decreased by myclobutanil) and type 4 (increased by triadimefon). These results correlate with those in Koh et al. suggesting triadimefon and myclobutanil are not carcinogenic in the liver. The decrease in these enzymes gene expression suggests there is a decrease in sex steroids reaching the liver.

3β HSD catalyzes the conversion of dihydroepiandrostenedione and pregnenolone to androstenedione and progesterone (respectively), precursors of gonadal steroids testosterone and estrogen; and adrenal steroids cortisol, corticosterone and aldosterone, respectively. 3β HSD activity is therefore essential for production of all steroid hormones and is found in all steroidogenic tissues (Bain et al, 1991). Additional work by Baine et al. has found 3β HSD activity in the liver as well. Myclobutanil decreased gene expression of 3β HSD in the liver and triadimefon increased 3β HSD in the testis (Tables 13 & 18). Increased expression of 3β HSD in the testis suggests there is an increased need for steroid metabolism in the testis due to conazole exposure.

qRT-PCR

The qRT-PCR results generally validated the microarray data on several gene expression changes. The decrease in liver Cyp2c40 expression by three of the four conazoles was confirmed by qRT-PCR, and a robust increase in liver Cyp 2c55 levels by all four conazoles was also detected. The microarrays did not detect the increase in Cyp 2c55 following fluconazole treatment detected by qRT-PCR. qRT-PCR indicated the fluconazole effects on Cyp2c55 transcript levels were lesser than the changes caused by the other three conazoles and perhaps the microarrays failed to detect these smaller changes. Both microarrays and qRT-PCR detected increased liver Cyp2b10 expression in propiconazole and fluconazole treatment groups, however the qRT-PCR findings were not statistically significant. qRT-PCR picked up other differences not found by microarray, such as the 2-fold decrease in liver Cyp2b10 levels by myclobutanil.

In the testis both qRT-PCR and microarray analysis detected changes in 3β HSD transcript levels. However, qRT-PCR indicated decreased 3β HSD by fluconazole, while microarrays indicated increased 3β HSD by myclobutanil.

The Cyp genes 8b1 and 24 were differentially expressed in both liver and testis, based on microarray results. Cyp24 was moderately elevated in the testis by propiconazole and myclobutanil according to the microarrays, but qRT-PCR detected a moderate decrease in testicular Cyp24 expression by fluconazole treatment only. More surprising, the same qRT-PCR primers and probe used for the testis samples was unable to detect Cyp24 expression in the liver, although, basal levels of Cyp24 in the liver are normally expressed at lower levels (Choudhary et al, 2003). This indicates that there may be a flaw in either the microarray probes, or the qRT-PCR assay for Cyp24. Cyp8b1 gene expression was decreased in the

testis by fluconazole and decreased by triadimefon in the liver according to microarray analyses. qRT-PCR results indicate a decrease in gene transcript levels of Cyp8b1 in fluconazole treated liver.

There was 67% agreement between the microarray and qRT-PCR results in the liver gene expression and gene transcript measurements and 80% agreement in the testis.

Summary

Traditional toxic end-points such as organ weights, histology and AROD assays were not able to discriminate between the conazoles that cause liver tumors or testis atrophy, and those that do not cause these outcomes. Thus there is a need for better approaches identifying adverse effects more closely linked to mode and mechanism of action. Differential gene expression unique to propiconazole and triadimefon in the liver, and myclobutanil in the testis, demonstrates there may be distinct gene expression patterns relating to specific toxicities of the different conazoles. Additional differential gene expression patterns common between the conazoles were found in the liver and testis, including genes related to stress response and the cell cycle. Common biological processes affected in the liver and testis by the conazoles in this study supports the hypothesis for possible common modes of action by the various conazoles.

Further work will be necessary to address the significance of these differentially expressed genes and their relationship to conazole toxicities of the liver and testis. These numerous genes represent possible links to understanding the modes of action for the various conazole toxicities. The methods and data from this study will be useful in future studies aimed at identifying modes and mechanisms of conazole toxicity in the developing rat

reproductive tract.

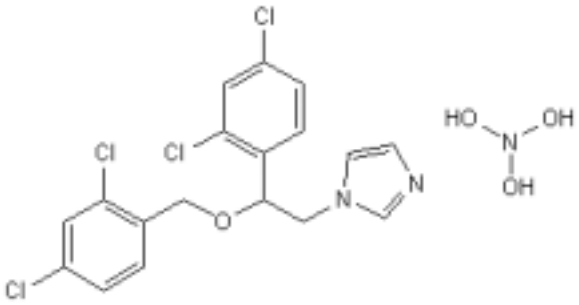

Miconazole nitrate

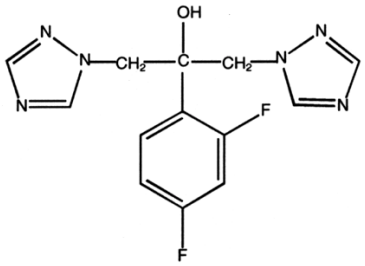

Fluconazole

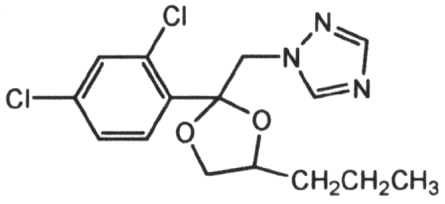

Propiconazole

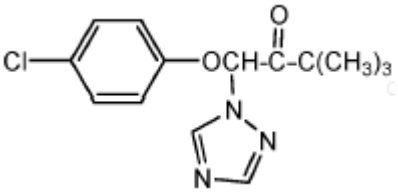

Myclobutanil

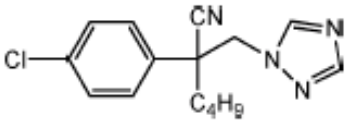

Triadimefon

Figure 1: Structures of 1,3 (miconazole nitrate) and 1,2,4-N substituted azole ring conazoles. Fluconazole (pharmaceutical), propiconazole, myclobutanil and triadimefon (agricultural use) are 1,2,4-triazole fungicides used in this study.

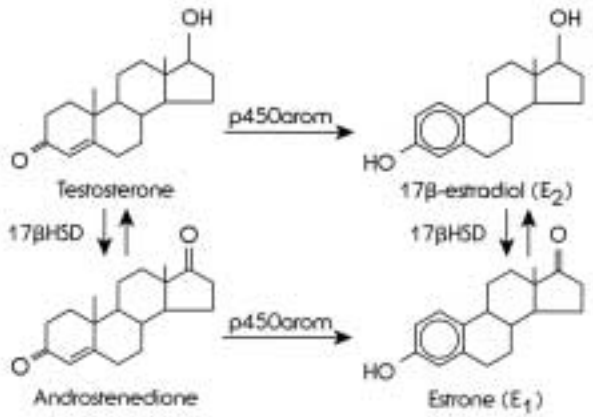

Figure 2: Role of Aromatase in steroidogenesis.

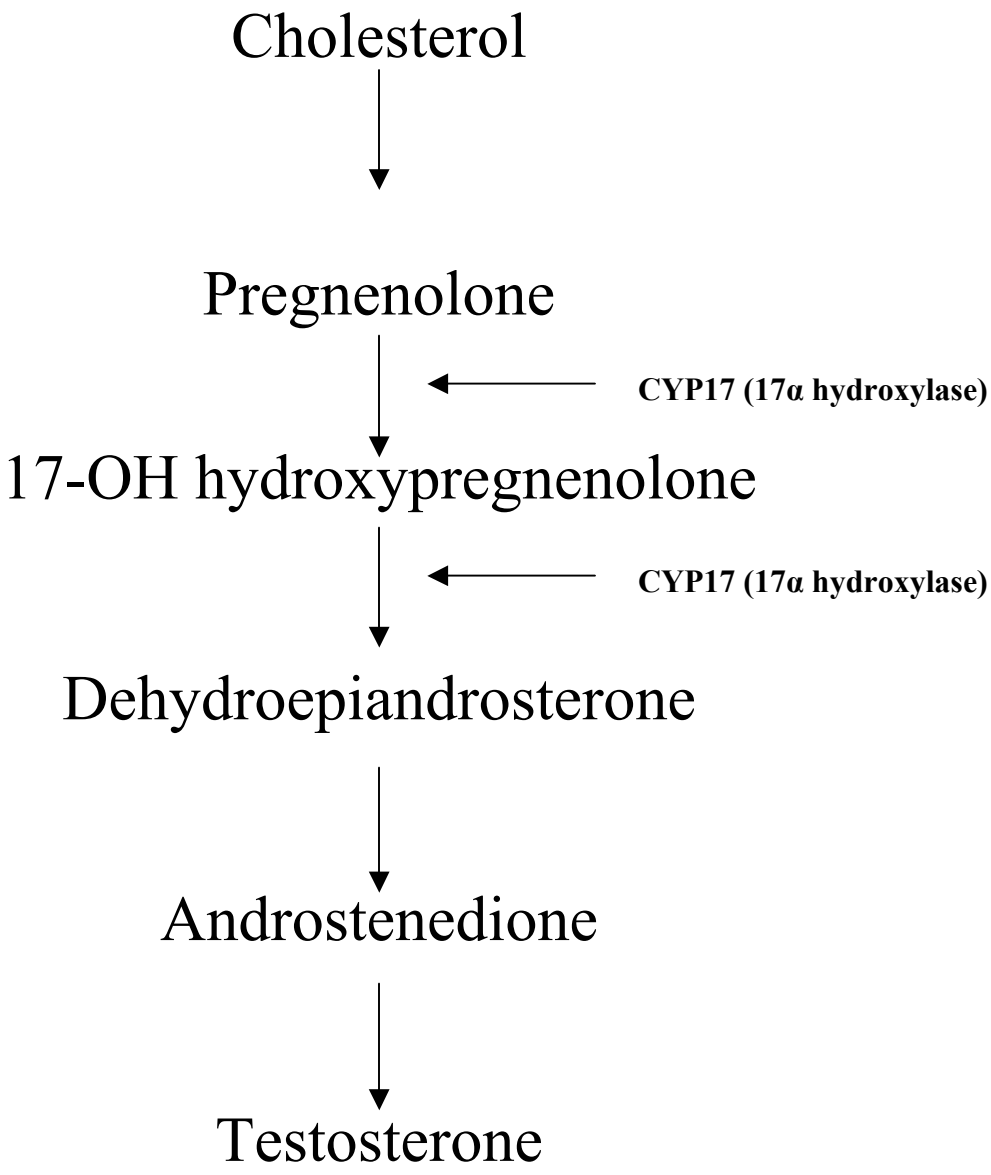

Figure 3: Role of CYP17 (17α hydroxylase) enzyme in the biosynthesis of steroids.

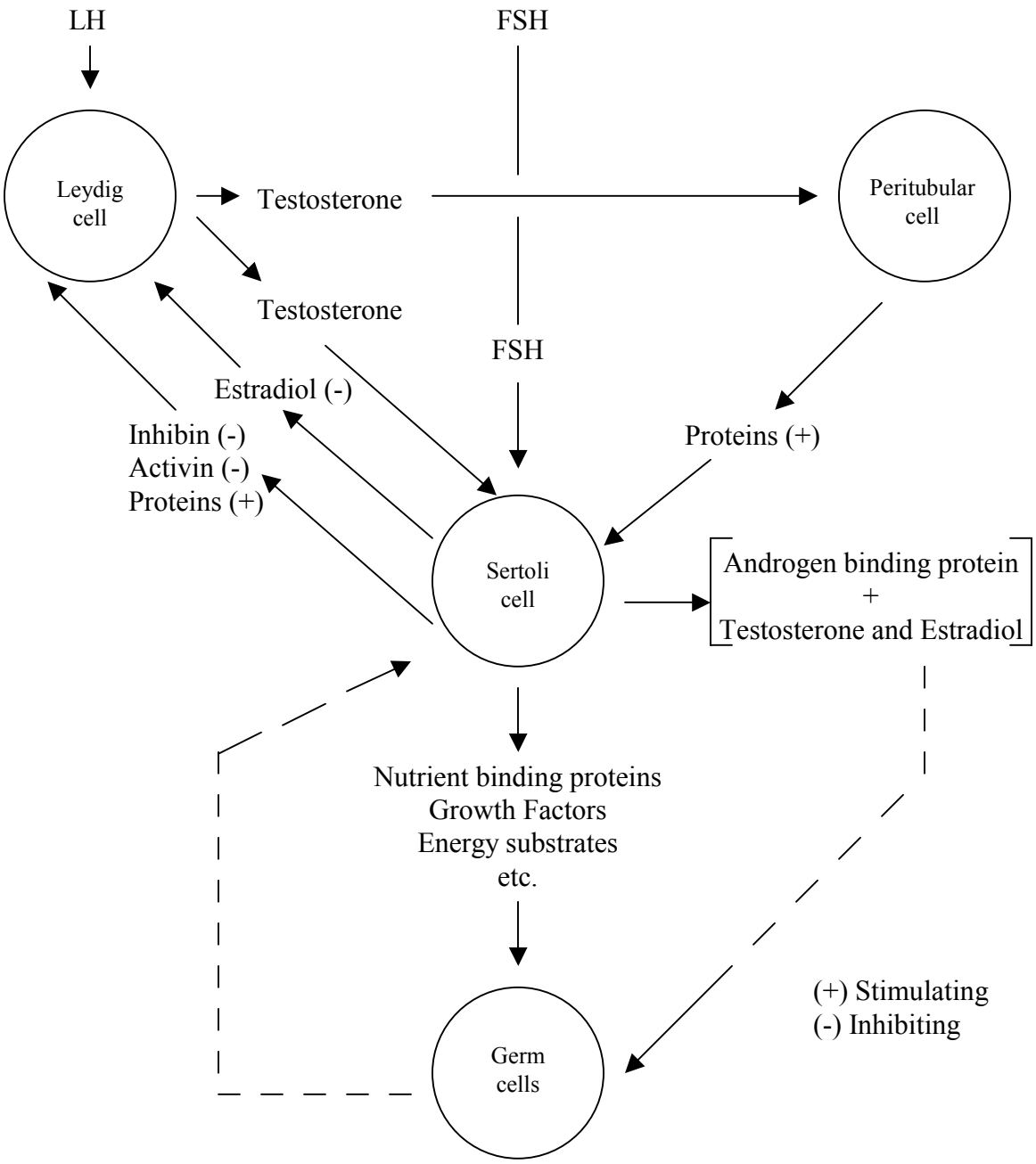

Figure 4: FSH and LH are important hormones in the hypothalamic-pituitary-gonadal axis that play key roles in testosterone production, sperm production and maturation.

Mouse Conazole Dosing Study

Experiment	Stage One			Stage Two		
Treatment Group	VCA**	Flu	Propi	VCB**	Myclo	Tri
Biological Replicates *						
low dose (NOAEL)	6	6	6	6	6	6
mid dose (LOAEL)	6	6	6	6	6	6
high dose (2x LOAEL)	6	6	6	6	6	6

Chemical	NOAEL (mg/kg/day)	LOAEL (mg/kg/day)	2xLOAEL (mg/kg/day)
Fluconazole	2	25	50
Propiconazole	10	75	150
Myclobutanil	10	75	150
Triadimefon	5	50	115

Figure 5: Experimental design set up for dosing. (VCA) Vehicle Control A, (Flu) Fluconazole (50 mg/kg), (Propi) Propiconazole (150 mg/kg), (VCB) Vehicle Control B, (Myclo) Myclobutanil (150 mg/kg), (Tri) Triadimefon (115 mg/kg).
* Mice were randomly assigned to different treatment groups with equal weight distribution.
** Vehicle Controls received Alkamuls EL-620.

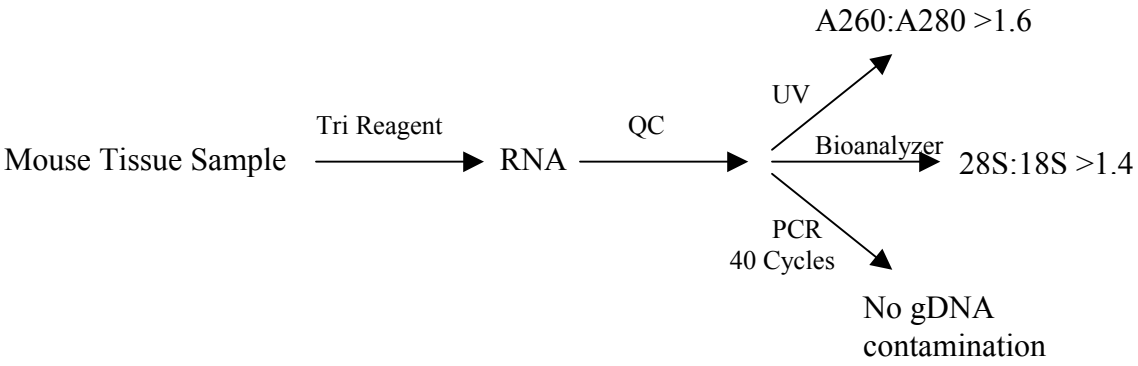

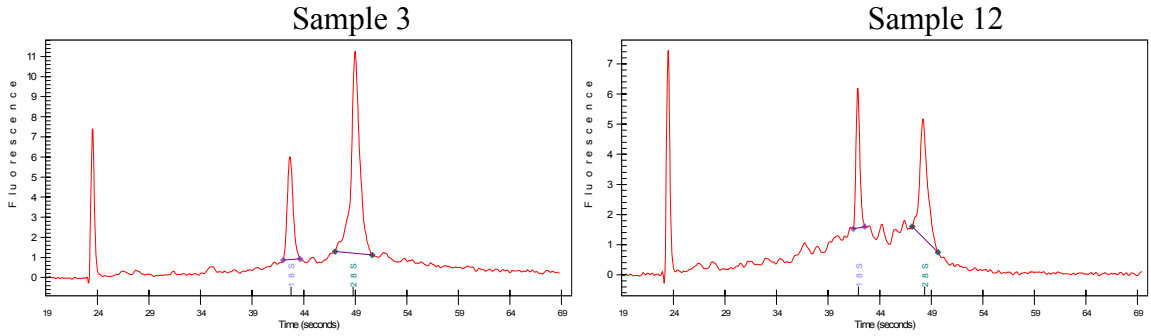

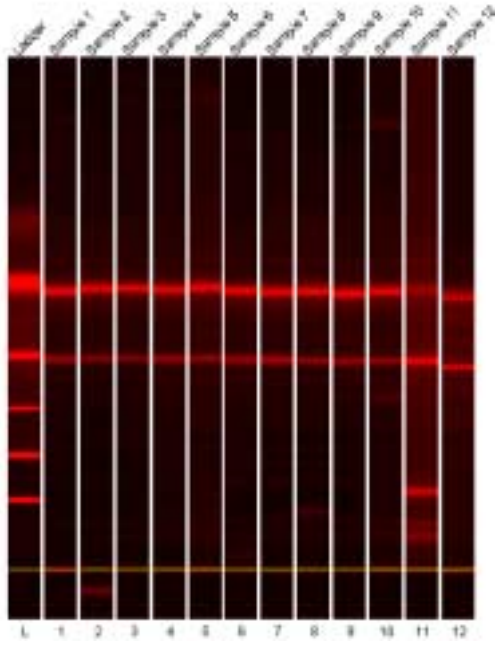

Sample 3 is a sample of good RNA that was used in the microarray analysis, sample 12 was refused and a new RNA sample was made from that tissue before continuing on for microarray analysis.

Figure 6: RNA isolation procedure and criteria that were met for quality microarray RNA. Samples that passed each of these quality criteria steps were used for reverse transcription before being hybridized to their respective microarrays.

Microarray Study Design

	Batch 1	Batch 2	Batch 3	Batch 4
Dose	high dose	high dose	high dose	high dose
Vehicle Control	VCA, VCB	VCA, VCB	VCA, VCB	VCA, VCB
Conazole	F, P, M, T	F, P, M, T	F, P, M, T	F, P, M, T

Figure 7: Microarray Study Design for hybridizing labeled cDNA probes to glass slide microarrays. Four RNA samples were run from each treatment and control group. One sample from each treatment group was run in each batch to decrease technical variation between batches. Each sample was run parallel with a reference RNA sample on each microarray for comparison between slides. A total of 24 microarrays were run for each target tissue. Vehicle control A (VCA), Vehicle control B (VCB), fluconazole (F), propiconazole (P), myclobutanil (M), triadimefon (T).

Labeling
Cy5: Individual liver RNAs
Cy3: Reference RNA (study specific, pooled)

Hybridization
- Hybridizations done in batches
- 1 Batch = 6 samples (one from each treatment group)
- Total of 4 batches (24 samples)

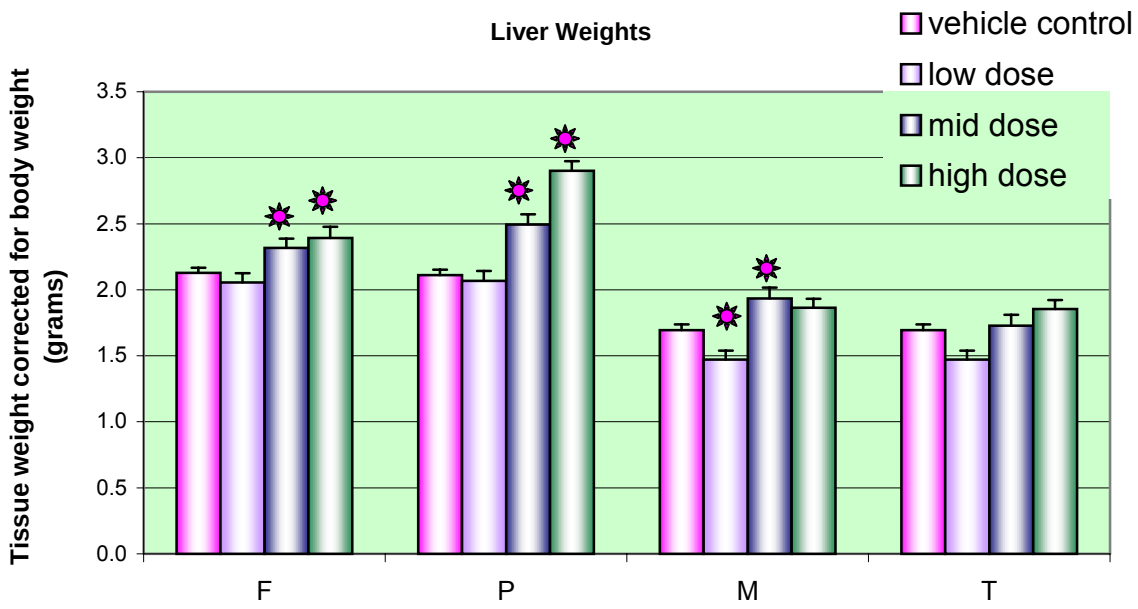

Figure 8: Analysis of Covariance of Conazole-treated Liver in Male CD1 Mice. (*) p-value < 0.05.

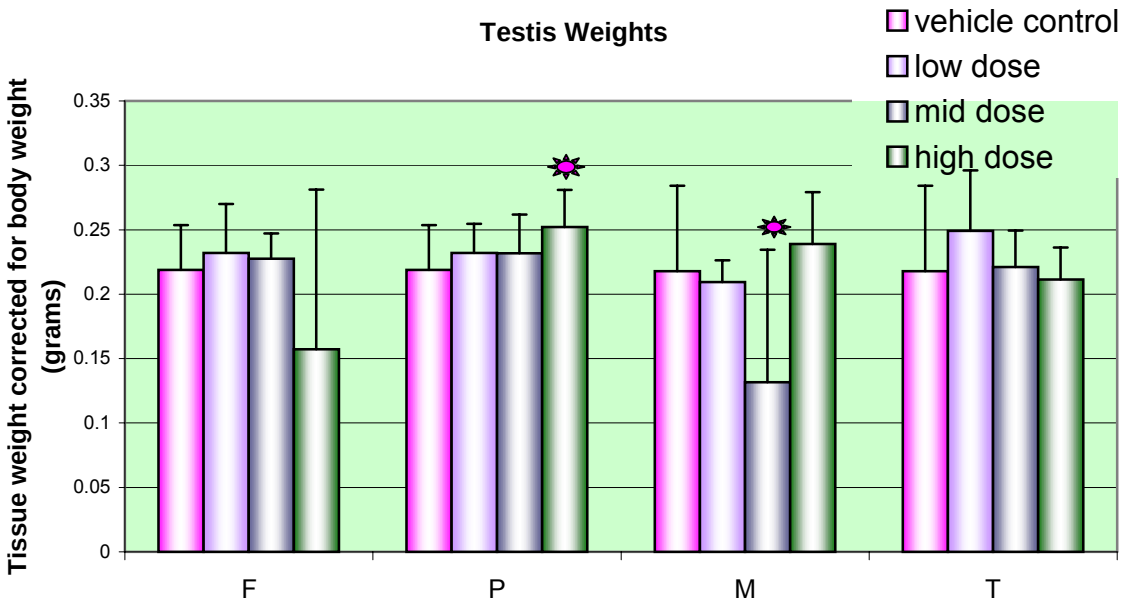

Figure 9: Analysis of Covariance of Conazole-treated Testis in Male CD1 Mice. (*) p-value < 0.05.

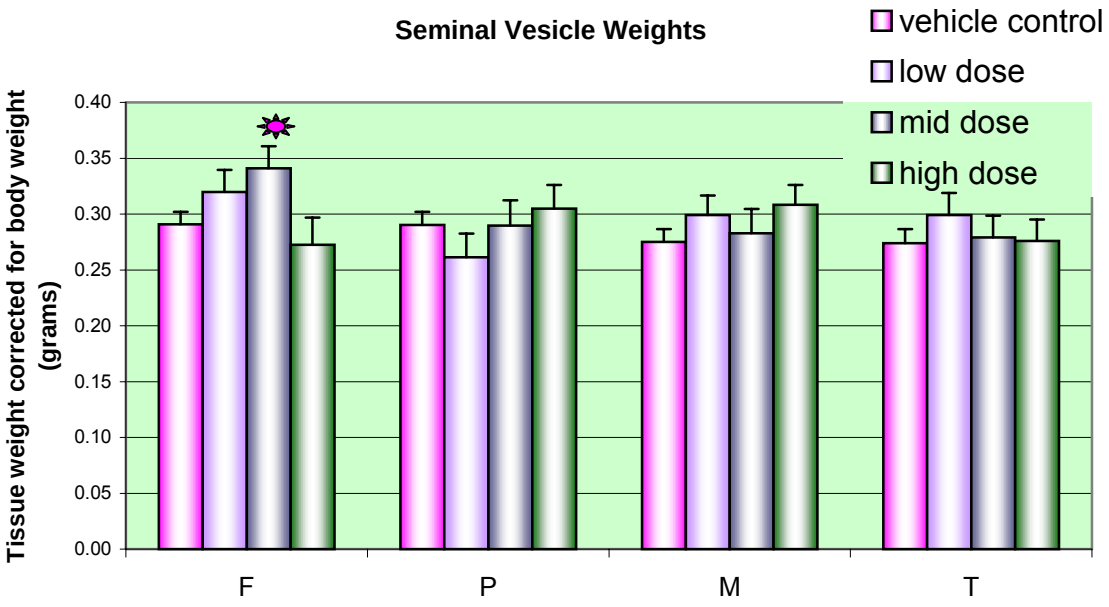

Figure 10: Analysis of Covariance of Conazole-treated Seminal Vesicle in Male CD1 Mice. (*) p-value < 0.05.

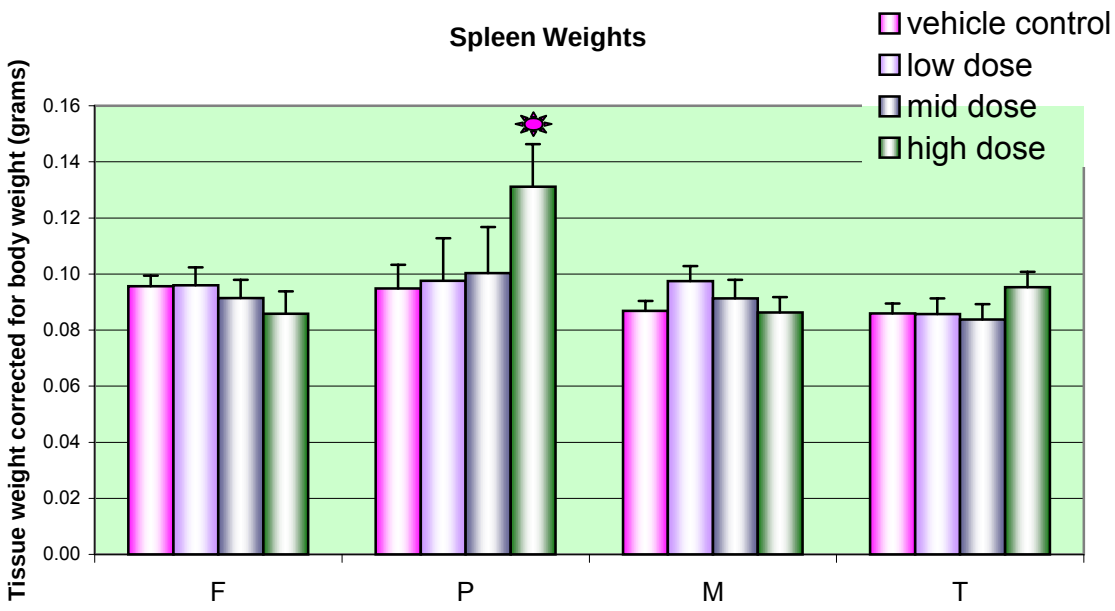

Figure 11: Analysis of Covariance of Conazole-treated Spleen in Male CD1 Mice. (*) p-value < 0.05.

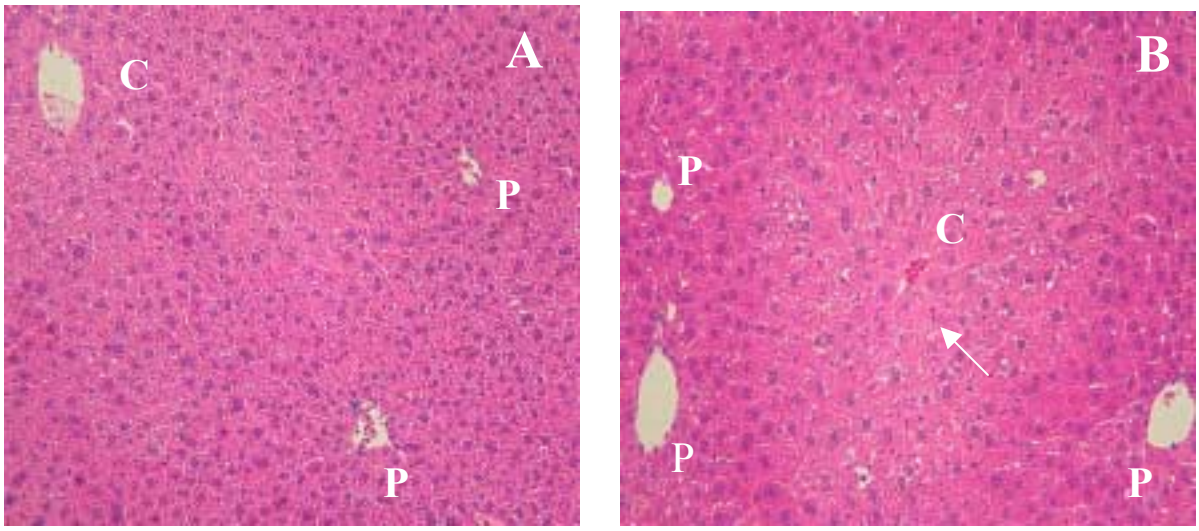

Figure 12: Histology of conazole-treated Male CD1 Mouse Liver. (A) Liver section from a control animal, showing normal hepatocyte conformation between the portal areas (P) and centrilobular veins (C). (B) Liver from high-dose propiconazole 150mg/kg treatment group with diffuse centrilobular hypertrophy (arrow). 20x magnification.

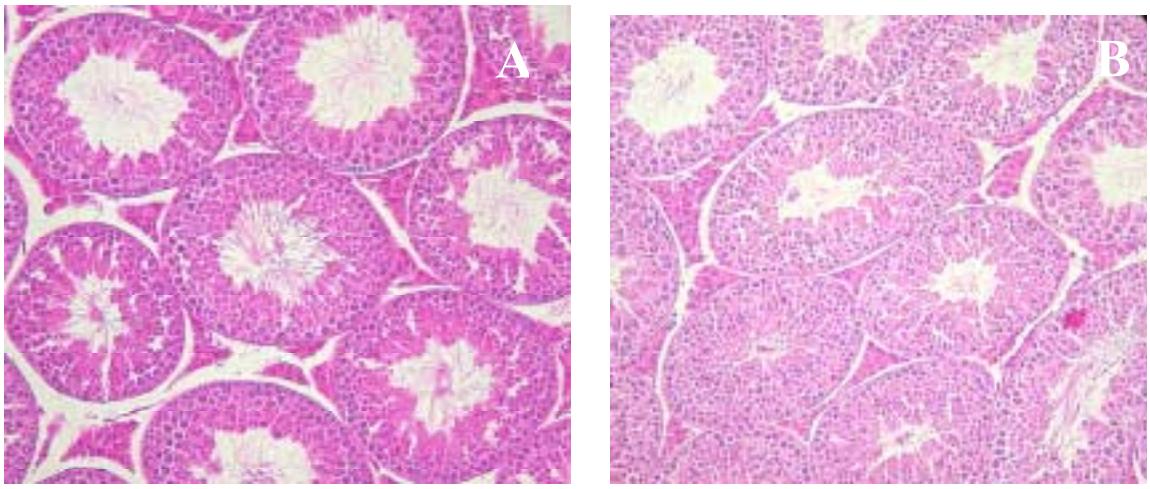

Figure 13: Histology of conazole-treated Male CD1 Mouse Testis. (A) Testis section from control animal, (B) high dose treated propiconazole testis section. No significant findings were found between the different doses. 20x magnification.

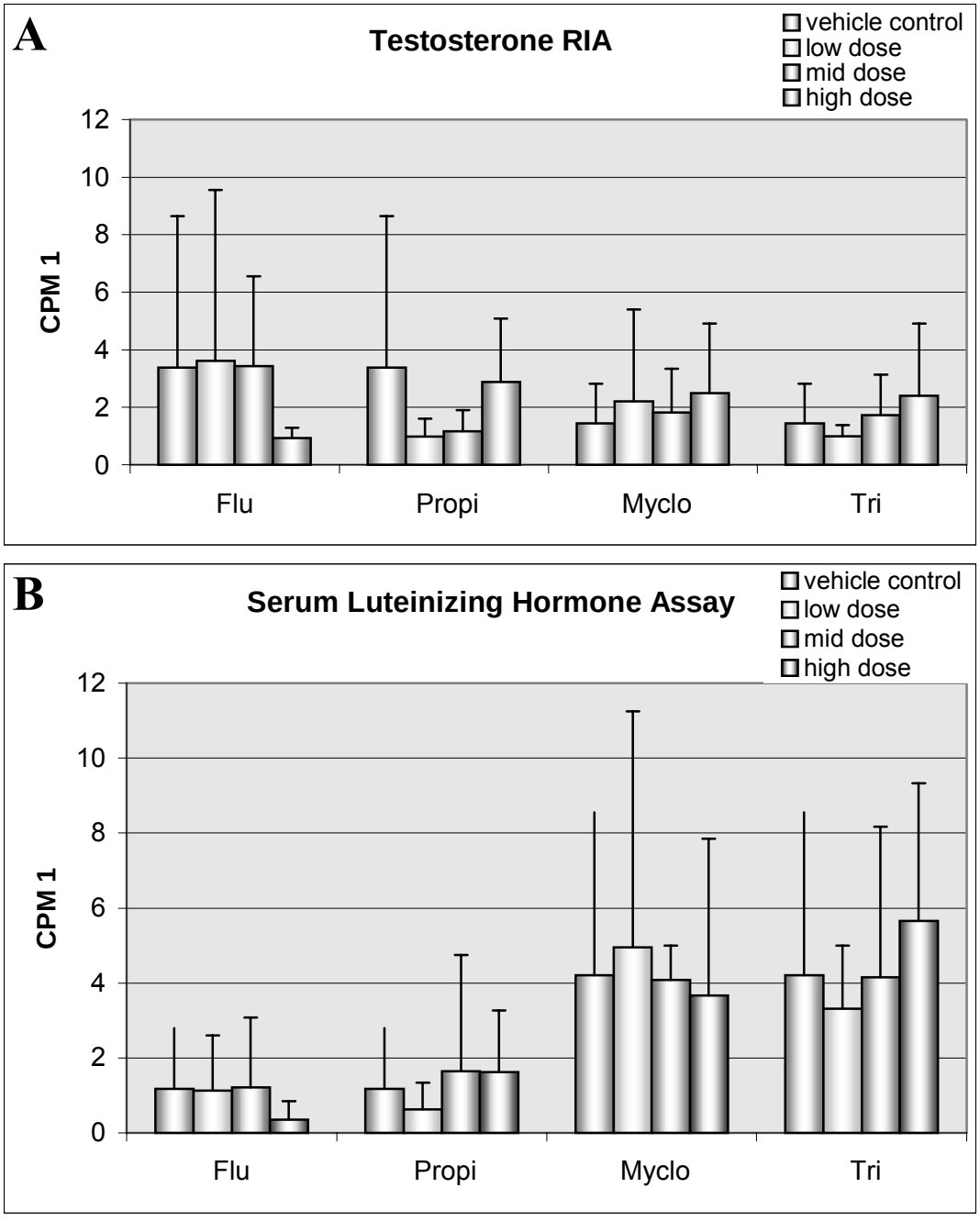

Figure 14: Serum hormone level results for (A) Testosterone ^{125} Iodine Radioimmunoassay (RIA) and (B) LH DELFIA assays. No significant treatment affects occurred in any of the four conazole treatment groups.

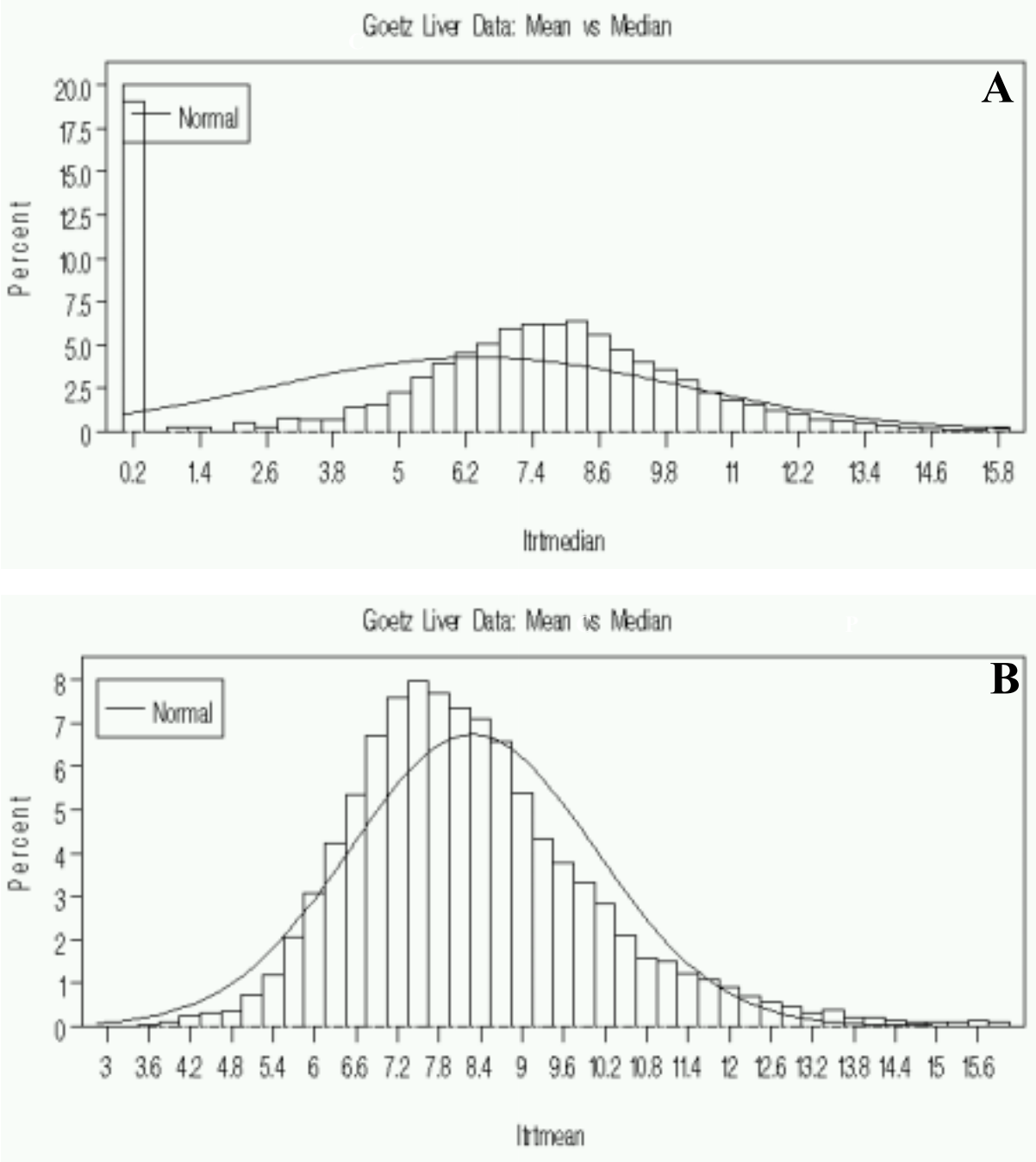

Figure 15: Microarray analysis: comparison of treatment median and mean values without background subtraction. (A) Log_2 of treatment median values are compared with (B) the log_2 of treatment means values to determine if median or mean intensity values should be used in the analysis. Data represented here are raw values without correction for background. Using the log_2 of the mean, all values are above zero and follow a normal distribution more closely.

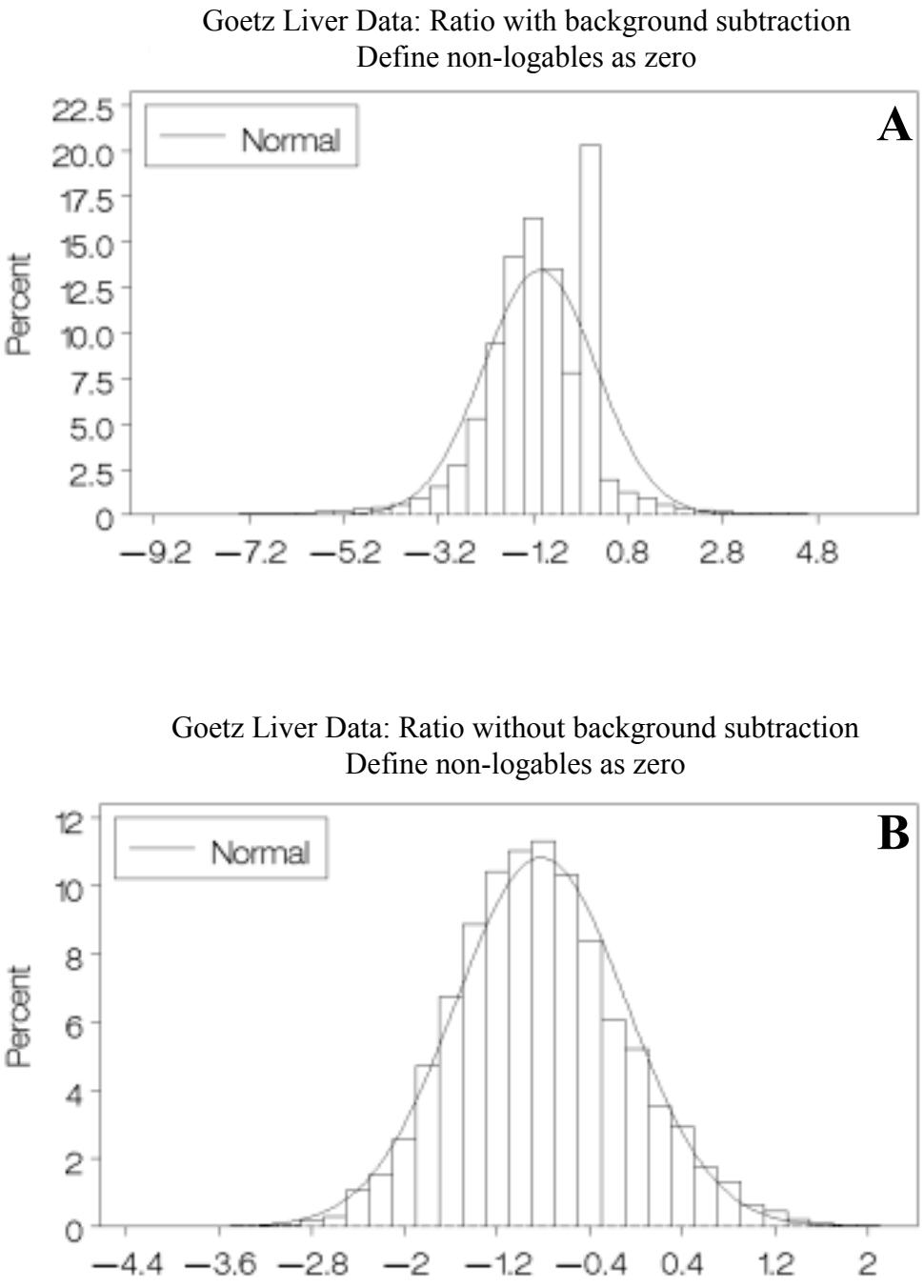

Figure 16: Microarray analysis: comparison of intensity-ratio with or without background subtraction. (A) Cy5/Cy3 ratios with background subtraction are compared with (B) Cy5/Cy3 intensity ratios to determine if intensity values should be corrected for background. Ratios without background subtraction follow a more normal distribution of intensity ratios and intensity values are brought closer into the same intensity range from one another.

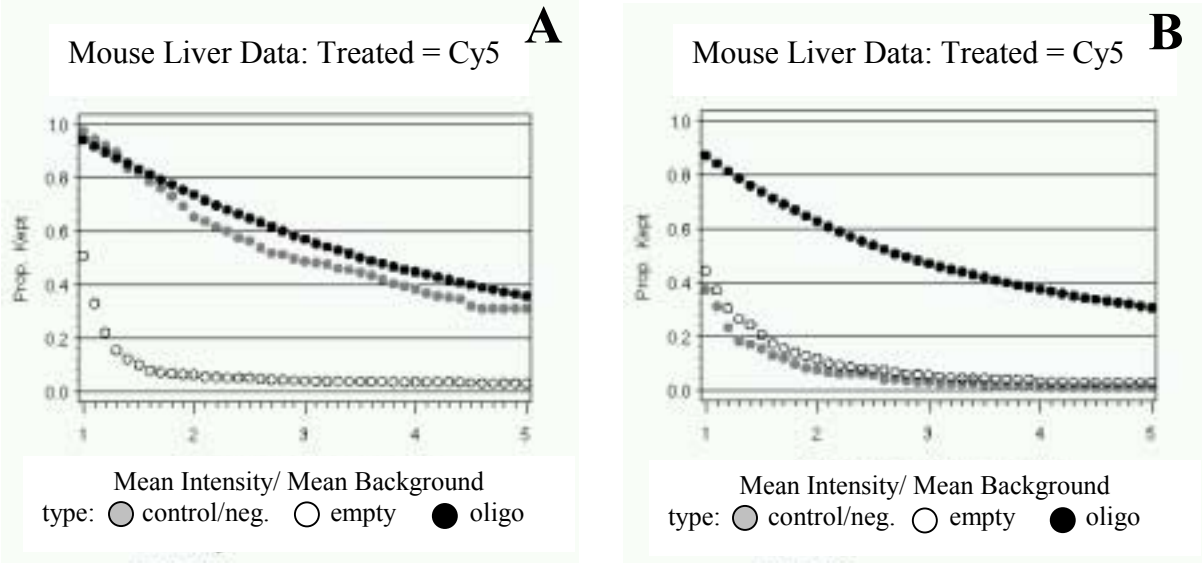

Figure 17: Use of Microarray Analysis Procedure (MAP) to determine threshold values for individual slides. (A) Example of a slide with high intensity values for control and negative spots. (B) A threshold value of roughly 1.7 defines the number of control and negative spots below 20%, empties below 10% and the proportion of oligos kept are over 80%. This process was done on a per slide basis to determine the percentage of 'present' spots on each slide. More importantly, this also defines which spots are 'present' for each slide. Spots defined as 'present' have stronger signal to background ratios than 80% of the controls/negatives and 90% of empty spot's signal to background values.

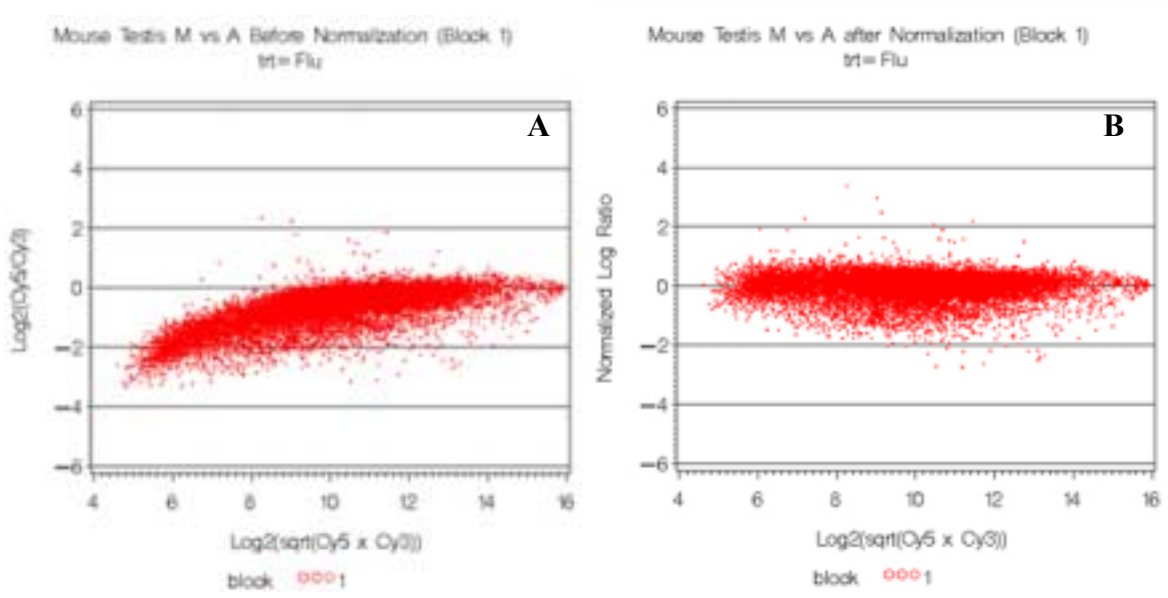

Figure 18: Ratio-Intensity Plot Raw Data, Normalization of average intensity of each gene. (A) Before normalization of an individual slide, lower range average intensity values produce negative log ratios. This type of ratio-intensity plot shows the intensity-specific artifacts from the $\log_2$ ratio measurements. After normalization (B) the average intensity values are centered more around zero. Outliers are relatively unchanged. When converting intensity ratios into $\log_2$, systematic dependence on intensity can occur. Through the use of the LOWESS normalization, intensity-dependent effects in the $\log_2$ ratio values are removed.

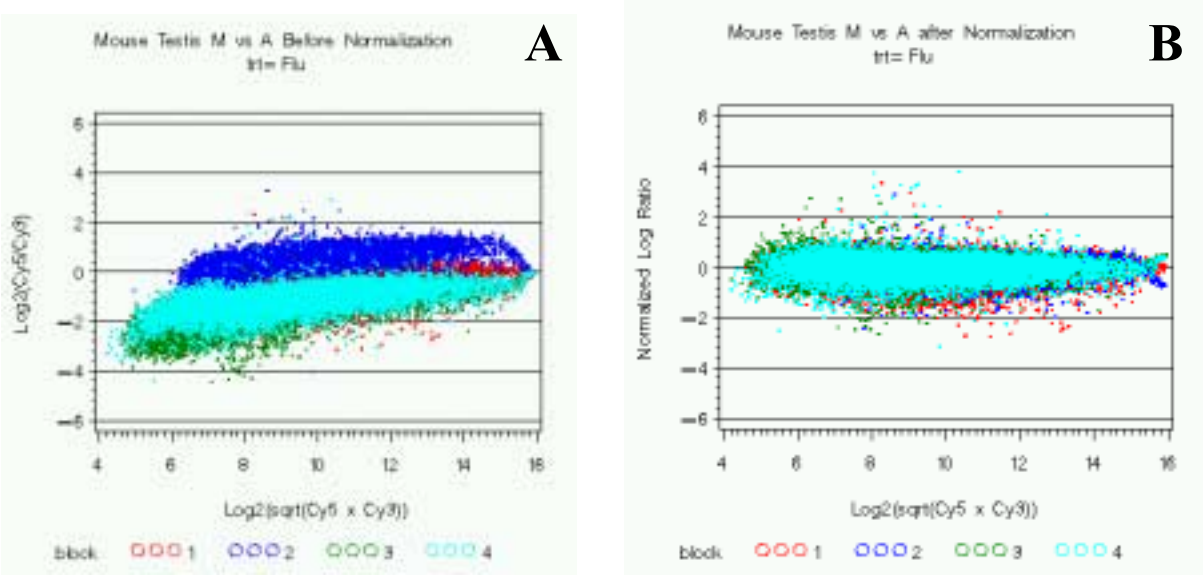

Figure 19: Microarray analysis: normalization of all four slides within one treatment block. (A) Four replicates from the same conazole treatment group compared with each other before normalization and (B) after normalization. X-axis [Log_2(Cy5/Cy3)] is log mean signal intensity ratio for each spotted oligo. Y-axis [Log2(sqrt(Cy5 x Cy3))] is the geometric average intensity plus error for each spotted oligo.

Conazole	Type of Azole derivative	Liver Cancer (Male Mouse)	Thyroid cancer (Male Rat)	Male Reproductive	Notes
Fluconazole * (Diflucan)	Bis-triazole			Inhibits CYP19 (Paulus et al., 1994)	Non-carcinogenic
Propiconazole *	1,2,4-triazole	2 yr. diet NOAEL 15mg/Kg (EPA, 1999)	N/A	Inhibits CYP19 (Sanderson, 2002) 2 gen diet, F1 and F2, decreased testis/ epi wt. LOAEL 2500ppm (Salamon et al., 1985)	Mouse liver tumors
Triadimenol (Baytan)	1,2,4-triazole	2 yr. diet NOAEL 18 mg/Kg LOAEL 72 mg/Kg (EPA, 1989)	(EPA, 1997)	Inhibits CYP19, weak ER agonist (Vinggaard et al., 1999,2000) GD6-GD15 gavage, triazole metabolite,LOAEL 100mg/Kg, undecended testis (Renhof, 1988)	Rat thyroid tumors Mouse liver tumors
Triadimefon * (Bayleton)	1,2,4-triazole	2 yr. diet NOAEL 300ppm (Bayer 1994)	2 yr. diet NOEAL 300ppm LOAEL 1800ppm (Bayer, 1994)	Inhibits CYP19, weak ER agonist (Vinggaard et al., 1999, 2000) 2 gen diet, decreased insemination, increased T, pubertal changes F1 males, NOAEL 50ppm (Bayer, 1984)	Rat thyroid tumors Mouse liver tumors
Myclobutanil *	1,2,4-triazole	N/A	N/A	2 yr chronic diet NOAEL 2.49 mg/Kg LOAEL 9.84 mg/Kg Testicular atrophy, decreased testis wts., bilateral aspermatogenesis, hypospermia (EPA, 1995)	Non-carcinogenic
Ketoconazole (Nizoral)	1,3 imidazole			Inhibits CYP19, 17,20-lyase, 17α-hydroxylase. Inhibitory effect on androgen receptors. 200mg/Kg reduces fertility in rats (Waller 1990)	

Table 1: Known Multiple Toxicities of Conazoles. (*) Chemicals used in this study

Treatment (mg/kg body weight)	Body weight (g)	Liver weight (g)	p-value	% body weight change
Control A	35.7 ± 0.4	2.11 ± 0.04		
Fluconazole 2	35.6 ± 1.0	2.06 ± 0.07	0.385	-3.52
Fluconazole 25	36.2 ± 0.3	2.32 ± 0.07	0.028	9.05
Fluconazole 50	35.1 ± 1.3	2.39 ± 0.09	0.010	12.97
Propiconazole 10	34.4 ± 0.4	2.07 ± 0.07	0.621	-2.18
Propiconazole 75	34.6 ± 0.9	2.49 ± 0.08	0.000	18.63
Propiconazole 150	36.4 ± 0.9	2.90 ± 0.07	0.000	36.59
Control B	33.9 ± 0.4	1.69 ± 0.06		
Myclobutanil 10	34.3 ± 0.6	1.47 ± 0.07	0.011	-12.52
Myclobutanil 75	33.5 ± 0.9	1.93 ± 0.08	0.017	13.88
Myclobutanil 150	34.8 ± 0.5	1.86 ± 0.07	0.052	11.11
Triadimefon 5	34.8 ± 0.5	1.66 ± 0.09	0.738	-1.41
Triadimefon 50	33.5 ± 0.9	1.73 ± 0.10	0.760	10.50
Triadimefon 115	33.7 ± 0.8	1.85 ± 0.09	0.141	9.70

Table 2: Effects of conazole treatment in mouse liver. Liver weights adjusted for body weights.

Gene	Primer Sequence (5'-3')	Fragment size (bp)	Annealing temperature (ºC)	Gene Bank accession no.
Heat Shock Protein 70-3	F: GGCAAGGCCAACAAGATCAC R: TGCACCATGCGCTCGAT Pb: ACAAGGGCCGCCTGAGCAAGGA	73	56	M12571
CYP 17α-OH	F: ACGGTGGGAGACATCTTTGG R: TGGTCAATCTCCTTTTGGATCTTC Pb: TCCTGGCTTTCCTGGTGCACAATCC	80	56	NM_012753
CYP 19	F: AGCATTTGGACAGGCTGGG R: ATGAGGGTCACCACGTCCAC Pb: CACTGACAACTCGGGCT	80	56	NM_017085
CYP 2c40	F: CGCAGCCCCTGTATGCA R: GCTGGACCTCATGCACCAT Pb: ATGCCTTACACAAATGC	70	56	NM_010004

Table 3: Details of primers used for qRT-PCR. Forward primer (F), reverse primer (R), Probe (Pb).

A

Chemical	All	Genes with increased expression	Genes with decreased expression	EPA Custom only (10 total)	Oligo (10068 total)	Oligo/Control (188 total)
Any	2081			5	2009	67
Flu	515	111	404	0	506	7
Propi	420	248	172	1	403	13
Myclo	505	136	369	2	492	6
Tri	983	590	393	2	929	48

B

Chemical	All	Genes with increased expression	Genes with decreased expression	EPA Custom only (1 total)	Oligo (10529 total)	Oligo/Control (176 total)
Any	1424			1	1399	24
Flu	492	223	269	0	484	3
Propi	229	108	121	0	217	9
Myclo	623	184	439	1	608	11
Tri	278	122	156	0	275	3

Table 4: Total number of differentially expressed genes in mouse (A) liver microarray data and (B) testis microarray data. Comparison of genes differentially expressed between the four conazoles and between tissues. Fluconazole (Flu), propiconazole (Propi), myclobutanil (Myclo), and triadimefon (Tri). (p-value ≤ 0.05).

Mouse P450	Rat P450	Human P450	Fluconazole	Myclobutanil	Propiconazole	Triadimefon
1a1	1A1	1A1	↑	↑	↑ ↑	↑
1a2	1A2	1A2	↑	↑	↑ ↑ ↑	
2b10	2B1	2B1	↑ ↑	↑	↑ ↑	↑
2b13	2B1/2	2B6	↑	↑	↑ ↑ ↑	↑
2c55	2C24	2C18/19		↑	↑	↑
2b9					↑	↑
2e1	2E1	2E1				↓
2c37, 2c50	2C37	2C18			↑	
2c40	2C13	2C18	↓	↓	↓	
2j9	2J4	2J2	↓			↑
2j5	2J4	2J2	↓			
2c29	2C7	2C18	↑			↓
3a13	3A1/2	3A4	↑	↑	↑ ↑	↑
4a10	4A8	4A11		↑		
8b1	8B1	8B1	↓			↓
19	19	19	↓		↓	↓
24	CC24	24A1		↑	↑ ↑	↑
51	51	51			↑	

↑ ↓ Cytochrome P450 activity results from Dr. Sun's lab
↑ ↓ Known inducers or inhibitors on enzyme activity
↑ ↓ Microarray data on mouse conazole-treated liver
↑ ↓ Microarray data on mouse conazole-treated testis

Table 5: Effects of conazoles on CYP activity and expression levels in mice.

Gene	C_T mean ± SD		Fold change	Array result	C_T mean ± SD		Fold change	Array result
Cyp 2b10	VCA	29.7 ± 0.70			VCB	28.8 ± 0.25		
	P	28.3 ± 0.90	2.64	1.91*	M	29.8 ± 0.21	0.50*	n/s
	F	29.2 ± 0.79	1.41	1.75*	T	29.2 ± 1.09	0.76	n/s
Cyp 2c40	VCA	18.9 ± 0.73			VCB	18.4 ± 0.19		
	P	20.2 ± 0.62	0.41*	0.50*	M	18.6 ± 0.19	0.87*	0.67*
	F	20.9 ± 0.24	0.25*	0.47*	T	19.2 ± 0.11	0.57	n/s
Cyp 2c55	VCA	27.0 ± 0.52			VCB	26.1 ± 0.21		
	P	22.2 ± 1.33	27.86*	5.87*	M	22.7 ± 0.72	10.56*	3.97*
	F	24.8 ± 0.42	4.59 *	n/s	T	23.2 ± 0.37	7.46*	4.12*
Cyp 8b1	VCA	19.8 ± 0.37			VCB	19.2 ± 0.31		
	P	20.1 ± 0.90	0.81	n/s	M	19.3 ± 0.47	0.93	n/s
	F	21.2 ± 0.30	0.38 *	n/s	T	19.4 ± 0.11	0.87	0.57*
HSP 70-3	VCA	25.5 ± 0.33			VCB	24.4 ± 0.67		
	P	25.8 ± 1.24	0.81	n/s	M	25.8 ± 0.57	0.38*	n/s
	F	26.0 ± 1.53	0.71	n/s	T	25.6 ± 0.69	0.44*	n/s

Table 6: Quantitative real time RT-PCR results for liver gene transcripts. Cycle Threshold (C_T), vehicle control for stage one (VCA), propiconazole (P), fluconazole (F), vehicle control for stage two (VCB), myclobutanil (M), triadimefon (T). (*) statistically significant from control (n/s) not significant from control. Samples were run in duplicate, 4 samples per treatment and control groups, same samples used in microarray analysis.

Gene	C_T mean ± SD	Fold change	Array result	C_T mean ± SD	Fold change	Array result
3β Hydroxysteroid Dehydrogenase	VCA 33.5 ± 1.45			VCB 35.9 ± 0.86		
	P 35.1 ± 1.08	0.33	n/s	M 35.9 ± 0.81	1.00	n/s
	F 35.9 ± 0.93	0.19*	n/s	T 35.4 ± 1.56	1.41	1.45*
Cyp 17	VCA 19.9 ± 0.73			VCB 20.1 ± 0.35		
	P 19.8 ± 0.43	1.07	n/p	M 19.4 ± 0.62	1.62	n/p
	F 19.9 ± 0.44	1.00	n/p	T 20.0 ± 0.27	1.07	n/p
Cyp 19	VCA 27.0 ± 0.31			VCB 29.2 ± 0.96		
	P 27.2 ± 0.22	0.87	n/p	M 27.9 ± 0.26	2.46*	n/p
	F 27.4 ± 0.61	0.76	n/p	T 28.1 ± 0.90	2.14	n/p
Cyp 24	VCA 31.2 ± 0.19			VCB 32.0 ± 0.66		
	P 31.5 ± 0.32	0.81	1.28*	M 31.4 ± 0.12	1.52	1.30*
	F 31.5 ± 0.07	0.81*	n/s	T 31.8 ± 0.12	1.15	n/s
Cyp 2c55	VCA 23.9 ± 0.13			VCB 24.3 ± 0.32		
	P 24.4 ± 0.48	0.71	n/s	M 24.2 ± 0.93	1.07	n/s
	F 24.0 ± 0.17	0.93	n/s	T 24.4 ± .046	0.93	n/s
Cyp 8b1	VCA 31.1 ± 0.32			VCB 31.8 ± 0.48		
	P 31.4 ± 0.31	0.81	n/s	M 31.4 ± 0.36	1.32	n/s
	F 31.3 ± 0.46	0.87	0.69*	T 31.9 ± 0.53	0.93	n/s
Glutathione S-transferase pi 2	VCA 22.3 ± 0.83			VCB 22.7 ± 0.37		
	P 21.9 ± 0.33	1.32	1.57*	M 22.4 ± 0.13	1.23	n/s
	F 22.5 ± 0.13	0.87	n/s	T 22.7 ± 0.38	1.00	n/s
HSP 70-3	VCA 20.4 ± 0.13			VCB 21.4 ± 0.89		
	P 20.6 ± 0.27	0.87	n/p	M 20.7 ± 0.16	1.62	n/p
	F 20.7 ± 0.10	0.81*	n/p	T 21.0 ± 0.21	1.32	n/p

Table 7: Quantitative real time RT-PCR results for testis gene transcripts. Cycle Threshold (C_T), vehicle control for stage one (VCA), propiconazole (P), fluconazole (F), vehicle control for stage two (VCB), myclobutanil (M), triadimefon (T). (*) statistically significant from control, (n/s) not significant from control, (n/p) not present on array. . Samples were run in duplicate, 4 samples per treatment and control groups, same samples used in microarray analysis.

Gene Name	GenBank	Propiconazole fold change/ p-value	Triadimefon fold change/ p-value	Biological Process
ATPase, H+ transporting, lysosomal (vacuolar proton pump), alpha 70 kDa, isoform 1	NM_007508	0.6681 / 0.037	0.6615 / 0.049	8
Cytochrome P450, 24	D89669	1.8738 / 0.017	1.7858/ 0.039	2
Glutathione S-transferase, alpha 2 (Yc2)	NM_008182	3.1052 / 0.000	1.7425/ 0.029	4
Glutathione S_transferase, theta 3	BC003903	2.4047 / 0.007	2.2614/ 0.018	4
Mitogen activated protein kinase kinase 6	U39066	0.8288 / 0.041	1.2679 / 0.021	7
Monoglyceride lipase	NM_011844	1.4233 / 0.016	0.6931 / 0.021	5
Protocadherin beta 16	NM_053141	1.8157 / 0.002	1.5005/ 0.031	3
* Protocadherin gamma subfamily C, 3	NM_033581	2.1970 / 0.000	1.7756/ 0.006	1
* RIKEN cDNA 4931406C07 gene	BC016078	2.2992 / 0.000	1.5316 / 0.002	
Topoisomerase (DNA) I	NM_009408	1.3017 / 0.039	1.3869 / 0.022	6
Transthyretin	NM_013697	0.5851 / 0.02	0.4640 / 0.004	9
Tumor suppressor region 10	NM_019720	1.5642 / 0.03	0.6332 / 0.041	

Table 8: Differentially expressed genes common to propiconazole and triadimefon in the liver. Of the genes exclusively modified by these two known liver carcinogenic conazoles, only 50% of them have been identified by their biological functions. Conazole treatment group (cnz), fluconazole (F), propiconazole (P), myclobutanil (M), triadimefon (T), testis (Ts), liver (L). (1) cell adhesion, (2) electron transport, (3) homophilic cell adhesion; regulation of transcription, DNA-dependent, (4) glutathione transferase activity, (5) proteolysis and peptidolysis; lipid metabolism; aromatic compound metabolism, (6) DNA topological change; DNA unwinding, (7) protein amino acid phosphorylation, (8) proton transport; ATP biosynthesis; hydrogen transport, (9) transport. (*) The 2 genes found common to propiconazole and triadimefon with a p-value less than 0.01.

Tissue	Gene Name	GenBank	cnz	Fold Change	p-value	Biological process
Ts	Cytochrome P450, 24	D89669	P	1.2805	0.032	1
Ts	Cytochrome P450, 24	D89669	M	1.2983	0.025	1
L	Cytochrome P450, 24	D89669	P	1.87388	0.017	1
L	Cytochrome P450, 24	D89669	T	1.7858	0.039	1
Ts	Cytochrome P450, 8b1, sterol 12 alpha-hydrolase	NM_010012	F	0.6897	0.028	1
L	Cytochrome P450, 8b1, sterol 12 alpha-hydrolase	NM_010012	T	0.5733	0.007	1
Ts	Arachidonate 5-lipoxygenase activating protein	AK004002	T	1.5619	0.007	2
L	Arachidonate 5-lipoxygenase activating protein	AK004002	T	0.508	0.009	2
Ts	Isocitrate dehydrogenase 1 (NADP+), soluble	NM_010497	M	1.3817	0.051	3
L	Isocitrate dehydrogenase 1 (NADP+), soluble	NM_010497	M	0.6814	0.027	3
Ts	Glutathione S-transferase, alpha 2 (Yc2)	NM_008182	F	1.1607	0.033	4
L	Glutathione S-transferase, alpha 2 (Yc2)	NM_008182	P	3.1052	0	4
L	Glutathione S-transferase, alpha 2 (Yc2)	NM_008182	T	1.7426	0.029	4
Ts	Adaptor-related protein complex AP-1, mu subunit 1	NM_007456	T	1.3633	0.042	5
L	Adaptor-related protein complex AP-1, mu subunit 1	NM_007456	F	1.5095	0.021	5
L	Adaptor-related protein complex AP-1, mu subunit 1	NM_007456	P	1.4763	0.017	5
Ts	Hydroxysteroid dehydrogenase-2, delta<5>-3-beta	M75886	T	1.4542	0.032	6
L	Hydroxysteroid dehydrogenase-2, delta<5>-3-beta	M75886	M	0.6417	0.032	6

Table 9: Differentially expressed genes common to both conazole treated liver and testis tissues in the adult CD-1 mouse. Conazole treatment group (cnz), fluconazole (F), propiconazole (P), myclobutanil (M), triadimefon (T), testis (Ts), liver (L). (1) electron transport, (2) leukotriene metabolism; leukotriene biosynthesis, (3) glutathione metabolism; tricarboxylic acid cycle; response to oxidative stress; glyoxylate cycle; main pathways of carbohydrate metabolism, (4) glutathione transferase activity, (5) protein transport; endocytosis; intracellular protein transport; vesicle-mediated transport, (6) steroid biosynthesis; C21-steroid hormone biosynthesis.

Gene Name	GenBank	cnz	Fold Change	p-value	Biological Process
Cytochrome P450, 1a2, aromatic compound inducible	NM_009993	P	1.4749	0.028	1
Cytochrome P450, 2b10, phenobarbitol inducible, type b	NM_009998	F	1.7505	0.046	1
Cytochrome P450, 2b10, phenobarbitol inducible, type b	NM_009998	P	1.9118	0.015	1
Cytochrome P450, 2c29	NM_007815	F	1.7053	0.044	1
Cytochrome P450, 2c29	NM_007815	T	0.5647	0.033	1
Cytochrome P450, 2c37	NM_010001	P	1.9750	0.003	1
Cytochrome P450, 2c40	NM_010004	F	0.4711	0.000	1
Cytochrome P450, 2c40	NM_010004	P	0.5053	0.000	1
Cytochrome P450, 2c40	NM_010004	M	0.6698	0.013	1
RIKEN cDNA 2010318C06 gene (Cyp2c55)	NM_028089	P	5.8679	0.002	
RIKEN cDNA 2010318C06 gene (Cyp2c55)	NM_028089	M	3.9717	0.016	
RIKEN cDNA 2010318C06 gene (Cyp2c55)	NM_028089	T	4.1195	0.013	
Cytochrome P450, 2e1, ethanol inducible	NM_021282	T	0.5327	0.008	1
Cytochrome P450, 2j9	AF336850	F	0.6691	0.05	1
Cytochrome P450, 2j9	AF336850	T	1.4967	0.049	1
Mus musculus, Similar to cytochrome P450, 4a10, clone MGC:18880	BC013476	M	1.6980	0.038	
Cytochrome P450, 8b1, sterol 12 alpha-hydrolase	NM_010012	T	0.5733**	0.007	1
Cytochrome P450, 24	D89669	P	1.8738*	0.017	1
Cytochrome P450, 24	D89669	T	1.7858*	0.039	1
Cytochrome P450, 51	NM_020010	P	1.3727	0.047	1,2,3

Table 10: Cytochrome P450 genes affected by conazole treatment in mouse liver. Conazole treatment group (cnz), fluconazole (F), propiconazole (P) , myclobutanil (M), triadimefon (T), (*) increased in testis, (**) decreased in testis, (1) electron transport, (2) cholesterol biosynthesis, (3) proteolysis and peptidolysis.

Gene Name	GenBank	cnz	Fold Change	p-value	Biological Process
Alcohol dehydrogenase 5	NM_007410	T	1.7669	0.002	
Aldehyde dehydrogenase 2, mitochondrial	NM_009656	M	0.8111	0.021	5
Aldehyde dehydrogenase family 1, subfamily A1	NM_013467	P	1.4680	0.049	5
Aldehyde dehydrogenase family 5, subfamily A1	AK016580	M	0.5362	0.037	
Aldehyde dehydrogenase family 3, subfamily A2	NM_007437	T	1.5162	0.034	5
Aldehyde dehydrogenase family 1, subfamily A7	NM_011921	P	1.5808	0.036	5
Glyceraldehyde-3-phosphate dehydrogenase	NM_008084	F	1.2943	0.014	1
Glyceraldehyde-3-phosphate dehydrogenase	NM_008084	P	1.3375**	0.002	1
Glyceraldehyde-3-phosphate dehydrogenase	NM_008084	M	0.6957**	0.000	1
Glyceraldehyde-3-phosphate dehydrogenase	NM_008084	T	0.2907**	0.000	1
Glycerol phosphate dehydrogenase 1, cytoplasmic adult	BC019391	T	0.5854	0.017	
Heme oxygenase (decycling) 1	NM_010442	F	0.7181	0.031	2
Heme oxygenase (decycling) 1	NM_010442	P	0.6287	0.003	2
Isocitrate dehydrogenase 2 (NADP+), mitochondrial	NM_008322	T	1.5693*	0.011	
NADH dehydrogenase (ubiquinone) 1 alpha subcomplex, 1	NM_019443	T	1.4377	0.021	
NADH dehydrogenase (ubiquinone) 1 alpha subcomplex, 4	AK005084	M	0.6770	0.023	
NADH dehydrogenase (ubiquinone) 1 alpha subcomplex, 6 (14kD, B14)	NM_025987	T	1.3775	0.04	
NADH dehydrogenase (ubiquinone) 1, subcomplex unknown, 1	NM_025523	T	1.5026	0.018	
NAD(P) dependent steroid dehydrogenase-like	AF100198	F	0.6029	0.022	6
NAD(P) dependent steroid dehydrogenase-like	AF100198	T	1.5917	0.033	6
Proline dehydrogenase	NM_011172	T	1.7595	0.018	7
Prostaglandin I2 (prostacyclin) synthase	NM_008968	P	0.6854	0.011	3,4

Table 11: Enzymes involved in metabolism of endogenous and exogenous (xenobiotic) substrates effected by conazole treatment in mouse liver. Conazole treatment group (cnz), fluconazole (F), propiconazole (P), myclobutanil (M), triadimefon(T), (*) increased in testis, (**) decreased in testis, (1) glycolysis, (2) heme oxidation, (3)electron transport, (4) prostaglandin biosynthesis, (5) metabolism, (6)cholesterol biosynthesis, cholesterol metabolism, steroid biosynthesis, (7) proline catabolism, proline metabolism, glutamate biosynthesis.

Gene Name	GenBank	cnz	Fold Change	p-value	Biological Process
Bile acid-Coenzyme A: amino acid N-acyltransferase	NM_007519	T	1.4695	0.026	12
Cyclin-dependent kinase 4	NM_009870	T	0.5476	0.015	13,18
Cyclin-dependent kinase 9 (CDC2-related kinase)	BC003901	T	0.6075	0.007	13,17,18
Diacylglycerol O-acyltransferase 1	NM_010046	F	0.5390	0.016	
Diacylglycerol O-acyltransferase 2	NM_026384	T	0.3712	0.047	10
Galactosyltransferase 3 beta 1, 4	D37791	T	0.5366	0.004	
Glutathione S-transferase, alpha 2 (Yc2)	NM_008182	P	3.1052	0.000	
Glutathione S-transferase, alpha 2 (Yc2)	NM_008182	T	1.7425	0.029	
Glutathione S-transferase, alpha 4	NM_010357	T	1.4154	0.026	8
Glutathione S-transferase, mu 1	NM_010358	F	1.6931	0.028	8
Glutathione S-transferase, mu 2	NM_008183	P	1.9281	0.003	8
Glutathione S-transferase, mu 3	J03953	F	1.6848	0.034	8
Glutathione S-transferase omega 1	NM_010362	F	0.5950	0.014	8
Glutathione S-transferase, theta 1	NM_008185	M	1.3934	0.043	
Glutathione S-transferase, theta 1	NM_008185	T	1.8196	0.001	
Glutathione transferase zeta 1 (maleylacetoacetate isomerase)	NM_010363	F	0.7095	0.029	9
Mitogen activated protein kinase kinase kinase 5	NM_008580	F	1.6771	0.005	13,15
Mitogen activated protein kinase kinase kinase 5	NM_008580	P	1.6307	0.004	13,15
Mitogen activated protein kinase kinase 6	U39066	P	0.8288	0.041	13
Mitogen activated protein kinase kinase 6	U39066	T	1.2679	0.021	13
Mitogen activated protein kinase 9	NM_016961	M	0.5680	0.035	13
Mitogen activated protein kinase kinase kinase 11	NM_022012	F	3.4652	0.047	

Table 11 continued: Enzymes involved in metabolism of endogenous and exogenous (xenobiotic) substrates effected by conazole treatment in mouse liver. Conazole treatment group (cnz), fluconazole (F), propiconazole (P), myclobutanil (M), triadimefon(T), (8) glutathione conjugation reaction, (9) tyrosine catabolism; phenylalanine catabolism, (10) triacylglycerol biosynthesis, (11) sulfate transport, (12) bile acid metabolism, (13) protein amino acid phosphorylation, (14) angiogenesis, (15) apoptosis, (16) DNA methylation, (17) RNA elongation from Pol II promoter, transcription initiation from Pol II promoter, cell proliferation, regulation of cell cycle (18) cell cycle.

Gene Name	GenBank	cnz	Fold Change	p-value	Biological Process
Mitogen activated protein kinase 14	NM_011951	F	1.3793	0.023	13,14
Mitogen activated protein kinase 14	NM_011951	T	0.7439	0.034	13,14
Protein kinase, cGMP-dependent, type II	NM_008926	T	0.6462	0.011	13
Receptor-like tyrosine kinase	L21707	T	0.4668	0.021	13
Serine/threonine kinase 5	BC003261	P	0.6167	0.025	13,16,18
Serine threonine kinase 31	AF285580	P	0.6224	0.04	13
Thiosulfate sulfurtransferase, mitochondrial	NM_009437	T	0.4017	0.000	11

Table 11 continued: Enzymes involved in metabolism of endogenous and exogenous (xenobiotic) substrates effected by conazole treatment in mouse liver. Conazole treatment group (cnz), fluconazole (F), propiconazole (P), myclobutanil (M), triadimefon(T), (8) glutathione conjugation reaction, (9) tyrosine catabolism; phenylalanine catabolism, (10) triacylglycerol biosynthesis, (11) sulfate transport, (12) bile acid metabolism, (13) protein amino acid phosphorylation, (14) angiogenesis, (15) apoptosis, (16) DNA methylation, (17) RNA elongation from Pol II promoter, transcription initiation from Pol II promoter, cell proliferation, regulation of cell cycle (18) cell cycle.

Gene Name	GenBank	cnz	Fold Change	p-value	Biological Process
Adaptor-related protein complex AP-1, mu subunit 1	NM_007456	F	1.5095	0.021	5
Adaptor-related protein complex AP-1, mu subunit 1	NM_007456	P	1.4763	0.017	5
ATPase, H+ transporting, lysosomal (vacuolar proton pump)	NM_024173	T	1.8055	0.005	20
CCAAT/enhancer binding protein (C/EBP), beta	NM_009883	T	1.8650	0.002	9,12,19
Cell division cycle 5-like (S. pombe)	AK004547	F	0.7358	0.045	6
Cell division cycle 37 homolog (S. cerevisiae)	NM_016742	F	0.5201	0.015	2
Cell division cycle 42 homolog (S. cerevisiae)	NM_009861	T	1.4176	0.007	3,7
Endothelial cell-selective adhesion molecule	AF361882	F	0.5524	0.002	8
Fas-associating protein with death domain	NM_010175	F	0.6826	0.042	9,10
Fibroblast growth factor inducible 14	NM_008015	M	0.6935	0.033	
Fibroblast growth factor (acidic) intracellular binding protein	NM_021438	F	0.6682	0.041	
Growth arrest specific 5	NM_013525	M	1.3705	0.037	
Growth differentiation factor 11	AF092734	T	0.5255	0.029	
Growth factor receptor bound protein 7	NM_010346	T	0.5941	0.005	10,11
Inhibitor of growth family, member 1-like	NM_023503	T	1.5056	0	12
Insulin-like growth factor binding protein 4	NM_010517	T	0.3918	0.004	1
Insulin-like growth factor binding protein 6	NM_008344	T	0.6145	0.001	1
Kangai 1 (suppression of tumorigenicity 6, prostate)	NM_007656	T	0.4025	0.001	
Large tumor suppressor 2	NM_015771	T	0.5889	0.032	
Platelet derived growth factor, B polypeptide	NM_011057	T	0.6116	0.041	1,2,13
Programmed cell death 1 ligand 1	NM_021893	P	0.6056	0.046	

Table 12: Cancer and cell cycle related genes significantly affected by conazole treatment in mouse liver. Conazole treatment group (cnz), fluconazole (F), propiconazole (P), myclobutanil (M), triadimefon (T), (*) increased in testis, (**) decreased in testis, (1) cell growth and/or maintenance, (2) regulation of cell cycle, (3) small GTPase mediated signal transduction, (4) RAS protein signal transduction, (5) protein transport; intracellular protein transport, (6) protein targeting, (7) actin filament organization; Rho protein signal transduction, (8) homophilic cell adhesion, (9) apoptosis, (10) signal transduction, (11) neuropeptide signaling pathway; intracellular signaling cascade, (12) regulation of transcription, DNA-dependent, (13) cell proliferation, (14) lymph gland development; myogenesis; negative regulation of cell proliferation; necrosis; skeletal development; defense response; inflammatory response; organogenesis; regulation of myogenesis, (15) extracellular matrix organization and biogenesis, (16) protein biosynthesis, (17) immune response, (18) potassium ion transport, (19) anti-apoptosis; neuron differentiation (20) proton transport; ATP biosynthesis.

Gene Name	GenBank	cnz	Fold-Change	p-value	Biological Process
Programmed cell death 1 ligand 1	NM_021893	M	1.8991	0.023	
Programmed cell death 6	NM_011051	T	1.5748	0.007	9
Programmed cell death 10	NM_019745	T	1.5838	0.001	
RAB3C, member RAS oncogene family	NM_023852	P	1.9292	0.02	3,5
RAB36, member RAS oncogene family	AK018269	F	0.6415	0.032	
RAB4B, member RAS oncogene family	BC007147	M	1.7127	0.02	
Related RAS viral (r-ras) oncogene homolog 2	NM_025846	P	2.0536	0.023	1,3,4
T lymphoma oncogene	NM_011601	F	1.3533	0.036	1,2
T lymphoma oncogene	NM_011601	P	1.3019	0.044	1,2
Transforming growth factor alpha	NM_031199	F	0.4791	0.026	2,13
Transforming growth factor alpha	NM_031199	P	0.4617	0.013	2,13
Transforming growth factor, beta 1	NM_011577	M	0.6794	0.046	1,2,14
Transforming growth factor, beta 2	NM_009367	T	0.5824	0.021	1,2,13,15
Transthyretin	NM_013697	P	0.5851	0.02	5
Transthyretin	NM_013697	T	0.4640	0.004	5
Tumor suppressor region 10	NM_019720	T	0.6332	0.041	
Tumor suppressor region 10	NM_019720	P	1.5642	0.030	
Tumor necrosis factor, alpha-induced protein 3	NM_009397	P	1.7990	0.014	9
Tumor necrosis factor receptor superfamily, member 5	NM_011611	M	1.4115	0.036	16
Tumor necrosis factor (ligand) superfamily, member 14	NM_019418	M	1.7909	0.035	17
Tumor necrosis factor, alpha-induced protein 1 (endothelial)	AK004593	M	0.6090	0.046	18

Table 12 continued: Cancer and cell cycle related genes significantly affected by conazole treatment in mouse liver. Conazole treatment group (cnz), fluconazole (F), propiconazole (P), myclobutanil (M), triadimefon (T), (1) cell growth and/or maintenance, (2) regulation of cell cycle, (3) small GTPase mediated signal transduction, (4) RAS protein signal transduction, (5) protein transport; intracellular protein transport, (6) protein targeting, (7) actin filament organization; Rho protein signal transduction, (8) homophilic cell adhesion, (9) apoptosis, (10) signal transduction, (11) neuropeptide signaling pathway; intracellular signaling cascade, (12) regulation of transcription, DNA-dependent, (13) cell proliferation, (14) lymph gland development; myogenesis; negative regulation of cell proliferation; necrosis; skeletal development; defense response; inflammatory response; organogenesis; regulation of myogenesis, (15) extracellular matrix organization and biogenesis, (16) protein biosynthesis, (17) immune response, (18) potassium ion transport, (19) anti-apoptosis; neuron differentiation (20) proton transport; ATP biosynthesis.

Gene Name	GenBank	cnz	Fold Change	p-value	Biological Process
Corticosteroid binding globulin	NM_007618	T	2.0925	0.009	1
Estrogen related receptor, alpha	NM_007953	F	1.7353	0.006	1,8
Hydroxysteroid dehydrogenase-2, delta<5>-3-beta	M75886	M	0.6416*	0.032	4,5
Hydroxysteroid 17-beta dehydrogenase 2	NM_008290	T	0.3466	0.002	3,4
Hydroxysteroid 17-beta dehydrogenase 3	NM_008291	M	0.5565	0.021	3,4
Hydroxysteroid 17-beta dehydrogenase 4	NM_008292	T	1.3480	0.049	2,3,4
Mus musculus, Similar to hydroxysteroid (17-beta) dehydrogenase 5, clone MGC:37825 IMAGE:5098938, mR	BC021607	F	0.6765	0.025	
Mus musculus, Similar to hydroxysteroid (17-beta) dehydrogenase 5, clone MGC:37825 IMAGE:5098938, mR	BC021607	P	0.6786	0.017	
Hydroxysteroid (17-beta) dehydrogenase 10	NM_016763	F	0.7271	0.032	3
NAD(P) dependent steroid dehydrogenase-like	AF100198	F	0.6029	0.022	4,7
NAD(P) dependent steroid dehydrogenase-like	AF100198	T	1.5917	0.033	4,7
Steroid receptor RNA activator 1	NM_025291	F	0.6883	0.011	6
Steroid receptor RNA activator 1	NM_025291	T	1.5431	0.004	6

Table 13: Steroidogenic-related genes significantly affected by conazole treatment in mouse liver. Conazole treatment group (cnz), fluconazole (F), propiconazole (P), myclobutanil (M), triadimefon(T), (*) increased in testis, (1) transport, (2) protein targeting,, (3) metabolism, (4) steroid biosynthesis, (5) C21-steroid hormone biosynthesis, (6) regulation of transcription from Pol II promoter, (7) cholesterol biosynthesis; cholesterol metabolism, (8) regulation of transcription, DNA-dependent.

Gene Name	GenBank	cnz	Fold Change	p-value	Biological Process
Ferritin light chain 1	NM_010240	T	0.4607	0.016	2
Ferritin light chain 2	NM_008049	T	0.6141	0.005	2
Ferredoxin 1	NM_007996	T	1.7426	0.014	1
Glucose-6-phosphatase, catalytic	NM_008061	F	0.4621	0.021	3
Heat shock protein, 70 kDa 4	NM_015765	F	0.5985**	0.023	8
Nuclear factor, interleukin 3, regulated	NM_017373	F	0.4100	0.002	9
Interleukin 4 receptor, alpha	NM_010557	T	0.5623	0.044	10
Interleukin 11 receptor, alpha chain 1	NM_010549	F	0.5962	0.01	10
Interleukin 15 receptor, alpha chain	NM_008358	M	0.4014	0.047	10
Interleukin 21	NM_021782	F	1.5891	0.046	
Interleukin 21	NM_021782	M	1.5880	0.047	
Tumor necrosis factor, alpha-induced protein 1 (endothelial)	AK004593	M	0.6090	0.046	5
Tumor necrosis factor, alpha-induced protein 3	NM_009397	P	1.7990	0.014	6
Tumor necrosis factor (ligand) superfamily, member 14	NM_019418	M	1.7909	0.035	4
Tumor necrosis factor receptor superfamily, member 5	NM_011611	M	1.4115	0.036	7

Table 14: Stress response related genes significantly affected by conazole treatment in mouse liver. Conazole treatment group (cnz), fluconazole (F), propiconazole (P), myclobutanil(M), triadimefon (T), (*) increased in testis, (**) decreased in testis, (1) electron transport, (2) iron ion homeostasis; iron ion transport, (3) glycogen biosynthesis, (4) immune response, (5) potassium ion transport, (6) apoptosis, (7) protein biosynthesis, (8) proteolysis and peptidolysis, (9) regulation of transcription, DNA-dependent, (10) cell surface receptor linked signal transduction.

Gene Name	GenBank	Fold Change	p-value	Biological Process
Apoptotic chromatin condensation inducer in the nucleus	NM_023190	0.7219	0.000	1
Arylsulfatase A	X73230	0.76543	0.01	2
5-azacytidine induced gene 1	NM_009734	0.6955	0.01	3
Beta-2 microglobulin	NM_009735	1.7459	0.002	4
Feminization 1 homolog a (C. elegans)	BC009161	0.7327	0.004	5
Mitogen activated protein kinase kinase 5	NM_011840	0.7431	0.003	6
Sphingomyelin phosphodiesterase 3, neutral	AK019476	0.7219	0.002	7
Type I transmembrane protein Fn14	NM_013749	0.6959	0.004	1,8
V-rel reticuloendotheliosis viral oncogene homolog A, (avian)	NM_009045	0.7914	0.005	5,9

Table 15: Differentially expressed genes exclusively modified by myclobutanil treatment in mouse testis. (1) apoptotic program, (2) binding of sperm to zona pellucida; physiological processes; metabolism, (3) spermatogenesis, (4) defense response; cellular defense response; antigen presentation, endogenous antigen; antigen processing, endogenous antigen via MHC class I, (5) regulation of transcription, DNA-dependent, (6) protein amino acid phosphorylations, (7) sphingomyelin metabolism; response to stress; signal transduction, (8) cell adhesion; angiogenesis; substrate-bound cell migration, cell attachment to substrate, (9) cell growth and/or maintenance; defense response; regulation of cell cycle; organogenesis.

Gene Name	GenBank	cnz	Fold Change	p-value	Biological Process
Cytochrome P450, 2b9, phenobarbitol inducible, type a	NM_010000	M	2.3238	0.015	1
Cytochrome P450, 2b9, phenobarbitol inducible, type a	NM_010000	T	2.0088	0.039	1
Cytochrome P450, 8b1, sterol 12 alpha-hydrolase	NM_010012	F	0.6896**	0.028	1
Cytochrome P450, 24	D89669	P	1.2805*	0.032	1
Cytochrome P450, 24	D89669	M	1.2982*	0.025	1

Table 16: Cytochrome P450 genes affected by conazole treatment in mouse testis. Conazole treatment group (cnz), fluconazole (F), propiconazole (P), myclobutanil (M), triadimefon (T), (*) increased in liver, (**) decreased in liver, (1) electron transport.

Gene Name	GenBank	cnz	Fold Change	p-value	Biological Process
1-acylglycerol-3-phosphate O-acyltransferase 1 (lysophosphatidic acid acyltransferase, alpha)	NM_018862	T	1.5316	0.044	5
Anaplastic lymphoma kinase	NM_007439	T	1.3534	0.038	6,8
Arachidonate 5-lipoxygenase activating protein	AK004002	T	1.5619**	0.007	1
B cell phosphoinositide 3-kinase adaptor	NM_031376	F	0.7327	0.039	
BMX non-receptor tyrosine kinase	NM_009759	M	2.1225	0.032	7,8,12
Calcium/calmodulin-dependent protein kinase II alpha	NM_009792	F	0.6695	0.006	8
Calcium/calmodulin-dependent protein kinase II alpha	NM_009792	P	0.7593	0.046	8
Dual-specificity tyrosine-(Y)-phosphorylation regulated kinase 1a	U58497	T	0.7167	0.033	8,9
Fucosyltransferase 4	NM_010242	M	0.7658	0.032	8
Glutathione S-transferase, pi 2	NM_013541	P	1.5748	0.017	10
Glyceraldehyde-3-phosphate dehydrogenase	NM_008084	P	0.9221**	0.008	4
Glyceraldehyde-3-phosphate dehydrogenase	NM_008084	M	0.8941**	0.000	4
Glyceraldehyde-3-phosphate dehydrogenase	NM_008084	T	1.2310**	0.000	4
Hexokinase 2	NM_013820	M	0.7274	0.008	4
Mitogen activated protein kinase kinase 5	NM_011840	M	0.7431	0.003	8
Mitogen-activated protein kinase kinase kinase kinase 4	NM_008696	M	1.5372	0.003	8
Mitogen-activated protein kinase kinase kinase kinase 4	NM_008696	T	1.3436	0.026	8

Table 17: Enzymes involved in metabolism of endogenous and exogenous (xenobiotic) compounds effected by conazole treatment in mouse testis. Conazole treatment group (cnz), fluconazole (F), propiconazole (P), myclobutanil (M), tridimefon (T), (*) increased in liver, (**) decreased in liver, (1) leukotriene metabolism; leukotriene biosynthesis, (2) protein modification, (3) proline catabolism; glutamate biosynthesis, (4) glycolysis, (5) phospholipid biosynthesis; metabolism; phospholipid metabolism, (6) transmembrane receptor protein tyrosine kinase signaling pathway; (7) mesoderm development, (8) protein amino acid phosphorylation, (9) peptidyl-tyrosine phosphorylation, (10) glutathione conjugation reaction, (11) transport, oxidoreductase activity, (12) intracellular signaling cascade, (13) signal transduction, (14) cell cycle, (15) ganglioside biosynthesis, (16) cytoskeleton organization and biogenesis, (17) DNA metabolism; DNA topological change.

Gene Name	GenBank	cnz	Fold Change	p-value	Biological Process
NADH dehydrogenase (ubiquinone) Fe-S protein 4	NM_010887	F	0.7299	0.028	11
Procollagen lysine, 2-oxoglutarate 5-dioxygenase 2	NM_011961	F	1.3392	0.044	2
Procollagen lysine, 2-oxoglutarate 5-dioxygenase 2	NM_011961	P	1.3294	0.049	2
Proline dehydrogenase (oxidase) 2	NM_019546	F	0.5042	0.034	3
Protein kinase C, mu	NM_008858	M	1.5421	0.046	8,12
Rho-associated coiled-coil forming kinase 1	NM_009071	M	1.4976	0.012	8,12,13
Ribosomal protein S6 kinase, 90kD, polypeptide 4	NM_019924	P	0.7004	0.037	8
Serum-inducible kinase	M96163	M	1.8100	0.014	8,14
Sialyltransferase 9 (CMP-NeuAc:lactosylceramide alpha-2,3-sialyltransferase)	NM_011375	F	0.6774	0.023	8
Sialyltransferase 4C (beta-galactosidase alpha-2,3-sialytransferase)	NM_009178	P	0.7600	0.05	8
Sialytransferase 7 ((alpha-N-acetylneuraminyl 2,3-betagalactosyl-1,3)-N-acetyl galactosaminide alpha	NM_016973	F	0.6052	0.031	8,15
Sterile-alpha motif and leucine zipper containing kinase AZK	NM_023057	F	0.7468	0.006	16
Topoisomerase (DNA) II alpha	NM_011623	F	0.7633	0.02	17

Table 17 continued: Enzymes involved in metabolism of endogenous and exogenous (xenobiotic) compounds effected by conazole treatment in mouse testis. Conazole treatment group (cnz), fluconazole (F), propiconazole (P), myclobutanil (M), tridimefon (T), (*) increased in liver, (**) decreased in liver, (1) leukotriene metabolism; leukotriene biosynthesis, (2) protein modification, (3) proline catabolism; glutamate biosynthesis, (4) glycolysis, (5) phospholipid biosynthesis; metabolism; phospholipid metabolism, (6) transmembrane receptor protein tyrosine kinase signaling pathway; (7) mesoderm development, (8) protein amino acid phosphorylation, (9) peptidyl-tyrosine phosphorylation, (10) glutathione conjugation reaction, (11) transport, oxidoreductase activity, (12) intracellular signaling cascade, (13) signal transduction, (14) cell cycle, (15) ganglioside biosynthesis, (16) cytoskeleton organization and biogenesis, (17) DNA metabolism; DNA topological change.

Gene Name	GenBank	cnz	Fold Change	p-value	Biological Process
Activator of CREM in testis	NM_021318	F	1.4530	0.006	2,3
Arylsulfatase A	X73230	M	0.7654	0.01	6
5-azacytidine induced gene 1	NM_009734	M	0.6955	0.01	10
Extraembryonic, spermatogenesis, homeobox 1	NM_007957	T	0.6682	0.055	1,2
Feminization 1 homolog a (C. elegans)	BC009161	M	0.7327	0.004	1,2,7
Growth arrest specific 11	NM_018855	F	0.6832	0.014	7,8
Hydroxysteroid dehydrogenase-2, delta<5>-3-beta	M75886	T	1.4542	0.032	5
Mus musculus adult male testis cDNA, RIKEN full-length enriched library, clone:4930404C15, full insert	AK015074	T	0.6856	0.026	
Prostatic steroid binding protein C1	NM_054069	F	0.6272	0.019	
Seminal vesicle secretion 6	NM_013679	M	1.5681	0.037	
T-complex testis-expressed 3	NM_009343	T	1.3357	0.029	1,2
T-complex expressed gene 1	NM_027141	M	0.7451	0.044	4
Tousled-like kinase 2 (Arabidopsis)	NM_011903	P	0.7313	0.006	9

Table 18: Genes involved in testicular function affected by conazole treatment in mouse testis. Conazole treatment group (cnz), fluconazole (F), propiconazole (P), myclobutanil (M), triadimefon (T), (*) increased in liver, (**) decreased in liver, (1) regulation of transcription, (2) DNA-dependenT, (3) electron transport; transcription, (4) intracellular signaling cascade, (5) steroid biosynthesis; C21-steroid hormone biosynthesis, (6) binding of sperm to zona pellucida; physiological processes; metabolism, (7) biological process unknown, (8) sperm motility, (9) protein amino acid phosphorylations, (10) spermatogenesis.

Gene Name	GenBank	cnz	Fold Change	p-value	Biological Process
Apoptotic chromatin condensation inducer in the nucleus	NM_023190	M	0.7219	0	7
Breast cancer 2	NM_009765	M	1.7976	0.011	
Breast cancer 2	NM_009765	T	1.5611	0.044	
Cyclin-dependent kinase 2	NM_016756	M	1.2968	0.027	2,8,9
Cyclin-dependent kinase 2	NM_016756	T	1.3409	0.014	2,8,9
Cyclin E1	NM_007633	T	1.8569	0.037	3,8
CDK2 (cyclin-dependent kinase 2)-asscoaited protein 1	AF396656	P	0.7570	0.038	
Fyn proto-oncogene	NM_008054	T	0.6473	0.021	1, 2, 3, 5
MAD homolog 1 (Drosophila)	U74359	F	1.3315	0.035	10,18
Met proto-oncogene	NM_008591	M	0.6975	0.016	1, 2, 3, 4
Met proto-oncogene	NM_008591	T	0.7221	0.027	1, 2, 3, 4
Proliferation-associated 2G4, 38kD	NM_011119	F	0.6746	0.004	11
RAB3B, member RAS oncogene family	NM_023537	P	1.3272	0.018	6,15
RAD50 homolog (S. cerevisiae)	NM_009012	M	1.3356	0.03	12,17
Ras suppressor protein 1	NM_009105	M	1.5050	0.02	
Synaptonemal complex protein 3	NM_011517	M	1.3198	0.035	9,13
Wnt1 responsive Cdc42 homolog	AB051827	F	1.4078	0.012	14,15
X-ray repair complementing defective repair in Chinese hamster cells 2	NM_020570	F	0.7514	0.047	16,17
RAR-related orphan receptor gamma	NM_011281	M	1.9832	0.007	18
RAR-related orphan receptor gamma	NM_011281	T	1.8222	0.015	18
Cellular retinoic acid binding protein II	BC018397	M	1.5268	0.012	19

Table 19: Cancer and cell cycle related genes affected by conazole treatment on mouse testis. Conazole treatment group (cnz), fluconazole (F), propiconazole (P), myclobutanil (M), triadimefon (T), (*) increased in liver, (**) decreased in liver, (1) cell growth and/or maintenance, (2) protein amino acid phosphorylation, (3) regulation of cell cycle (4) brain development; adult behavior, (5) intracellular signaling cascade, (6) protein transport; intracellular protein transport, (7) apoptotic program, (8) cell cycle, (9) mitosis, (10) SMAD protein heteromerization; regulation of transcription from Pol II promoter; common-partner SMAD protein phosphorylation; organogenesis; BMP receptor signaling pathway, (11) proteolysis and peptidolysis, (12) transport, (13) meiosis, (14) G1/S transition of mitotic cell cycle; regulation of cell shape; RAC protein signal transduction; actin cytoskeleton organization and biogenesis, (15) small GTPase mediated signal transduction, (16) response to DNA damage; DNA recombination, (17) DNA repair, (18) regulation of transcription, DNA-dependent, (19) transport.

Gene Name	GenBank	cnz	Fold Change	p-value	Biological Process
Catalase 1	NM_009804	M	1.3264	0.037	3
Chaperonin subunit 7 (eta)	NM_007638	F	0.6628	0.018	4
Cytochrome b-245, alpha polypeptide	AK021200	T	1.5748	0.039	1,2
Cytochrome c oxidase, subunit Vb	NM_009942	F	1.3833	0.004	5
Diaphorase 4 (NADH/NADPH)	NM_008706	M	1.7332	0.001	5
DnaJ (Hsp40) homolog, subfamily C, member 4	NM_020566	M	0.7512	0.01	
Excision repair cross-complementing rodent repair deficiency, complementation group 4	NM_015769	F	0.7672	0.009	6
Forkhead box J1	L13204	M	0.6638	0.006	7,11,12
Forkhead box O1	AJ252157	F	1.3576	0.035	7,12
Glutathione S-transferase, pi 2	NM_013541	P	1.5748	0.017	13
Heat shock factor 2	NM_008297	F	1.3282	0.011	7,12
Heat shock factor 1	BC013716	T	0.7272	0.011	7,12
Heat shock protein, 70 kDa 4	NM_015765	P	0.7380**	0.008	8
Interleukin 13 receptor, alpha 2	NM_008356	M	1.5373	0.021	9
Tumor necrosis factor receptor superfamily, member 13c	NM_028075	F	0.7075	0.036	10

Table 20: Stress response related genes affected by conazole treatment on mouse testis. Conazole treatment group (cnz), fluconazole (F), propiconazole (P), myclobutanil (M), triadimefon (T), (*) increased in liver, (**) decreased in liver, (1) electron transport, (2) superoxide metabolism, (3) response to oxidative stress; catalase reaction; peroxidase reaction, (4) protein folding, (5) electron transport, (6) nucleotide-excision repair; DNA repair, (7) regulation of transcription, (8) proteolysis and peptidolysis, (9) cell surface receptor linked signal transduction, (10) immune response; biological process unknown, (11) pattern specification, (12) DNA-dependent, (13) glutathione conjugation reaction.

REFERENCES

1. Adachi K, Katsuyama M, Song S, Oka T. (2000) Genomic organization, chromosomal mapping and promoter analysis of the mouse selenocysteine tRNA gene transcription-activating factor (mStaf) gene. *Journal of Biochemistry*. 346: 45-51.

2. Akeno N, Saikatsu S, Kawane T, Horiuchi N. (1997) Mouse Vitamin D-24-Hydroxylase: Molecular Cloning, Tisse Distribution, and Transcriptional Regulation by 1α,25-Dihydroxyvitamin D_3. *Endocrinology*. 138(6): 2233-2240.

3. Andersson U, Yang YZ, Bjorkhem I, Einarsson C, Eggertsen G, Gafvels M. (1999) Thyroid hormone suppresses hepatic sterol 12alpha-hydroxylase (CYP8B1) activity and messenger ribonucleic acid in rat liver: failure to define known thyroid hormone response elements in the gene. *Biochim Biophys Acta*. 1438(2): 167-174.

4. Aoto H, Tsuchida J, Nishina Y, Nishimune Y, Asano A, Tajima S. (1995) Isolation of a novel cDNA that encodes a protein localized to the pre-acrosome region of spermatids. *Eur. J. Biochem*. 234(1): 8-15.

5. Bain PA, Yoo M, Clarke T, Hammon SH, Payne AH. (1991) Mulitple forms of mouse 3β-hydroxysteroid dehydrogenase/ Δ5-Δ4 isomerase and differential expression in gonads, adrenal glands, liver, and kidneys of both sexes. *Proc. Natl. Acad. Sci. USA*. 88: 8870-8874.

6. Barbosa MD, Johnson SA, Achey K, Gutierrez MJ, Wakeland EK, Zerial M, Kingsmore SF. (1995) The Rab protein family: genetic mapping of six Rab genes in the mouse. *Genomics*. 30(3): 439-444.

7. Bondy SC, Naderi S. (1994) Contribution of hepatic cytochrome P450 systems to the generation of reactive oxygen species. *Biochemical Pharmacology*. 48(1): 155-159.

8. Burke MD, Thompson S, Elcombe CR, Halpert J, Haaparanta T, Mayer RT. (1985) Ethoxy-, pentoxy- and benzyloxyphenoxazoles and homologues: a series of substrates to distinguish between different induced cytochromes P-450. *Biochem. Pharmacol*. 34(18): 3337-3345.

9. Buzdar AU. (2002) Anastrazole (Arimidex) in clinical practice versus the old 'gold standard', tamoxifen. *Expert Review of Anticancer Therapy*. 2(6): 623-629.

10. Carreau S, Bourguiba S, Lambard S, Galeraud-Denis I, Genissel C, Bilinska B, Benahmed M, Leallet J. (2001) Aromatase expression in male germ cells. *Journal of Steroid Biochemistry & Molecular Biology*. 79: 203-208.

11. Chiao Y, Cho W, Wang PS. (2002) Inhibition of Testosterone Production by Propylthiouracil in Rat Leydig Cells. *Biology of Reproduction*. 67: 416-422.

12. Choudhary D, Jansson I, Schenkman JB, Sarfarazi M, Stoilov I. (2003) Comparitive expression profiling of 40 mouse cytochrome P450 genes in embryonic and adult tissues. *Archives of Biochemistry and Biophysics*. 414: 91-100.

13. Chuaqui RF, Bonner RF, Best CJM, Gillespie JW, Flaig MJ, Hewitt SM, Phillips JL, Krizman DB, Tangrea MA, Ahram M, Linehan WM, Knezevic V, Emmert-Buck MR. (2002) Post-analysis follow-up and validation of microarray experiments. *Nature Genetics Supplement*. 32: 509-514.

14. Cornwall GA, Hann SR. (1995) Transient appearance of CRES protein during spermatogenesis and caput epididymal sperm maturation. *Molecular Reproduction and Development*. 41(1): 37-46.

15. Cornwall GA, Hsia N. (2002) CRES (cystatin-related epididymal spermatogenic) gene regulation and function. *Zhonghua Nan Ke Xue*. 8(5): 313-318.

16. Di Matteo G, Fuschi P, Zerfass K, Moretti S, Ricordy R, Cenciarelli C, Tripodi M, Jansen-Durr P, Lavia P. (1995) Transcriptional control of the Htf9-A/RanBP-1 gene during the cell cycle. *Cell Growth and Differentiation*. 6(10): 1214-1224.

17. Egaas E, Sandvik M, Fjeld E, Källqvist T, Goksøyr A, Svensen A. (1999) Some effects of the fungicide propiconazole on cytorchrome P450 and glutathione S-transferase in brown trout (*Salmo trutta*). *Comparative Biochemistry and Physiology Part C* 122: 337-344.

18. EPA. (1995) Myclobutanil; Pesticide Tolerances. Federal Register, 60(153): 40500-40503.

19. EPA. (2000) Myclobutanil; Pesticide Tolerances. Federal Register, 65(91): 29963-29973.

20. EPA. (1999) Propiconazole; Establishment of Time-Limited Pesticide Tolerances. Federal Register, 64(51): 13080-13086.

21. EPA. (1996) Triadimefon; Pesticide Tolerances for Emergency Exemptions. Federal Register, 61(232): 63721-63726.

22. EPA. (1994) Triadimenol (Baytan); Pesticide Tolerance. Federal Register Document 94-21256. 40, CFR Part 180.

23. Farhan H, Cross HS. (2002) Transcriptional inhibition of CYP24 by genistein. *Annals of the New York Academy of Sciences*. 973: 459-462.

24. Fleming I. (2001) Cytochrome P450 Enzymes in Vascular Homeostasis. *Circulation Research*. 89: 753-762.

25. Food and Agriculture Organization of the United Nations, Rome (1985): Triadimefon. www.inchem.org

26. Ghannoum M, Rice L. (1999) Antifungal Agents: Mode of Action, Mechanisms of Resistance, and Correlation of These Mechanisms with Bacterial Resistance. *Clinical Microbiology Reviews.* 12(4): 501-517.

27. Gilbert SF. (1997) Developmental Biology 5th Ed.

28. Giordano S, Maffe A, Williams TA, Artigiani S, Gual P, Bardelli A, Basilico C, Michieli P, Comoglio PM. (2000) Different point mutations in the met oncogene elicit distinct biological properties. *Journal of the Federation of American Societies for Experimental Biology.* 14: 401-408.

29. Gottlieb RA, Dosanjh A. (1996) Mutant cystic fibrosis transmembrane conductance regulator inhibits acidification and apoptosis in C127 cells: Possible relevance to cystic fibrosis. *Proceedings of the National Academy of Sciences*. 93: 3587-3591.

30. Halline AG, Davidson NO, Skarosi SF, Sitrin MD, Tietze C, Alpers DH, Brasitus TA. (1994) Effects of 1,25-Dihydroxyvitamin D3 on Proliferation and Differentiation of Caco-2 Cells. *Endocrinology*. 134(4): 1710-1717.

31. Hancock JT, Desikan R, Neill SJ. (2001) Does the redox status of cytochrome C act as a fail-safe mechanism in the regulation of programmed cell death? Free *Radic Biol Med.* 31(5): 697-703.

32. Harada T, Yamaguchi S, Ohtsuka R, Takeda M, Fujisawa H, Yoshida T, Enomoto A, Chiba Y, Fukumori J, Kojima S, Tomiyama N, Saka M, Ozaki M, Maita K. (2003) Mechanisms of promotion and progression of preneoplastiv lesions in Hepatocarcinogenesis by DDT in F344 rats. *Toxicology and Pathology*. 31(1): 87-98.

33. Harris KA, Weinberg V, Bok RA, Kakefuda M, Small EJ. (2002) Low dose ketoconazole with replacement doses of hydrocortisone in patients with progressive androgen independent prostate cancer. *Journal of Urology*. 168(2): 542-545.

34. Hayes JD, Judah DJ, McLellan LI, Kerr LA, Peacock SD, Neal GE. (1991) Ethoxyquin-induced resistance to aflatoxin B1 in the rat is associated with the expression of a novel alpha-class glutathione S-transferase subunit, Yc2, which possesses high catalytic activity for aflatoxin B1-8,9-epoxide. *Journal of Biochemistry.* 15(279): 385-398.

35. He H, Dai F, Yu L, She X, Zhao Y, Jiang J, Chen X, Zhao S. (2002) Identification and characterization of nine novel human small GTPases showing variable expressions in liver cancer tissues. *Gene Expression*. 10(5-6): 231-242.

36. Hess RA, Bunick D, Bahr J. (2001) Oestrogen, its receptors and function in the male reproductive tract – a review. *Molecular and Cellular Endocrinology*. 178: 29-38.

37. Hogdson E, Smart R. (2001) Introduction to Biochemical Toxicology 3rd Ed.

38. Honkakoski P, Negishi M. (2000) Review Article: Regulation of cytochrome P450 (CYP) genes by nuclear receptors. *Journal of Biochemistry*. 347: 321-337.

39. Hunt MC, Yang Y, Eggertsen G, Carneheim CM, Gåfvels M, Einarsson C, Alexson SEH. (2000) The Peroxisome Proliferator-activated Receptor α (PPARα) Regulates Bile Acid Biosynthesis. *The Journal of Biological Chemistry*. 275(37): 28947-28953.

40. Hurley PM, Hill RN, Whiting RJ. (1998). Mode of Carcinogenic Action of Pesticides Inducing Thyroid Follicular Cell Tumors in Rodents. *Environmental Health Perspectives*. 106(8): 437-445.

41. Ko BCB, Lam AKM, Kapus A, Fan L, Chung SK, Chung SSM. (2002) Fyn and p38 Signaling Are Both Required for Maximal Hypertonic Activation of the Osmotic Response Element-binding Protein/ Tonicity-responsive Enhancer-binding Protein (OREBPT/TonEBP). *The Journal of Biological Chemistry*. 277(48): 46085-46092.

42. Kreysing J, Polten A, Lukatela G, Matzner U, von Figura K, Gieselmann V. (1994) Translational Control of Arylsulfatase A Expression in Mouse Testis. *The Journal of Biological Chemistry*. 269(37): 23255-23261.

43. Kukiełka E. Cederbaum AI. (1996) Ferritin Stimulation of Lipid Peroxidation by Microsomes after Chronic Ethanol Treatment: Tole of Cytochrome P4502E1. *Archives of Biochemistry and Biophysics*. 332(1): 121-127.

44. Lavrentiadou SN, Chan C, Kawcak T, Ravid T, Tsaba A, van der Vliet A, Rasooly R, Goldkorn T. (2001) Ceramide-Mediated Apoptosis in Lung Epithelial Cells is Regulated by Glutathione. *Am. J. Respir. Cell Mol. Biol.* 25: 676-684.

45. Lewin B. (2000) Genes VII.

46. Lewis DFV. (2001) Guide to Cytochromes P450 Structure and Function. 1st Ed.

47. Li-Hawkins J, Gåfvels M, Olin M, Lund EG, Andersson U, Schuster G, Björkhem I, Russell DW, Eggertsen G. (2002) Cholic acid mediates negative feedback regulation of bile acid synthesis in mice. *The Journal of Clinical Investigation*. 110(8): 1191-1200.

48. Liu H, Lightfoot R, Stevens JL. (1996) Activation of Heat Shock Factor by Alkylating Agents Is Triggered by Glutathione Depletion and Oxidation of Protein Thiols. *The Journal of Biological Chemistry*. 271(9): 4805-4812.

49. Livak KJ, Schmittgen TD. (2001) Analysis of Relative Gene Expression Data Using Real-Time Quantitative PCR and the $2^{-\Delta\Delta C}{}_T$ Method. *Methods*. 25: 402-408.

50. Luo G, Zeldin DC, Blaisdell JA, Hodgson E, Goldstein JA. (1998) Cloning and Expression of Murine CYP2Cs and Their Ability to Metabolize Arachidonic Acid. *Archives of Biochemistry and Biophysics*. 357(1): 45-57.

51. McGinnity DF, Riley RJ. (2001) Predicting drug pharmacokinetics in humans from in vitro metabolism studies. *Biochemical Society Transactions*. 29(Pt 2): 135-139.

52. Miners JO, Birkett DJ. (June 1998) Cytochrome P4502C9: an enzyme of major importance in human drug metabolism. *British Journal of Clinical Pharmacology*. 45(6): 525-538.

53. Mitra AK, Thummel KE, Kalhorn TF, Kharasch ED, Unadkat JD, Slattery JT. (March 1996) Inhibition of sulfamethoxazole hydroxylamine formation by fluconazole in human liver microsomes and healthy volunteers. *Clinical Pharmacology Therapy*. 59(3): 332-340.

54. Mustonen MVJ, Poutanen MH, Isomaa VV, Vihko PT, Vihko RK. (1997) Cloning of mouse 17β-hydroxysteroid dehydrogenase type 2, and analyzing expression of the mRNAs for types 1, 2, 3, 4 and 5 in mouse embryos and adult tissues. *Biochem. J.* 325: 199-205.

55. Nanji AA, Griniuviene B, Yacoub LK, Sadrzadeh SM, Levitsky S, McCully JD. (1995) Heat-shock gene expression in alcoholic liver disease in the rat is related to the severity of liver injury and lipid peroxidation. *Proc. Soc. Exp. Biol. Med.* 210(1): 12-19.

56. National Center for Biotechnology Information (NCBI) website: http://www.ncbi.nlm.nih.gov

57. Nebert DW, Russell DW. (2002) Clinical importance of the cytochromes P450. *The Lancet*. 360: 1155-1162.

58. Nelson DR. (2003) Comparison of P450s from human and fugu: 420 million years of vertebrate P450 evolution. *Archives of Biochemistry and Biophysics*. 409: 18-24.

59. Nitta H, Bunick D, Hess RA, Janulis L, Newton SC, Millette CF, Osawa Y, Shizuta Y, Toda K, Bahr JM. (1993) Germ Cells of the Mouse Testis Express P450 Aromatase. *Endocrinology*. 132(3): 1396-1401.

60. Office of Prevention, Pesticides and Toxic Substances (1996) Carcinogenicity Peer Review of Bayleton. U.S. EPA, Washington, DC.

61. Ohmori S, Misaizu T, Nakamura T, Takano N, Kitagawa H, Kitada M. (1993) Differential role in lipid peroxidation between rat P450 1A1 and P450 1A2. *Biochemical Pharmacology*. 46(1): 55-60.

62. Okazaki N, Takahashi N, Kojima S, Masuho Y, Koga H. (2002) Protocadherin LKC, a new candidate for a tumor suppressor of colon and liver cancers, its association with contact inhibition of cell proliferation. *Carcinogenesis*. 23(7): 1139-1148.

63. Operon website: http://oligos.qiagen.com

64. Paulus G, Longeart L, Monro AM. (1994) Human Carcinogenic Risk Assessment Based on Hormonal Effects in a Carcinogenicity Study in Rats With the Antifungal Agent, Fluconazole. *Teratogenesis, Carcinogenesis, and Mutagenesis*. 14: 251-257.

65. Pellinen P, Stenback F, Kojo A, Honkakoski P, Gelboin HV, Pasanen M. (1996) Regenerative changes in hepatic morphology and enhanced expression of CYP2B10 and CYP3A during daily administration of cocaine. *Hepatology*. 23(3): 515-523.

66. Peterson JA, Graham SE. (1998) A close family resemblance: the importance of structure in understanding cytochromes P450. *Structure*. 6:1079-1085.

67. Pezzi V, Panno ML, Sirianni R, Forastieri P, Casaburi I, Lanzino M, Rago V, Giordano F, Giordano C, Carpino A, Andò S. (2001) Effects of tri-iodothyronine on alternative splicing events in the coding region of cytochrome P450 aromatase in immature rat Sertoli cells. *Journal of Endocrinology*. 170: 381-393.

68. Pfizer Inc. (1998) Diflucan®: Fluconazole administration. 70-4526-00-7. www.pfizer.com/hml/pi's/diflucanpi.html

69. Pierce RH, Campbell JS, Stephenson AB, Franklin CC, Chaisson M, Poot M, Kavanagh TJ, Rabinovitch PS, Fausta N. (2000) Disruption of Redox Homeostasis in Tumor Necrosis Facto-Induced Apoptosis in a Murine Hepatocyte Cell Line. *American Journal of Pathology*. 157(1): 221-236.

70. Quackenbush J. (Dec. 2002) Microarray data normalization and transformation. *Nature Publishing Group (Review).* 32: 496-501.

71. Rajeevan MS, Vernon SD, Taysavang N, Unger ER. (2001) Validation of Array-Based Gene Expression Profiles by Real-Time (Kinetic) RT-PCR. *Journal of Molecular Diagnostics*. 3(1): 26-31.

72. Rashba-Step J, Cederbaum AI. (1994) Generation of reactive oxygen intermediates by human liver microsomes in the presence of NADPH or NADH. *Mol. Pharmacol*. 45(1): 150-157.

73. Raza H, Robin M, Fang J, Avadhani NG. (2002) Multiple isoforms of mitochondrial Glutathione S-transferase and their differential induction under oxidative stress. *Biochem. J.* 366: 45-55.

74. Reyes JL, Hernandez ME, Melendez E, Gomez-Lojero C. (1995) Inhibitory effect of the antioxidant ethoxyquin on electron transport in the mitpchondrial respiratory chain. *Biochem Pharmacol*. 39(3): 283-289.

75. Reyes JC. (2001) PML and COP1 – two proteins with much in common. *Trends in Biochemical Sciences*. 26(1): 18-20.

76. Roman RJ. (2002) P-450 Metabolites of Arachidonic Acid in the Control of Cardiovascular Function. *Physiology Review*. 82: 131-185.

77. Ronis MJ, Celander M, Badger TM. (1998) Cytochrome P450 enzymes in the kidney of the bobwhite quail (Colinus virginianus): induction and inhibition by ergorsterol biosynthesis inhibiting fungicides. *Comparative Biochemistry and Physiology Part C* 121: 221-229.

78. Ronis MJ, Ingleman-Sundberg M, Badger TM. (Nov. 1994) Induction, suppression and inhibition of multiple hepatic cytochrome P450 isozymes in the male rat and bobwhite quail (Colinus virginianus) by ergosterol biosynthesis inhibiting fungicides (EBIFs). *Biochemical Pharmacology*. 48(10): 1953-1965.

79. Russell LD, Ettlin RA, Sinha Hikim AP, Clegg ED. (1990) Histological and Histopathological Evaluation of the Testis 1st Ed. Clearwater, FL: Cache River Press.

80. Sanderson JT, Boerma J, Lansbergen GWA, van den Berg M. (2002) Induction and Inhibtion of Aromatase (CYP19) Activity by Various Classes of Pesticides in H295R Human Adrenocortical Carcinoma Cells. *Toxicology and Applied Pharmacology*. 182: 44-54.

81. SAS Institute Inc. (1999), SAS/STAT User's Guide, Version 8, Cary, NC: SAS Institute Inc.

82. Schlüter G, Schmidt U. (1988) Toxicology of azoles. Institute for Toxicology – Pharma and Institue for Toxicology – Agrochemicals, Bayer AG, FRG.

83. Schmidt U. (1983) Interaction of triadimefon with liver microsomes, studies on rat and mouse *in vivo* and *in vitro*. Bayer Ag, Institute for Toxicology, Report No. 11812 submitted to WHO by Bayer AG. (unpublished).

84. Seddon B, Zamoyska R. (2002) TCR signals mediated by Src family kinases are essential for the survival of naïve T cells. *Journal of Immunology*. 169(6): 2997-3005.

85. Shalom S, Don J. (1999) Tlk, a novel evolutionarily conserved murine serine threonine kinase, encodes multiple testis transcripts. *Mol Reprod Dev*. 52(4): 392-405.

86. Shetty G, Krishnamurthy H, Krihnamurthy HN, Bhatnagar AS, Moudgal NR. (1998) Effect of long-term treatment with aromatase inhibitor on testicular function of adult male bonnet monkeys (M. radiata). *Steroids*. 63(7-8): 414-420.

87. Shrikhande S, Friess H, Issenegger C, Martignoni ME, Yong H, Gloor B, Yeats R, Kleeff J, Büchler MW. Fluconazole Penetration into the Pancreas. *Antimicrobial Agents and Chemotherapy*. 44(9): 2569-2571.

88. Sousa MM, Saraiva MJ. (2001) Internalization if Transthyretin. *The Journal of Biological Chemistry*. 276(17): 14420-14425.

89. Student's t-test website: http://www.physics.csbsju.edu/cgi-bin/stats/t-test

90. Su C, Chong K, Edelstein K, Lille S, Khardori R, Lai C. (1999) Constitutive hsp 70 Attenuates Hydrogen Peroxide-Induced Membrane Lipid Peroxidation. *Biochemical and Biophysical Research Communications*. 265: 279-284.

91. Tantibhedhyangkul J, Weerachatyanukul W, Carmona E, Xu H, Anupriwan A, Michaud D, Tanphaichitr N. (2002) Role of Sperm Surface Arylsulfatase A in Mouse Sperm-Zona Pellucida Binding. *Biology of Reproduction*. 67: 212-219.

92. Tiboni GM, Iammarrone E, Giampietro F, Lamonaca D, Bellati U, Di Ilio C. (1999) Teratological Interaction Between the Bis-Triazole Antifungal Agent Fluconazole and the Anticonvulsant Drug Phenytoin. *Teratology*. 59: 81-87.

93. Vallet V, Antoine B, Chafey P, Vandewalle A, Kahn A. (1995) Overproduction of a Truncated Hepatocyte Nuclear Factor 3 Protein Inhibits Expression of Liver-Specific Genes in Hepatoma Cells. *Molecular and Cellular Biology*. 15(10): 5453-5460.

94. Vanden Bossche H, Marichal P, Gorrens J, Coene M-C. (1990) Biochemical basis for the activity and selectivity of oral antifungals drugs. *Br J Clin Pract Suppl* 71: 41-46.

95. Veal EA, Toone WM, Jones N, Morgan BA. (2002) Distinct Roles for Glutathione D-Transferases in the Oxidative Stress Response in *Schizosaccharomyces pombe*. *The Journal of Biological Chemistry*. 277(38): 35523-35531.

96. Ventura-Holman T, Seldin MF, Li W, Maher JF. (1998) The murine fem1 gene family: homologs of the Caenorhabditis elegans sex-determination protein FEM-1. *Genomics*. 54(2): 221-230.

97. Vinggaard AM, Breinholt V, Larsen JC. (1999) Screening of selected pesticides for oestrogen receptor activation in vitro. *Food Addit Contam*. 16(12): 533-542.

98. Vinggaard AM, Hnida C, Breinholt V, Larsen JC. (2000) Screening of Selected Pesticides for Inhibition of CYP19 Aromatase Activity *In Vitro*. *Toxicology in Vitro*. 14: 227-234.

99. Waller DP, Martin A, Vickery BH, Zaneveld LJ. (1990) The effects of ketoconazole on fertility of male rats. *Contraception*. 41(4): 411-417.

100. Wassler M, Syntin P, Sutton-Walsh HG, Hsia N, Hardy DM, Cornwall GA. (2002) Identification and characterization of cystatin-related epididymal spermatogenic protein in human spermatozoa: localization in the equatorial segment. *Biology of Reproduction*. 67(3): 795-803.

101. WHO and FAO. (1983) Triadimefon: Pesticide Residues in Food, Evaluations 1983. *INCHEM documents*. #643.

102. Yang YH, Dudoit S, Luu P, Speed T. (2002) Normalization for cDNA microarray data: a robust composite method addressing single and multiple slide systematic variation. *Nucleic Acids Research*. 30(4): e15.

103. Yang Y, Zhang M, Eggertsen G, Chiang JY. (2002) On the mechanism of bile acid inhibition of rat sterol 12alpha-hydroxylase gene (CYP8B1) transcription: roles of alpha-fetoprotein transcription factor and hepatocyte nuclear factor 4alpha. *Biochim Biophys Acta*. 1583(1): 63-73.

104. Zarn JA, Brüschweiler BJ, Schlatter JR. (2003) Azole Fungicides Affect Mammaliam Steroidogenesis by Inhibiting Sterol 14α-Demethylase and Aromatase. *Environmental Health Perspectives*. 111(3): 255-261.

APPENDIX

Hepatic Microsomal Alkoxyresorufin Dealkylase Activities Induced in Rats and Mice by Tumorigenic and Non-Tumorigenic Triazole Conazoles[§]

Guobin Sun[1], Amber K. Goetz*, Douglas B. Tully[1], Guy R. Lambert[1], David J. Dix[1], and Stephen Nesnow[1]**

*Amber Goetz is a North Carolina State University trainee under U.S. EPA Cooperative Research Agreement No. CT826512010.

[1] National Health and Environmental Effects Research Laboratory, Office of Research and Development, U.S. Environmental Protection Agency, Research Triangle Park, NC 27711, USA

[§] The research described in this article has been reviewed by the National Health and Environmental Effects Research Laboratory, US Environmental Protection Agency, and approved for publication. Approval does not signify that the contents necessarily reflect the views and the policies of the Agency, nor does mention of trade names or commercial products constitute endorsement or recommendation for use.

**To whom correspondence requests for reprints and editorial correspondence should be addressed, E-mail: nesnow.stephen@epa.gov

Abstract

Conazoles are N-substituted azole antifungal agents used as both pesticides and drugs. Some of these compounds are hepatotumorigenic in mice and some can induce thyroid tumors in rats. Many of these compounds are able to induce and/or inhibit mammalian hepatic cytochrome P450s that are responsible for the metabolism of endogenous as well as exogenous compounds including drugs and xenobiotic chemicals. Since both thyroid and liver cancers have been associated in part with alterations in P450 and related enzyme activities, we sought to examine P450s activity profiles induced by tumorigenic and non-tumorigenic triazole-containing conazoles: fluconazole, myclobutanil, propiconazole, and triadimefon. Sprague-Dawley rats and CD-1 mice were treated with the four conazoles at tumorigenic and non-tumorigenic doses by gavage daily for 14 days: fluconazole (2, 25, and 50 mg/kg body weight), myclobutanil (10, 75, and 150 mg/kg body weight), propiconazole (10, 75, and 150 mg/kg body weight), or triadimefon (5, 50, and 115 mg/kg body weight). Four alkoxyresorufin O-dealkylation (AROD) assays were used as measures of P450 enzyme activities. All four conazoles significantly induced pentoxyresorufin O-dealkylation (PROD) and benzyloxyresorufin O-dealkylation (BROD) at the mid and high doses in liver microsomes from mice. In rats, propiconazole, triadimefon, and myclobutanil also induced PROD and BROD activities at mid and high doses, while fluconazole induced PROD and BROD activities at the high dose only. No induction or slight induction of methoxyresorufin O-dealkylation or ethoxyresorufin O-dealkylation was detected in both species. Based on the associations between AROD specificities in induced liver microsomes, our results indicated that these four triazole-based conazoles induced cytochrome 2B and/or 3A families of isozymes. BROD and PROD fold-inductions were highly correlated within rats and within mice, suggesting that the two substrates were responding to similar groups of isozymes. The levels of induction of AROD activities were the greatest for PROD and BROD activities in triadimefon-treated rats at a dose that induced thyroid tumors. These levels were greater than 2-fold that obtained from rats treated with the three other conazoles at doses that did not induce tumors, suggesting a possible relationship between P450 and related activities and the thyroid tumors. In the mice no associations could be made between AROD induction patterns and hepatotumorigenic activity.

Key words: fluconazole; myclobutanil; propiconazole; triadimefon; cytochrome P450; alkoxyresorufin O-dealkylation

1. Introduction

Conazoles are N-substituted azole antifungal agents that are in the class of ergosterol biosynthesis inhibiting fungicides and are used as both pesticides and drugs (Hutson, 1998; Sheehan *et al.*, 1999). Some of these compounds are hepatotumorigenic in mice and some can induce thyroid tumors in rats (Hurley, 1998; Medical Economic Company, 1998; California EPA, 2003; Cornell University, 2003). While the mode of antifungal action of conazoles has been demonstrated to be the inhibition of CYP51 (lanosterol-14-α-demethylase)(Vanden Bossche *et al.*, 1987; Hutson, 1998; Lamb *et al.*, 2001; Zarn *et al.*, 2003), the modes of conazole-based toxicity and tumorigenicity are not known. It has been shown that many N-substituted azoles are able to induce and/or inhibit mammalian hepatic cytochrome P450s (Houston *et al.*, 1988; Leslie *et al.*, 1988; Harmsworth and Franklin, 1990; Maurice *et al.*, 1992; Ronis *et al.*, 1994; Ronis *et al.*, 1998; Slama *et al.*, 1998; Egaas *et al.*, 1999; Suzuki *et al.*, 2000; Kobayashi *et al.*, 2001). P450s are responsible for the metabolism of endogenous (e.g. steroids) as well as exogenous compounds including drugs and xenobiotic chemicals. Induction of P450-mediated metabolism can lead to the metabolic activation of carcinogens and drugs whose metabolites might exert toxic or carcinogenic effects. Alternatively, induction of P450 enzymes can lead to increased metabolism and hepatic clearance of substrates, reducing toxicity. Inhibition of P450 enzymes can decrease metabolism and hepatic clearance of substrates metabolized by that specific isoenzyme, and inhibition of specific steroidogenic P450s (e.g. CYP19) is associated with adverse effects on development and reproduction (Cummings *et al.*, 1997; Zarn *et al.*, 2003).

Although many N-substituted azoles have been studied regarding their ability to induce P450s from different sources, most of the research has focused on imidazole-containing compounds. In this regard, only a few triazole-containing antifungal agents have been studied *in vivo* in rats and mice. The objective of this study was to perform a systematic analysis of the profiles of mouse and rat hepatic P450 induction by four triazole-containing conazoles at tumorigenic and non-tumorigenic doses to look for similarities or differences in induction patterns. Four conazoles were studied: myclobutanil, fluconazole, propiconazole, and triadimefon (Fig. 1). Each conazole had been previously tested in manufacturer-sponsored bioassays in mice and rats and the data reported to regulatory authorities. Myclobutanil was selected because it was not tumorigenic in mice or rats (California EPA,

2003). Fluconazole and propiconazole were selected because they were hepatotumorigenic in mice (Medical Economic Company, 1998; California EPA, 2003). Triadimefon was selected because it induced rat thyroid tumors and mouse liver tumors (Hurley, 1998; California EPA, 2003). Alkoxyresorufin O-dealkylation (AROD) methods were used as measures of P450 enzyme activities and ethoxyresorufin O-dealkylation (EROD), pentoxyresorufin O-dealkylation (PROD), methoxyresorufin O-dealkylation (MROD), and benzyloxyresorufin O-dealkylation (BROD) activities were measured in microsomes from treated rodents. The different alkoxyresorufins have some specificities towards specific cytochromes. Therefore, AROD methods, in general (with some exceptions), can identify the cytochrome type. It has been found that EROD activity was associated with CYP1A1, PROD activity was associated with CYP2B1, MROD activity was associated with CYP1A2, and BROD activity was associated with several CYPs including CYP2B and CYP3A families (Burke *et al.*, 1994). This paper is the first in a series that seeks to define toxicological modes of action of conazoles using traditional, genomic, and proteomic approaches.

2. Materials and methods

2.1. Materials

Ethoxyresorufin, pentoxyresorufin, methoxyresorufin, benzyloxyresorufin, resorufin, β-nicotinamide adenine dinucleotide phosphate (NADP, 98%), glucose-6-phosphate (98%), glucose-6-phosphate dehydrogenase, KCl, $MgCl_2$, K_2HPO_4, $CuSO_4 \cdot 5H_2O$, DL-dithiothreitol (Cleland's Reagent, 99%), EDTA (99.8%), glycerol (99%), sucrose (99.5%), bovine serum albumin, Folin-Ciocalteau reagent, and K-Na tartrate (99%) were purchased from Sigma Chemical Co. (St. Louis, MO). Na_2CO_3 and Na_2HPO_4 were purchased from Fisher Scientific International Inc. (Fairlawn, NJ). Propiconazole was a gift from Syngenta Crop Protection Inc. Fluconazole and myclobutanil were obtained from LKT Laboratories Inc. (St. Paul, MN). Triadimefon was a gift from Bayer Crop Sciences.

2.2. Conazole purity analyses

Each conazole was dissolved in dichloromethane and analyzed by GC-MS using a Finnigan Voyager GC-MS system (San Jose, CA). One-microliter injections of the analytes

were made by autosampler onto a Phenomenex (Torrance, CA) Zebron ZB-5 capillary column (30 m x 0.25 mm ID x 0.25 μm film thickness). Helium was used as the carrier gas at a constant flow of 1 ml/min. The injector was operated in splitless mode at 250 ˚C for 1 minute at which time the split valve was opened and the injector was swept with a split flow of 50 ml/min. The initial oven temperature was set at 35 ˚C and held for 5 min. The oven temperature was then raised to 300 ˚C at a rate of 10 ˚C/min. The final temperature was held for 10 minutes. Full scan electron impact mass spectral data was collected from 65–485 amu at a rate of 2.5 scans/sec. Mass calibration was performed using perfluorotributylamine. A dichloromethane blank was run prior to each conazole.

2.3. Animal treatment

Adult male CD-1 mice at postnatal day (PND) 35-39 and adult male Sprague-Dawley rats at PND 43 were obtained from Charles River Laboratories. All animals were acclimated for at least 10 days before dosing and singly housed in the animal facility with a 12:12-h light:dark cycle under controlled temperature (22 ˚C) and humidity (45%) with ad libitum access to feed and water. The animals were assigned to treatment groups by randomization to insure equivalent body weight means across the dose groups prior to dosing. Each experimental group consisted of six animals treated with a given test compound and eighteen animals treated with the respective vehicle solvent as controls. Each conazole was dissolved in a 7.5% Alkamuls EL-620 (an ethoxyated castor oil) (Rhodia-USA, Cranbury, NJ)/distilled water solution for mice or a 15% Alkamuls EL-620/ distilled water solution for rats. The mice were dosed from PND50 to PND64. The rats were dosed from PND 60 to PND74. All treatments were administered by gavage each morning. Mice received dosing volumes of 10 ml/kg and rats 5 ml/kg of conazole solutions. Propiconazole treatment groups received 10, 75, or 150 mg/kg/day (0.10, 0.75, or 1.50% solution for mice; 0.20, 1.50 or 3.00% solution for rats). Fluconazole treatment groups received 2, 25, or 50 mg/kg/day (0.02, 0.25, 0.50% solution for mice; 0.04, 0.50 or 1.00% solution for rats). Triadimefon treatment groups received 5, 50, or 115 mg/kg/day (0.05, 0.50, 1.15% solution for mice; 0.10, 1.00, 2.30% solution for rats). Myclobutanil treatment groups received 10, 75, or 150 mg/kg/day (0.10, 0.75, 1.50% solution for mice; 0.20, 1.50 or 3.00% solution for rats). Rats and mice were treated for 14 consecutive days with each conazole. Twenty-four hr after the last dose the

animals were sacrificed and the livers harvested. Due to the size of this study, the dosing was conducted in two separate parts in order to evaluate all four conazoles. Each part consisted of two conazoles and a vehicle control (part one: fluconazole and propiconazole, part two: triadimefon and myclobutanil). At the end of part one dosing, the mice were euthanized using an intraperitoneal injection of Nembutal (pentobarbital) at 90 mg/kg body. This was done to collect blood samples for studies not reported in this paper. At the end of part two dosing mice were euthanized using CO_2. Rats in both part one and part two segments were sacrificed by guillotine. The livers were removed immediately, weighed, cooled in ice, and microsomes prepared. All aspects of the study were conducted in facilities certified by the American Association for Accreditation of Laboratory Animal Care in compliance with the guidelines of that association and the EPA/NHEERL Animal Care Committee.

2.4. Dose selection

The doses selected for each conazole were based on those used in the chronic cancer bioassays. For tumorigenic conazoles, the lowest doses that induced tumors in the chronic cancer bioassays were selected as the highest dose in these studies. For non-tumorigenic conazoles the highest dose tested was used (California EPA, 2003; Cornell University, 2003).

2.5. Preparation of rat and mouse liver microsomes

Four animals from each group were randomly chosen for liver microsomal AROD assays. Rat and mouse liver microsomes were prepared as described with some modifications (Matsuura et al., 1991). Briefly, the fresh liver was washed with cold 1.15% KCl and 0.25 M sucrose and minced into small pieces. The liver was transferred to a cold Beckman centrifuge tube, to which 15 ml of cold 0.25 M sucrose was added. The sample was homogenized on ice with a tissue tearer and centrifuged at 9,000 X g for 20 min at 4 °C in a Beckman L8 70 Ultracentrifuge. The supernatant was transferred to a Beckman centrifuge tube and centrifuged at 105,000 X g for 60 min at 4 °C. The supernatant was discarded and the pellets were scraped into a homogenizing vessel containing cold storage buffer (pH,7.5, K_2HPO_4: 10 mM, DTT: 0.1 mM, EDTA: 1 mM, glycerol: 20% (v/v)) diluted 1:1 with cold 0.25 M sucrose. The pellets were resuspended by hand manipulation. The

resulting microsomal suspension was aliquoted into Nunc vials (Nunc-Nalgene, Rochester, NY) and stored in liquid nitrogen until the assays were performed. The protein levels in the microsomes were determined by the Lowry assay (Lowry et al., 1951). Bovine serum albumin was used as the protein standard.

2.6. Alkoxyresorufin O-dealkylation (AROD) assays

AROD activities of liver microsomes were measured using the method described by Burke et al. (Burke et al., 1985) with some modifications. The reaction mixture (in a 4.5-ml 4-clear-sided methacrylate cuvette, FisherBrand) containing sodium phosphate buffer (0.1 M, pH, 7.4), $MgCl_2$ (3.3 mM), alkoxyresorufin (4.9 μM), NADP (78 mM), glucose-6-phosphate (198 mM), and glucose-6-phosphate dehydrogenase (24 U/ml) was incubated at 37 °C for 2 minutes. Liver microsomes were added to the mixtures to initiate the reaction (final concentration of microsome ~0.1 mg protein/ml). The final volume of the mixture was 3 ml. The fluorescence intensity of the mixture was measured at 37 °C on a Perkin-Elmer LS-50 fluorometer with an excitation wavelength of 550 nm and an emission wavelength of 585 nm. Data were collected every 3 seconds for 5 minutes and slopes obtained. AROD activities were expressed as the rate of resorufin formation and were calculated based on the fluorescence of resorufin standards. Each sample was assayed in duplicate. Variability in the duplicates was less than 10%.

2.7. Statistics

Statistical analyses of animal body and liver weights (6 animals/group and 18 animals for control) were performed by analysis of covariance (Shirley, 1977) using SAS Proc-GLM (SAS, Cary, NC). The data are presented as mean ± SD. Statistical analyses of AROD assay data (4 animals/group) were performed by Dunnett's multiple comparison method using SigmaStat (SPSS, Chicago, IL). Differences between treatment and control groups were considered statistically significant when $P < 0.05$. The AROD data are presented as mean ± SD.

3. Results

3.1. Conazole purity analyses

The purity analyses of the conazoles were performed by GC-MS. Myclobutanil eluted as a single peak at retention time (RT) 26.07 with no impurities observed and with the correct monoisotopic mass (*m/z* = 288.1). Triadimefon eluted as a single peak at RT 24.13 min with no impurities detected and with the correct monoisotopic mass (*m/z* = 293.1). Propiconazole afforded two major peaks observed in the chromatogram at 27.26 and 27.38 min with small amounts of impurities present (0.007%), consistent with the two diastereomeric forms of this agent and a monoisotopic molecular fragment mass of *m/z* = 259.0. Fluconazole eluted as one peak observed in the chromatogram at 25.63 min with no impurities present with a protonated monoisotopic mass of *m/z* = 307.

3.2. Effects of conazoles on body and liver weights in rats and mice

Propiconazole, fluconazole, triadimefon, and myclobutanil had no effect on rat or mouse body weights after 14 days of treatment (Table 1). Rat liver weights were increased by propiconazole, fluconazole, and triadimefon at mid and high doses in a dose-related manner. Myclobutanil increased rat liver weights at mid and high doses without a dose response. Mouse liver weights were increased by mid and high doses of propiconazole and fluconazole in a dose-related manner. Myclobutanil increased mouse liver weights at the mid dose, and triadimefon had no effect on mouse liver weights.

3.3. Effects of conazoles on hepatic AROD activities in conazole-treated rats

The effects of propiconazole, fluconazole, triadimefon, and myclobutanil on rat liver microsomal AROD activities are shown in Table 2. All four conazoles produced significant increases in BROD and PROD activities at the high dose and all but fluconazole produced significant increases in BROD and PROD activities at the mid dose. No significant AROD induction occurred at low doses of any conazole. Triadimefon produced the greatest activities of BROD and PROD of all the four conazoles at the highest dose. However, triadimefon had no effect on the induction of EROD and MROD activities. Qualitatively, myclobutanil presented a similar pattern as triadimefon, inducing BROD and PROD but not EROD and MROD activities. Propiconazole significantly induced BROD and PROD activities at the mid and high doses. It also induced some EROD and MROD activities.

Fluconazole was similar to propiconazole, inducing BROD, PROD, and EROD activities at the highest dose tested. In general, the induction of AROD activities for each of the four conazoles appeared to be dose dependent. Quantitatively within conazoles, BROD activities were greater than PROD activities for fluconazole, triadimefon, and myclobutanil. BROD activities for the four conazoles measured as fold induction ranged from 3.32 (propiconazole) to 27.7-fold (triadimefon), while PROD activities measured as fold induction for the four conazoles ranged from 5.19 (fluconazole) to 18.5-fold (triadimefon). The correlations between BROD and PROD activities were examined for all conazoles at all doses (Fig. 2A). BROD and PROD induction activities were highly correlated in conazole-induced AROD activities in rats with a correlation coefficient of 0.952. The highest dose of the thyroid tumorigenic conazole, triadimefon produced a 27.7-fold induction of BROD and a 18.5-fold induction of PROD. The other non thyroid tumorigenic conazoles (myclobutanil, fluconazole, and propiconazole) induced BROD and PROD activities to less than one-half that of triadimefon.

3.4. Effects of conazoles on hepatic AROD activities in conazole-treated mice

The effects of propiconazole, fluconazole, triadimefon, and myclobutanil on mouse liver microsomal AROD activities are shown in Table 3. Fluconazole and myclobutanil produced significant increases in all four AROD activities at the mid and high doses. Propiconazole produced significant induction in BROD, PROD, and MROD, but not EROD activities at mid and high doses. Triadimefon significantly induced BROD and PROD, but not EROD and MROD activities. As observed with the rats, BROD activities exceeded those of PROD. BROD fold induction ranged from 2.41 (triadimefon) to 7.24 (fluconazole). PROD fold induction ranged from 1.90 (triadimefon) to 8.68 (fluconazole). The induction of AROD activities for each conazole was dose-dependent. No significant AROD induction occurred at the low dose except for fluconazole treatment. The correlations between BROD and PROD activities were examined for all conazoles at all doses (Fig. 2B). A high correlation was found between BROD and PROD induction in mice with a correlation coefficient of 0.943. Triadimefon and propiconazole, the two hepatotumorigenic conazoles, induced BROD activities of 2.41-fold and 3.84-fold respectively at tumorigenic doses, while

fluconazole and myclobutanil, the two non hepatotumorigenic conazoles, induced BROD activities of 7.24-fold and 2.74-fold, respectively.

The expected lower control activities for PROD and BROD in mice in part one compared to part two was probably due to the residual Nembutal (pentobarbital) carried over to the microsomes as it was administered to the mice immediately prior to sacrifice. Pentobarbital was used to anesthetize the mice in part one during the cardiac puncture procedure. Pentobarbital is metabolized by mice *in vivo* (Rosin and Martin, 1983) and by rat liver microsomes (Jacobson *et al.*, 1973) to a series of hydroxylated products and can serve as an inhibitor of other P450 substrates including alkoxyresorufins. The extent of inhibition of AROD by pentobarbital is assumed to be similar in the microsomes from control and conazole treated mice. Therefore, the normalized enzyme activities (fold-induction) should not have been affected and can be compared between the four conazoles. It is interesting to note that the extents of induction were similar between rats and mice treated with propiconazole and the same was observed with fluconazole.

4. Discussion

The dealkylations of alkoxyresorufins are widely used methods for measuring cytochrome p450 activities and they provide partial identification of the specific cytochromes involved in their metabolism (Burke *et al.*, 1985; Nerurkar *et al.*, 1993; Burke *et al.*, 1994). Burke *et al.* (burke *et al.*, 1994) have reported a thorough study on cytochrome p450 specificities of alkoxyresorufin o-dealkylations. They used a series of resorufins with different chain lengths, and examined the dealkylation activities of both purified rat liver p450s and microsomes from rats treated with p450 inducers. They also confirmed their findings with antibody inhibition, and chemical inhibitor studies. In summary, they found that EROD was associated with cyp1a1, the predominant form found in liver microsomes from 3-methylcholanthrene-induced rats and inhibited by α-naphthoflavone. However, in microsomes from phenobarbital-induced rats, EROD activity was associated with cyp2b1 and in microsomes from control rats, erod activity was associated with cyp2c6. MROD activity was associated with cyp1a2, a form found in 3-methylcholanthrene-induced and isosafrole-induced rat liver microsomes and inhibited by furafylline. MROD activity was not an accurate indicator of cyp1a2 in phenobarbital-induced rat liver microsomes. Prod activity

was an excellent indicator of cyp2b1 in phenobarbital-induced rat liver microsomes, but not in control microsomes. BROD was found to measure several p450 forms. In phenobarbital-induced rat liver microsomes it detected mainly cyp2b1 with some cyp2c6 and cyp3a1/2 activities. In 3-methcholanthrene-induced rat liver it detected cyp1a1. Burke *et al.* (burke *et al.*, 1994) concluded that the AROD specificities were dependent on the type of induced CYPs in microsomes. Using the study by burke *et al*. (burke *et al.*, 1994) and based on the specificities of ARODs in rat liver microsomes, we interpret our results to indicate that the AROD induction patterns of fluconazole, myclobutanil, propiconazole, and triadimefon in rats are consistent with the induction of cyp2b and possibly cyp3a families of isozymes. This would explain the observed large increases in PROD and BROD activities and in some cases the small increases in EROD. There is less information on AROD activities and specific mouse liver cytochromes. However, it has been shown that hepatic microsomal prod and BROD activities from phenobarbital-treated mice are partially inhibited by monoclonal antibodies inhibitory for cyp2b1/2b2. Therefore we concluded that cyp2b forms are induced by these conazoles in mice (Nerurkar *et al.*, 1993). The high correlations of BROD and PROD inductions within mice and within rats demonstrate that both AROD substrates are detecting the same group of isoforms in the conazole-induced livers. This is not an uncommon finding as some chlorinated aromatic compounds and nitrogenous drugs (both with some structural similarities to the conazoles) such as methoxychlor (Oropeza-Hernandez *et al.*, 2003) and several benzodiazepines (Nims *et al.*, 1997) induced both BROD and PROD activities to significant extents in male rat liver.

Of the four conazoles examined here, only the effects of propiconazole on p450 in rats have been reported previously in two studies. Sprague-Dawley rats were treated daily by gavage for 3 days with propiconazole (400 mg/kg/day), the livers harvested 48 later, and the effects on p450 were measured (Ronis *et al.*, 1994). Propiconazole induced p450, cytochrome b_5 and p450 reductase protein content and induced prod, BROD, EROD, and MROD activities. Cyp3a-dependent erythromycin n-demethylase activity was also induced by propiconazole. Western blot analyses revealed large increases in cyp3a and cyp2b1 proteins and smaller increase in cyp1a1 protein. In the second study, hepatic microsomal activities were reported from male Sprague-Dawley rats after 7 days of propiconazole treatment by intraperitoneal administration (Leslie *et al.*, 1988). Microsomes were prepared

24 hr after the last treatment. These authors reported significant increases in p450 protein contents by propiconazole treatment and induced activities for aldrin epoxidase, aminopyrine-n-demethylase, ethoxycoumarin o-deethylase, and erod at a dose of 100 mg/kg/day. Aldrin epoxidase, and ethoxycoumarin o-deethylase have been associated with cyp2b (Guengerich *et al.*, 1982), and aminopyrine-n-demethylase activity has been associated with cyp3a (Bauer *et al.*, 1994). Qualitatively, our results and conclusions for propiconazole are consistent with the previous reports (Leslie *et al.*, 1988; Ronis *et al.*, 1994). The quantitative differences in AROD induction patterns between those studies and the results reported here can be reasonably attributed to the different treatment conditions (dose, route of administrations, treatment times, and harvest times) used in the three studies. Propiconazole has been reported to induce some of the same p450s as phenobarbital (Leslie *et al.*, 1988). Waxman and Azaroff (Waxman and Azaroff, 1992) have shown that the same isozymes (cyp2b1, cyp2b2, cyp3a1, and cyp3a2) are inducible by phenobarbital in male rats. However, the p450 induction pattern in rat liver induced by propiconazole cannot be attributed to phenobarbital-inducible isozymes alone (Leslie *et al.*, 1988).

In the present work, we studied the effects of triadimefon, propiconazole, myclobutanil, and fluconazole on hepatic cytochrome P450s in mice and rats by use of ARODs as probes for P450 activities. Both triadimefon and propiconazole were hepatocarcinogenic in mice. Triadimefon was also a rat thyroid carcinogen, while myclobutanil and fluconazole were not carcinogenic in rats and mice. We selected these four compounds with the goal of comparing their modulation of liver P450s with their toxicological effects at doses that were toxicologically significant. While propiconazole and triadimefon were hepatocarcinogenic in mice and myclobutanil and fluconazole were not, the observed patterns of AROD induction were similar for all four conazoles. At this level of analysis, the overall induction profiles and levels of induction of AROD activities do not seem to correlate with their hepatocarcinogenic activities.

Triadimefon is the only one among these four conazoles that induces rat thyroid tumors. Although there are many mechanisms that lead to thyroid cancer, thyroid tumors can be induced by overproduction of TSH (thyroid-stimulating hormone) as part of a negative feedback loop in the pituitary-hypothalamus thyroid axis (Hurley, 1998). Overproduction of TSH has been associated with the increased metabolism of thyroxine by the phase ii enzyme,

UDPGT (uridine diphosphate glucuronyl transferase). While UDPGT activities were not measured in this study, co-induction of UDPGT with p450 enzymes has been reported (Bock *et al.*, 1990; Hanioka *et al.*, 1995; Siess *et al.*, 1997). Since triadimefon induced AROD activities to a much greater extent in the rat than the other three conazoles, we suggest that one explanation for the different rat thyroid carcinogenic activities of the four conazoles studied may be through the over-induction of UDPGT. Whether UDPGT is co-induced with p450s by triadimefon requires further study.

As previously noted, the AROD probes are not selective enough to definitively distinguish between the different P450s. Further resolution of the relationships between P450 activities and toxicological activities of these conazoles should come from microarray gene expression studies, antibody inhibition studies, and RT-PCR studies. These approaches may help to identify specific P450s induced by these conazoles and their potential roles in the tumorigenesis process. It must be noted that this analysis has only focused on a limited number of the many CYPs found in rat and mouse livers. These assays would not detect CYPs involved in steroid biosynthesis, or the biosyntheses of other endogenous compounds. More extensive analyses of the effects of these four conazoles on CYP expression will come from microarray gene expression analyses and RT-PCR studies that are currently underway.

ACKNOWLEDGEMENTS

We would like to thank Alvin Moore (Charles River Laboratory, Raleigh, NC) and Vivian Wilson (Priority One Services) for excellent animal care support, and Judy Schmid (US EPA) for assistance in statistical analyses. We thank Rhodia USA for the gift of Alkamuls EL620. We also thank Jim Stevens of Syngenta CropScience for the gift of propiconazole, and Ghona Sangha of Bayer CropScience for the gift of triadimefon. We thank Rex Pegram and Jeff Ross (US EPA) for their reviews of this manuscript. Finally, we also thank the many other members of the P450/Conazole Research Program Project at the US EPA, who contributed to the execution of this study.

Table 1. The effects of propiconazole, fluconazole, triadimefon, and myclobutanil on body and liver weights in rats and mice[a]

Conazole	Dose (mg/kg body weight)	Mice			Rat		
		Body weight (g)	Liver		Body weight (g)	Liver	
			Weight (g)	P[b]		Weight (g)	P[b]
Propiconazole	Control	35.7 ± 1.7	2.13 ± 0.19		407 ± 36	16.0 ± 1.7	
	10	34.4 ± 1.4	2.00 ± 0.06	0.621	406 ± 25	16.0 ± 1.1	0.818
	75	34.6 ± 2.0	2.44 ± 0.20	0	406 ± 21	18.0 ± 1.0	0
	150	36.4 ± 2.2	2.96 ± 0.33	0	421 ± 26	19.7 ± 1.7	0
Fluconazole	Control	35.7 ± 1.7	2.13 ± 0.19		407 ± 36	16.0 ± 1.7	
	2	35.6 ± 2.4	2.05 ± 0.26	0.385	399 ± 23	16.1 ± 1.3	0.320
	25	36.2 ± 0.8	2.35 ± 0.22	0.028	402 ± 28	17.3 ± 1.7	0.015
	50	35.1 ± 2.7	2.35 ± 0.25	0.010	412 ± 38	19.3 ± 3.1	0
Triadimefon	Control	33.9 ± 1.4	1.68 ± 0.19		388 ± 29	14.7 ± 1.5	
	5	34.8 ± 1.2	1.70 ± 0.15	0.738	399 ± 22	16.4 ± 1.4	0.873
	50	33.5 ± 2.3	1.74 ± 0.34	0.760	402 ± 28	17.2 ± 2.6	0.007
	115	33.7 ± 1.8	1.83 ± 0.28	0.141	386 ± 54	18.8 ± 3.2	0
Myclobutanil	Control	33.9 ± 1.4	1.68 ± 0.19		388 ± 29	14.7 ± 1.5	
	10	34.3 ± 1.4	1.49 ± 0.28	0.011	399 ± 27	16.4 ± 2.6	0.068
	75	33.5 ± 1.7	1.89 ± 0.14	0.017	393 ± 53	17.3 ± 2.5	0
	150	34.8 ± 1.1	1.91 ± 0.07	0.052	378 ± 32	16.4 ± 1.5	0.001

[a]Results are expressed as mean ± SD. [b]P from statistical comparisons to respective control value.

Table 2. Effects of treatment of rats with conazoles on liver microsomal alkoxyresorufin O-dealkylation activities

Conazole	Dose	BROD	EROD	MROD	PROD
	mg/kg body wt.	pmol resorufin formed /min/mg protein			
Propiconazole	Control	37.9 ± 6.8 (1)	99 ± 10 (1)	49 ± 14 (1)	21 ± 10 (1)
	10	37.7 ± 3.5 (0.99)	93 ± 19 (0.94)	55 ± 10 (1.12)	11.3 ± 6.0 (0.54)
	75	125 ± 35[b] (3.32)	134 ± 34 (1.35)	75 ±11[b] (1.53)	84 ± 21[b] (4)
	150	218 ± 44[b] (5.75)	145[b] ± 31 (1.46)	85.2 ± 6.5[b] (1.74)	150 ± 64[b] (7.14)
Fluconazole	Control	37.9 ± 6.8 (1)	99 ± 10 (1)	49 ± 14 (1)	21 ± 10 (1)
	2	35.5 ± 6.3 (0.94)	100 ± 31 (1.01)	39.9 ± 6.3 (0.81)	27.6 ± 9.0 (1.31)
	25	91 ± 35 (2.40)	167 ± 51 (1.69)	42 ± 12 (0.86)	59 ± 33 (2.81)
	50	268 ± 117[b] (7.07)	193 ± 66[b] (1.95)	46.9 ± 8.6 (0.96)	109 ± 55[b] (5.19)
Triadimefon	Control	57.6 ± 6.9 (1)	148 ± 33 (1)	57 ± 10 (1)	22.7 ± 6.4 (1)
	5	96 ± 20 (1.56)	122 ± 24 (0.82)	51 ± 10 (0.89)	34.9 ± 8.6 (1.54)
	50	654 ± 149[b] (11.4)	152 ± 32 (1.03)	61 ± 12 (1.07)	179 ± 37[b] (7.89)
	115	1593 ± 121[b] (27.7)	176 ± 21 (1.19)	53.0 ± 8.1 (0.93)	419 ± 57[b] (18.5)
Myclobutanil	Control	57.6 ± 6.9 (1)	148 ± 33 (1)	57 ± 10 (1)	22.7 ± 6.4 (1)
	10	93 ± 20 (1.61)	126 ± 23 (0.85)	51 ± 10 (0.89)	37.1 ± 8.9 (1.63)
	75	628 ± 154[b] (10.9)	154 ± 33 (1.04)	49.8 ± 7.9 (0.87)	161 ± 33[b] (6.65)
	150	766 ± 180[b] (13.3)	152 ± 23 (1.03)	51.4 ± 5.7 (0.91)	184 ± 61[b] (8.11)

[a]Results are expressed as mean ± SD (fold induction); n = 4 animals. Microsomes from each animal were assayed in duplicate. Variability in the duplicates was less than 10%. [b]Significantly different from control by Dunnett's test (P < 0.05).

Table 3

Effects of treatment of mice with conazoles on liver microsomal alkoxyresorufin O-dealkylation activities

Conazole	Dose	BROD	EROD	MROD	PROD
	mg/kg body wt.	pmol resorufin/min/mg protein			
Propiconazole	Control	80 ± 17 (1)	100 ± 23 (1)	130 ± 13 (1)	13.6 ± 2.2 (1)
	10	119 ± 33 (1.49)	106 ± 11 (1.06)	151 ± 24 (1.16)	15.1 ± 1.6 (1.11)
	75	224 ± 44[b] (2.8)	117 ± 13 (1.17)	200 ± 26[b] (1.54)	48.2 ± 6.6 [b] (3.54)
	150	307 ± 47[b] (3.84)	129 ± 33 (1.29)	194 ± 26[b] (1.49)	73.6 ± 7.2 [b] (5.41)
Fluconazole	Control	80 ± 17 (1)	100 ± 23 (1)	130 ± 13 (1)	13.6 ± 2.2 (1)
	2	145 ± 30 (1.81)	160 ± 35 (1.60)	165 ± 13[b] (1.27)	35.4 ± 9.1 (2.60)
	25	364 ± 83[b] (4.55)	236 ± 54[b] (2.36)	239 ± 17[b] (1.84)	69 ± 12 [b] (5.07)
	50	579 ± 111[b] (7.24)	261 ± 57[b] (2.61)	253 ± 35[b] (1.95)	118 ± 27 [b] (8.68)
Triadimefon	Control	303 ± 22 (1)	113 ± 17 (1)	181 ± 28 (1)	48 ± 12 (1)
	5	190 ± 38 (0.63)	84 ± 17 (0.74)	207 ± 50 (1.14)	46.0 ± 9.9 (0.96)
	50	538 ± 93[b] (1.78)	115 ± 22 (1.02)	237 ± 24 (1.31)	91 ± 23 [b] (1.90)
	115	730 ± 141[b] (2.41)	131 ± 47 (1.16)	218 ± 24 (1.20)	125 ± 22 [b] (2.60)
Myclobutanil	Control	303 ± 22 (1)	113 ± 17 (1)	181 ± 28 (1)	48 ± 12 (1)
	10	388 ± 108 (1.28)	122 ± 12 (1.08)	209 ± 25 (1.15)	53.4 ± 7.5 (1.11)
	75	737 ± 162[b] (2.43)	164 ± 40[b] (1.45)	247 ± 43[b] (1.36)	93 ± 25 [b] (1.94)
	150	831 ± 169[b] (2.74)	197 ± 39[b] (1.74)	260 ± 45[b] (1.44)	110 ± 13 [b] (2.29)

Results are expressed as means ± SD (fold induction); n = 4 animals. Microsomes from each animal were assayed in duplicate. Variability in the duplicates was less than 10%. [b]Significantly different from control by Dunnett's test ($p < 0.05$).

Figure legends

Figure 1. Structures of triazole containing conazoles used in these studies.

Figure 2 Correlation plots of the relationships between conazole induced BROD and PROD fold induction activities. Data points represent fold induction levels of four conazoles for all doses from rat (**A**) and mouse (**B**) studies. The correlation coefficients: (R^2) were 0. 952 based on the rat data and 0.943 based on the mouse data.

References

Bauer, C., Corsi, C., Paolini, M., 1994. Stability of microsomal monooxygenases in murine liver S9 fractions derived from phenobarbital and beta-naphthoflavone induced animals under various long-term conditions of storage. Teratog. Carcinog. Mutagen. 14, 13-22.

Bock, K. W., Lipp, H. P., Bock-Hennig, B. S., 1990. Induction of drug-metabolizing enzymes by xenobiotics. Xenobiotica 20, 1101-1111.

Burke, M. D., Thompson, S., Elcombe, C. R., Halpert, J., Haaparanta, T., Mayer, R. T., 1985. Ethoxy-, pentoxy- and benzyloxyphenoxazones and homologues: a series of substrates to distinguish between different induced cytochromes P-450. Biochem. Pharmacol. 34, 3337-3345.

Burke, M. D., Thompson, S., Weaver, R. J., Wolf, C. R., Mayer, R. T., 1994. Cytochrome P450 specificities of alkoxyresorufin O-dealkylation in human and rat liver. Biochem. Pharmacol. 48, 923-936.

California EPA 2003. Summary of toxicology data. California Environmental Protection Agency, Department of Pesticide Regulation. In *http://www.cdpr.ca.gov/docs/toxsums/toxsumlist.htm*.

Cornell University 2003. The Pesticide Management Education Program at Cornell University. In *http://pmep.cce.cornell.edu/profiles/fung-nemat/*.

Cummings, A. M., Hedge, J. L., Laskey, J., 1997. Ketoconazole impairs early pregnancy and the decidual cell response via alterations in ovarian function. Fundam. Appl. Toxicol. 40, 238-246.

Egaas, E., Sandvik, M., Fjeld, E., Kallqvist, T., Goksoyr, A., Svensen, A., 1999. Some effects of the fungicide propiconazole on cytochrome P450 and glutathione S-transferase in brown trout (Salmo trutta). Comp. Biochem. Physiol. C Pharmacol. Toxicol. Endocrinol. 122, 337-344.

Guengerich, F. P., Dannan, G. A., Wright, S. T., Martin, M. V., Kaminsky, L. S., 1982. Purification and characterization of microsomal cytochrome P-450s. Xenobiotica 12, 701-716.

Hanioka, N., Nakano, K., Jinno, H., Hamamura, M., Takahashi, A., Yoda, R., Nishimura, T., Ando, M., 1995. Induction of hepatic drug-metabolizing enzymes by chlornitrofen (CNP) and CNP-amino in rats and mice. Chemosphere 30, 1297-1309.

Harmsworth, W. L., Franklin, M. R., 1990. Induction of hepatic and extrahepatic cytochrome P-450 and monooxygenase activities by N-substituted imidazoles. Xenobiotica 20, 1053-1063.

Houston, J. B., Humphrey, M. J., Matthew, D. E., Tarbit, M. H., 1988. Comparison of two azole antifungal drugs, ketoconazole, and fluconazole, as modifiers of rat hepatic monooxygenase activity. Biochem. Pharmacol. 37, 401-408.

Hurley, P. M., 1998. Mode of carcinogenic action of pesticides inducing thyroid follicular cell tumors in rodents. Environ. Health Perspect. 106, 437-445.

Hutson, D. H. 1998. Azoles and analogues. In *Metabolic pathways of agrochemicals, part II* (T. R. Roberts, Ed.), pp. 1011-1070. Royal Society of Chemistry.

Jacobson, M., Levin, W., Lu, A. Y., Conney, A. H., Kuntzman, R., 1973. The rate of pentobarbital and acetanilide metabolism by liver microsomes: a function of lipid

peroxidation and degradation of cytochrome P-450 heme. Drug Metab. Dispos. 1, 766-774.

Kobayashi, Y., Suzuki, M., Ohshiro, N., Sunagawa, T., Sasaki, T., Tokuyama, S., Yamamoto, T., Yoshida, T., 2001. Climbazole is a new potent inducer of rat hepatic cytochrome P450. J. Toxicol. Sci. 26, 141-150.

Lamb, D. C., Cannieux, M., Warrilow, A. G., Bak, S., Kahn, R. A., Manning, N. J., Kelly, D. E., Kelly, S. L., 2001. Plant sterol 14 alpha-demethylase affinity for azole fungicides. Biochem. Biophys. Res. Commun. 284, 845-849.

Leslie, C., Reidy, G. F., Stacey, N. H., 1988. The effects of propiconazole on hepatic xenobiotic biotransformation in the rat. Biochem. Pharmacol. 37, 4177-4181.

Lowry, O. H., Rosebrough, N. J., Randall, R. J., 1951. Protein measurement with the Folin phenol reagent. J. Biol. Chem. 193, 265-275.

Matsuura, Y., Kotani, E., Iio, T., Fukuda, T., Tobinaga, S., Yoshida, T., Kuroiwa, Y., 1991. Structure-activity relationships in the induction of hepatic microsomal cytochrome P450 by clotrimazole and its structurally related compounds in rats. Biochem. Pharmacol. 41, 1949-1956.

Maurice, M., Pichard, L., Daujat, M., Fabre, I., Joyeux, H., Domergue, J., Maurel, P., 1992. Effects of imidazole derivatives on cytochromes P450 from human hepatocytes in primary culture. Faseb J. 6, 752-758.

Medical Economic Company 1998. *Physicians' Desk Reference*. Medical Economic Company, Inc.

Nerurkar, P. V., Park, S. S., Thomas, P. E., Nims, R. W., Lubet, R. A., 1993. Methoxyresorufin and benzyloxyresorufin: substrates preferentially metabolized by

cytochromes P4501A2 and 2B, respectively, in the rat and mouse. Biochem. Pharmacol. 46, 933-943.

Nims, R. W., Prough, R. A., Jones, C. R., Stockus, D. L., Dragnev, K. H., Thomas, P. E., Lubet, R. A., 1997. In vivo induction and in vitro inhibition of hepatic cytochrome P450 activity by the benzodiazepine anticonvulsants clonazepam and diazepam. Drug Metab. Dispos. 25, 750-756.

Oropeza-Hernandez, L. F., Lopez-Romero, R., Albores, A., 2003. Hepatic CYP1A, 2B, 2C, 2E and 3A regulation by methoxychlor in male and female rats. Toxicol. Lett. 144, 93-103.

Ronis, M. J., Celander, M., Badger, T. M., 1998. Cytochrome P450 enzymes in the kidney of the bobwhite quail (Colinus virginianus): induction and inhibition by ergosterol biosynthesis inhibiting fungicides. Comp. Biochem. Physiol. C Pharmacol. Toxicol. Endocrinol. 121, 221-229.

Ronis, M. J., Ingelman-Sundberg, M., Badger, T. M., 1994. Induction, suppression and inhibition of multiple hepatic cytochrome P450 isozymes in the male rat and bobwhite quail (Colinus virginianus) by ergosterol biosynthesis inhibiting fungicides (EBIFs). Biochem. Pharmacol. 48, 1953-1965.

Rosin, D. L., Martin, B. R., 1983. Comparison of the effects of acute and subchronic administration of Aroclor 1254, a commercial mixture of polychlorinated biphenyls, on pentobarbital-induced sleep time and [14C]pentobarbital disposition in mice. J. Toxicol. Environ. Health 11, 917-931.

Sheehan, D. J., Hitchcock, C. A., Sibley, C. M., 1999. Current and emerging azole antifungal agents. Clin. Microbiol. Rev. 12, 40-79.

Shirley, E., 1977. The analysis of organ weight data. Toxicology 8, 13-22.

Siess, M. H., Le Bon, A. M., Canivenc-Lavier, M. C., Suschetet, M., 1997. Modification of hepatic drug-metabolizing enzymes in rats treated with alkyl sulfides. Cancer Lett. 120, 195-201.

Slama, J. T., Hancock, J. L., Rho, T., Sambucetti, L., Bachmann, K. A., 1998. Influence of some novel N-substituted azoles and pyridines on rat hepatic CYP3A activity. Biochem. Pharmacol. 55, 1881-1892.

Suzuki, S., Kurata, N., Nishimura, Y., Yasuhara, H., Satoh, T., 2000. Effects of imidazole antimycotics on the liver microsomal cytochrome P450 isoforms in rats: comparison of in vitro and ex vivo studies. Eur. J. Drug Metab. Pharmacokinet. 25, 121-126.

Vanden Bossche, H., Marichal, P., Gorrens, J., Bellens, D., Verhoeven, H., Coene, M.-C., Lauwers, W., Janssen, P. A. J., 1987. Interaction of azole derivatives with cytochrome P-450 isozymes in yeast, fungi, plants and mammalian cells. Pestic. Sci. 21, 289-306.

Waxman, D. J., Azaroff, L., 1992. Phenobarbital induction of cytochrome P-450 gene expression. Biochem. J. 281 (Pt 3), 577-592.

Zarn, J. A., Bruschweiler, B. J., Schlatter, J. R., 2003. Azole fungicides affect mammalian steroidogenesis by inhibiting sterol 14 alpha-demethylase and aromatase. Environ. Health Perspect. 111, 255-261.

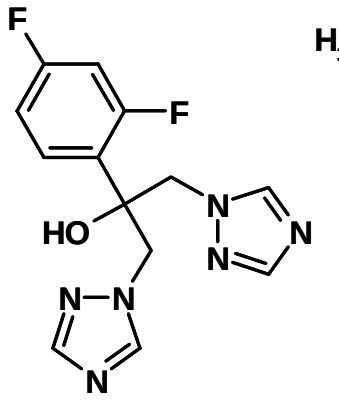

Fluconazole

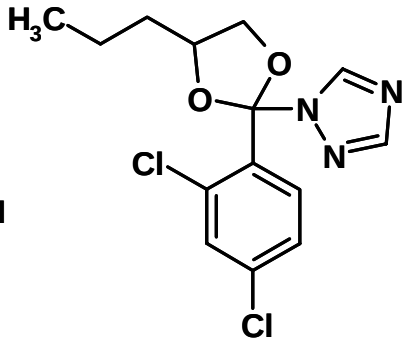

Propiconazole

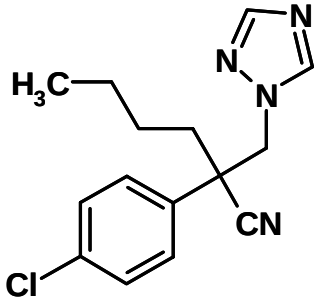

Myclobutanil

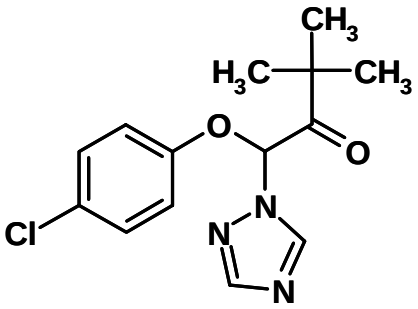

Triadimefon

Figure 1

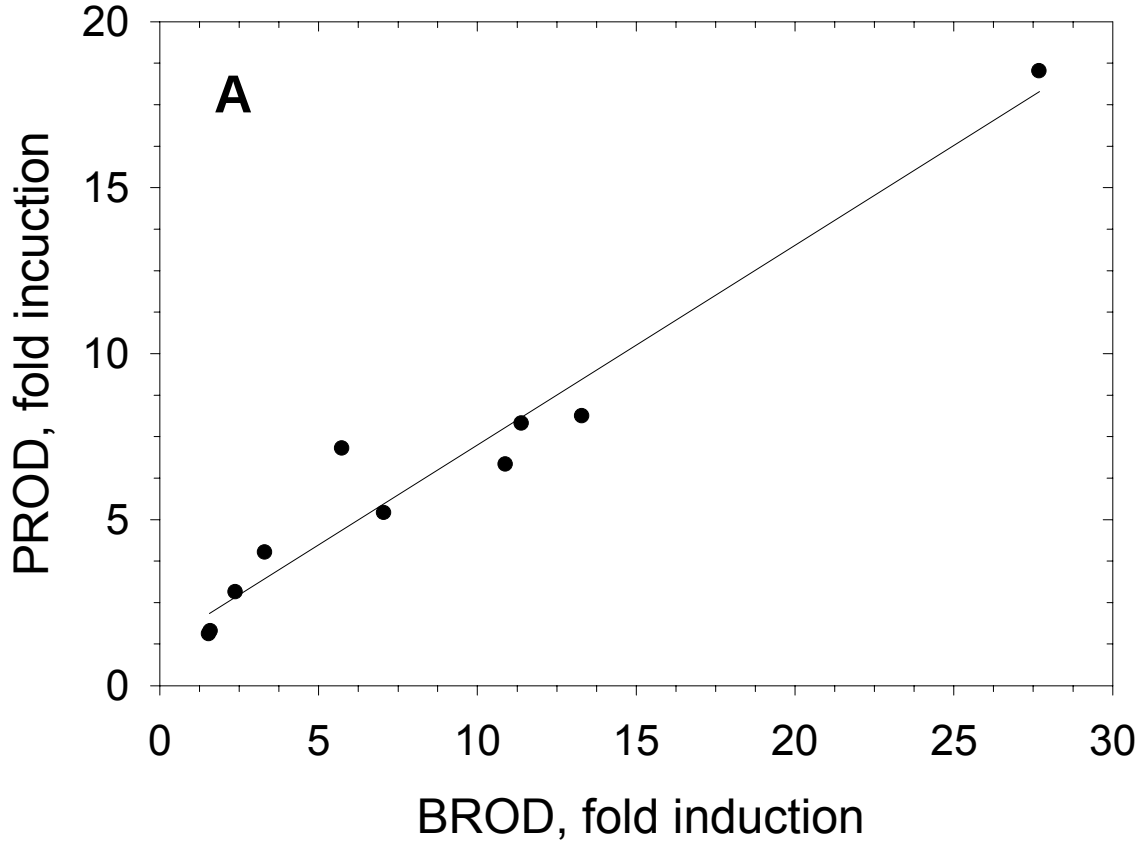
A
PROD, fold incuction
BROD, fold induction
0
5
10
15
20
25
30

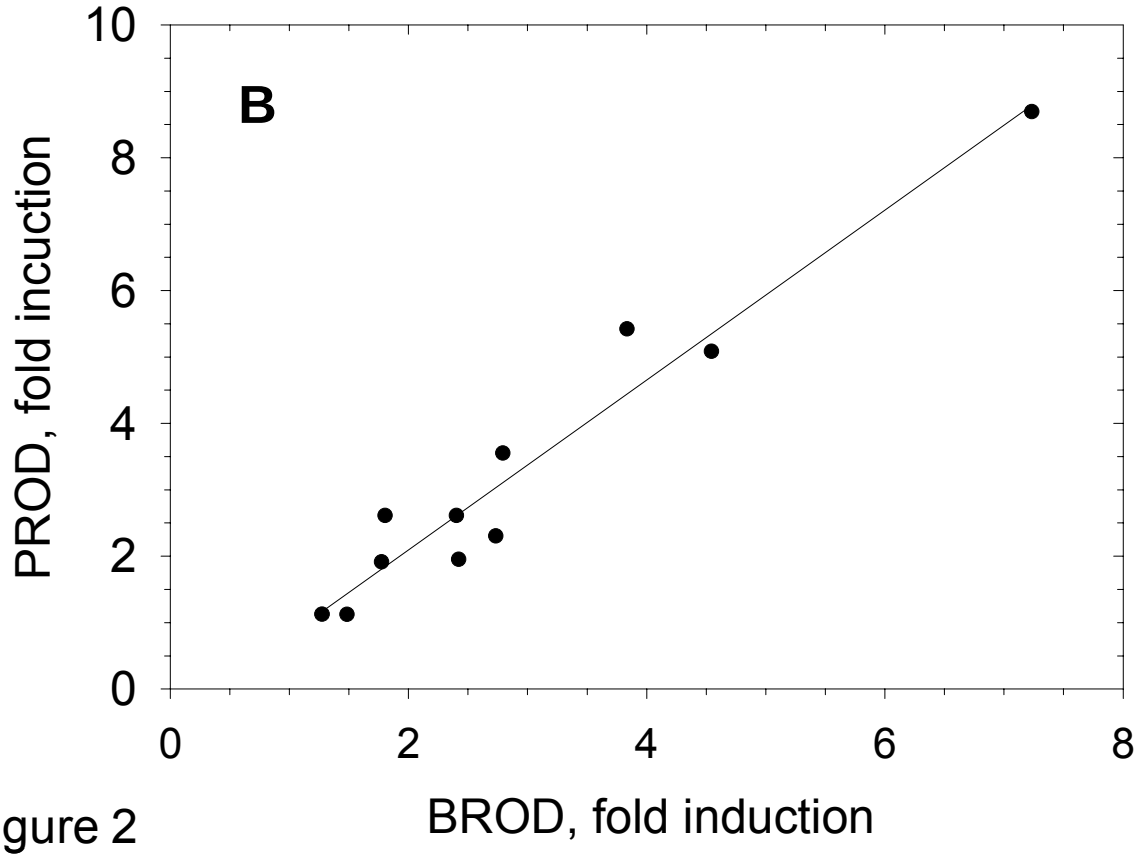
B
PROD, fold incuction
BROD, fold induction
0
2
4
6
8
10

Figure 2